VOLUME 2 (1956/57) No. 2

NUCLEAR PHYSICS

MONTHLY JOURNAL DEVOTED TO THE EXPERIMENTAL AND THEORETICAL STUDY OF ATOMIC NUCLEI, NUCLEAR FIELDS AND THE FUNDAMENTAL ASPECTS OF COSMIC RADIATION

EDITOR: L. ROSENFELD - MANCHESTER

M. CERINEO, Energy levels of C^{11} and angular distributions of some neutron groups from the B^{10} (d, n) reaction . . . 113

H. NAUTA, Differential elastic scattering of 14 MeV neutrons in lead, mercury and zinc 124

H. E. GOVE, G. A. BARTHOLOMEV, E. PAUL and A. E. LITHERLAND, Properties of low lying levels in Mg^{25} 132

A. Z. DOLGINOV and I. N. TOPTIGIN, Effect of distribution of nuclear charge on angular correlation in beta-decay . . 147

P. C. MACQ et M. DE HEMPTINNE, Interpretations des résultats expérimentaux de correlation angulaire 160

R. J. BLIN-STOYLE, Collective nuclear motion and the effective mass of a nucleon 169

A. SALAM, The interaction lagrangian for fundamental particles 173

S. N. BISWAS and H. S. GREEN, Radially symmetric solutions of Bethe-Salpeter equation 177

RIAZUDDIN, On the charge independence of nuclear forces 188

Book Review 192

NORTH - HOLLAND PUBLISHING COMPANY - AMSTERDAM

October 1956

EDITORIAL BOARD

AUSTRIA:	B. Karlik (Vienna), H. Thirring (Vienna)
BELGIUM:	M. de Hemptinne (Louvain), J. Verhaeghe (Ghent)
CANADA:	G. Volkoff (Vancouver)
DENMARK:	C. Møller (Copenhagen), S. Rozental (Copenhagen)
EGYPT & ARAB COUNTRIES:	F. El Bedewi (Alexandria), M. G. Nooh (Cairo)
FINLAND:	L. Simons (Helsinki)
FRANCE:	A. Berthelot (Saclay), S. Gorodetzky (Strasbourg), F. Joliot (Paris)
GERMANY (FED. REP.):	W. Gentner (Freiburg i. B.) J. H. D. Jensen (Heidelberg)
GERMANY (DEM. REP.):	G. Hertz (Leipzig)
GREAT BRITAIN:	S. Devons (Manchester)
HUNGARY:	L. Janossy (Budapest)
INDIA:	H. Bhabha (Bombay), B. Peters (Bombay), R. Ramanna (Trombay)
IRISH REPUBLIC:	J. McConnell (Maynooth)
ISRAEL:	G. Racah (Jerusalem)
ITALY:	E. Amaldi (Rome)
JAPAN:	S. Kikuchi (Tokyo), S. Tomonaga (Tokyo)
NETHERLANDS:	H. Brinkman (Groningen), S. R. de Groot (Leiden)
NORWAY:	E. Hylleraas (Oslo), A. Lundby (Oslo), H. Wergeland (Trondheim)
POLAND:	L. Infeld (Warsaw)
PORTUGAL:	J. M. Araújo (Porto), J. R. de Almeida Santos (Coimbra)
SOUTH AMERICA:	G. Beck (Saõ Paulo), J. Leite Lopes (Rio de Janeiro)
SPAIN:	J. M. Otero (Madrid), C. Sanchez del Rio (Madrid)
SWEDEN:	O. Klein (Stockholm), K. Siegbahn (Uppsala), I. Waller (Uppsala)
SWITZERLAND:	P. Huber (Basel), P. Scherrer (Zürich)
U.S.S.R.:	M. A. Markov (Moscow), I. S. Shapiro (Moscow), D. V. Skobeltzyn (Moscow)
YUGOSLAVIA:	I. Supek (Zagreb)
U.S.A. & MEXICO:	V. Weisskopf (Cambridge, Mass.)
AUSTRALIA & NEW ZEALAND:	H. Messel (Sydney), M. L. Oliphant (Canberra)

CONTRIBUTIONS may be sent to the Editor, Professor L. Rosenfeld, Dept. of Theoretical Physics, The University, Manchester, either directly, or preferably through the intermediary of one of the members of the Editorial Board of the country or region in which the author is working. They may be written in English, French or German.

BOOKS FOR REVIEW should be sent to Professor Rosenfeld.

NUCLEAR PHYSICS is published in monthly issues. The subscription price of a volume of 700 pages is fl 57.00; 114s; $ 15.00. Postfree.

SUBSCRIPTIONS should be sent to the publishers, NORTH-HOLLAND PUBLISHING COMPANY, P.O.Box 103, Amsterdam or to any subscription-agent. Subscriptions for U.S.A. are to be sent exclusively to INTERSCIENCE PUBLISHERS, INC., 250 Fifth Avenue, New York 1, N.Y.

Printed in the Netherlands.

Nuclear Physics **2** (1956/57) 113—123; *North-Holland Publishing Co., Amsterdam*

ENERGY LEVELS OF C^{11} AND ANGULAR DISTRIBUTIONS OF SOME NEUTRON GROUPS FROM THE B^{10}(d, n) REACTION

M. CERINEO

Institute "R. Bošković", Zagreb, Yugoslavia †

Received 7 July 1956

Abstract: The energy spectrum and the angular distributions of separated neutron groups from the B^{10}(d, n) reaction at 7.55 MeV deuteron mean energy have been determined. The resulting information on the excited states of C^{11} is presented in the table I. The angular distributions obtained are in agreement with the stripping theory.

1. Introduction

Recent work on the angular distribution of neutrons from the B^{10}(d, n)C^{11} reaction [1, 2]) has created some controversy about the assignment of spin and parity to some of the first excited states of C^{11}. Especially after the work of Evans and Parkinson [3]) on the mirror nucleus B^{11}, it was felt desirable to measure the angular distributions of separated neutron groups from the B^{10}(d, n) reaction at higher deuteron energies. This would at the same time enable one to cover the region above 9 MeV of excitation of C^{11}, which so far has not been done with a (d, n) reaction.

2. Experimental

The present experiment was carried out using the external beam of deuterons of a mean energy of 7.55 ± 0.10 MeV from the Cambridge cyclotron. After passing through a focusing magnet [4]), the beam was collimated by a system of lead stops ending in one 12 mm in diameter, placed 24 cm before the target. The target chamber was 3″ in diameter, and the target was mounted on a rectangular brass framework. It could be rotated and vertically displaced for background measurements. The monitoring of the beam during the

† This work was carried out while the author was at the Cavendish Laboratory, Cambridge, England.

exposure was performed by scattering deuterons from a thin gold foil before they entered the target chamber [5]). The elastically scattered deuterons were allowed to enter a scintillation counter placed about 27 cm from the scatterer at an angle of 15° to the forward direction.

The target was isotopically enriched boron (95 % B^{10}), about 1 mg per cm^2, mounted on a thin gold foil. The deuteron beam was stopped in the lead lining the target chamber.

Energies of emitted neutrons were obtained by measuring the ranges of recoil protons in 400 microns thick Ilford C 2 nuclear emulsions. The plates were mounted around the target chamber in a light-tight plateholder, with their inner edges 7.62 cm from the center of the target. The following angles were covered: 0°, 5°, 10°, 15°, 20°, 30°, and at 15° intervals to 165°. Three additional plates were mounted at −75°, −90°, and −105° to check possible dissymmetry in the experimental set-up.

The plates were treated by the Blau-De Felice two baths development method [6]). The shrinkage was found to be 2.38 ± 0.04, in agreement with the figure cited for C 2 emulsions [7]).

The scanning of the plates was made with a Cooke, Troughton and Simms M 4000 binocular microscope. For the angular distributions ×6 compensating eyepieces with an internal measuring scale and ×45 oil immersion objective were used, accepting all tracks projected into a cone of 15° aperture in respect to the direction of incident neutrons. For the low energy region of neutron spectra this angle was reduced to 10°, using ×10 Kellner eyepieces. The plates were scanned at a mean distance of 12 cm from the target. Altogether some 15000 tracks have been measured.

Conversion from range to energy was made by means of the range-energy relation of Baroni *et al.* [8]). Taking into account the knock-on angle of the recoil proton and the shrinkage of the emulsion, the energies of the neutron were calculated and plots of their number in 0.1 MeV intervals were then made. Where necessary the data were corrected for the (n,p) cross-section variation [9]), and escape probability [10]).

Because of the very low intensity of the beam (about 0.01 μ A) the plates were exposed for 116 hours, the plates at forward angles being renewed after half the total exposure. This long exposure resulted in a rather heavy γ-ray background, which made the scanning of the plates difficult. A separate exposure of 16 hours

of four plates at 20°, under different geometrical conditions was also made.

For background measurements the beam was allowed to strike a dummy target of gold backing for one fifth of the total exposure time, with plates disposed at all angles.

3. Energy Levels of C^{11}

In fig. 1 a plot is given of the actual number of neutrons at 20° in 0.1 MeV intervals, up to 9 MeV excitation of C^{11}. Apart from the

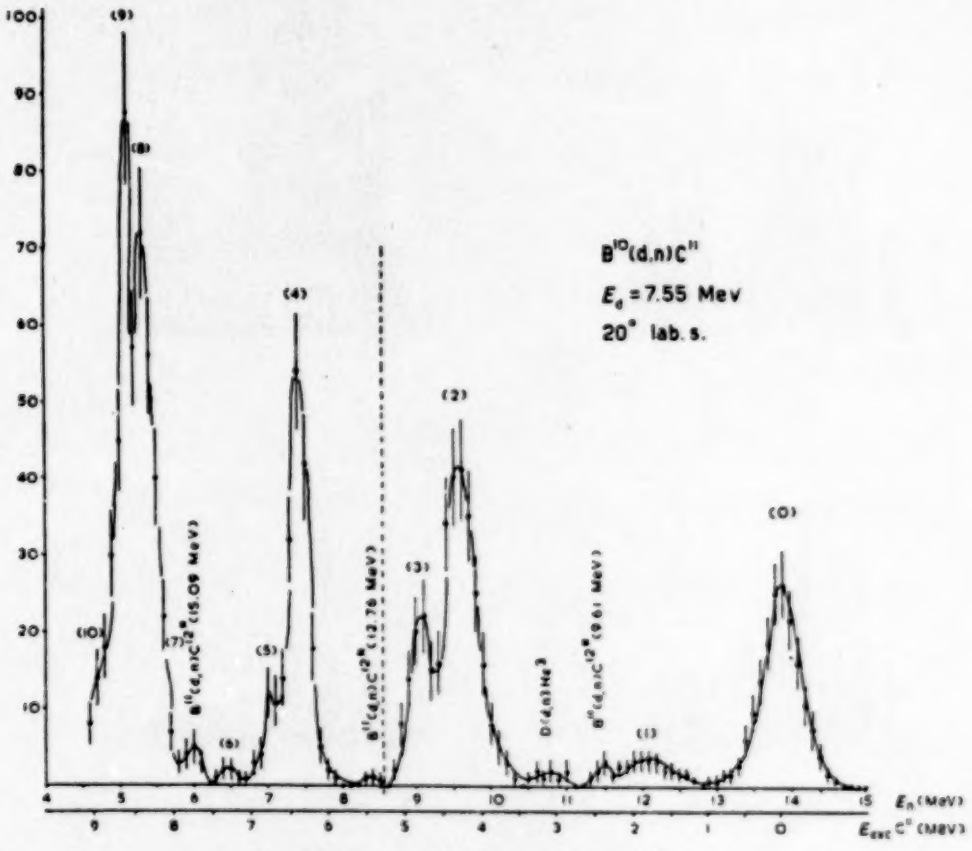

Fig. 1. Neutron spectrum at 20°.

background, which is subtracted, the spectrum is uncorrected. The part of the spectrum corresponding to the excitation energies of C^{11} above 8.7 MeV, was separately measured at 0°, 20°, 45°, and 75° (fig. 2). By comparing the spectra at different angles it was possible to assign a few new levels to C^{11}.

Table I summarizes the results. The Q values (column c) were obtained from the superposition of neutron spectra at all angles at which the measurements were made, plotted against the excitation

energy of C^{11}. The indicated errors include the uncertainty in the Q_0 value and in the range-energy relation.

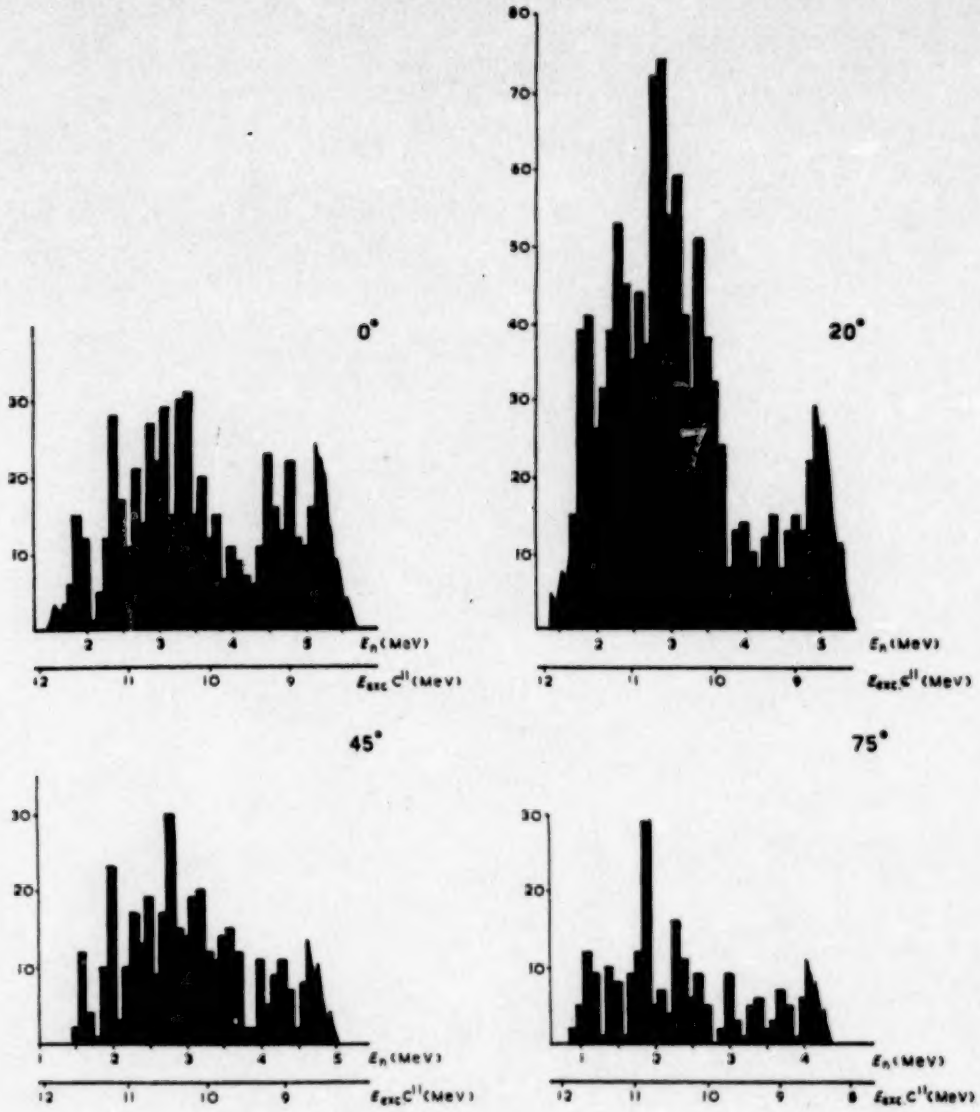

Fig. 2. Neutron spectra at various angles.

The levels below 9 MeV are in good agreement with those already reported [11]). It may be noted that the values for the 7, 8, and 9-th level agree with those found by Johnson [12]), and are consistently smaller than those given by Marion *et al.* [13]) who find 8.107, 8.430, and 8.660 MeV respectively.

The 0.05 MeV larger value for the second excited state must be assigned to the interference of the 11.74 MeV state of C^{12} from the $B^{11}(d, n)C^{12}$ reaction. At forward angles the neutrons from this

C^{12} state fall in the low energy tail of the 4.23 C^{11} state. The B^{11}(d, n) reaction was found to be responsible for a number of neutron groups throughout the spectrum.

The measured halfwidths (column b) of individual neutron groups are consistently smaller than 5 %, except for low intensity

TABLE I

Energy levels of C^{11}.

a	b	c	d	e	f	g	h
0	0.78	6.472±0.001	1.5	1.1	2.3	1.1	2.1
1.86	0.54	4.61 ±0.06	0.3	0.3	2.7	0.8	3.4
4.28	0.46	2.19 ±0.05	1.7	1.4	2.7	1.6	1.7
4.77	0.35	1.70 ±0.05	1.0	1.0	3.9	1.9	2.1
6.40	0.31	0.07 ±0.04	3.4	5.9	8.0	3.5	2.3
6.78	0.31	−0.31 ±0.05	1.0	1.0		2.1	
7.41	0.36	−0.94 ±0.05	0.3	0.2		0.8	
8.09	0.22	−1.62 ±0.04	0.9	0.2	3.1	1.3	2.4
8.40	0.17	−1.93 ±0.04	5.0	5.0	28	12.2	2.3
8.62	0.16	−2.14 ±0.04	5.2	9.2	17.5	8.3	2.1
8.98	0.18	−2.51 ±0.03	1.4				
9.28	0.16	−2.81 ±0.03	1.7				
9.69	0.22	−3.22 ±0.03	1.4				
10.09	0.16	−3.62 ±0.02	1.4				
10.69	0.15	−4.22 ±0.02	2.1				
10.89	0.14	−4.42 ±0.02	1.5				
(11.26)	0.17	−4.79 ±0.02					
11.52	0.17	−5.05 ±0.02					

groups and low energy neutron groups where the errors in measurement are necessarilly larger. This indicates that in spite of the unusually long exposure, the mean energy of the deuteron beam did not vary much more than 1 %, since all other errors (geometry, straggling of the proton tracks, thickness of the target, errors in measurements, etc.) are responsible for a 4.5 % spread.

In column d the intensities of individual neutron groups at 0° in the c.m.s. are given, in comparison with those (column e) given by Johnson [12]). It is interesting to compare the ratios of the intensities at 0° to those at 80° (column f) with the ones obtained at 3.64 MeV bombarding energy (column g). The given values (column h) might suggest that at least in this energy region the contribution due to the stripping is proportional to the energy, the ratios of the two energies being 2.1. The rather different values for the first and second excited state could perhaps be due to the fact that in these cases the stripping maximum does not fall at 0°.

Fig. 2 gives the part of the neutron spectrum above 8.7 MeV excitation at four angles. The scanned areas are not the same for all angles.

The reported level [12]) at 8.98 MeV is well established. There remains, however, some doubt about the 9.13 MeV level which was not observed in present experiment. On the other hand, a level at 9.28 MeV was found. Although at forward angles this neutron group could be attributed to the formation of C^{12} in 16.57 MeV state from the B^{11}(d, n) reaction, its presence at 45° and 75° excludes this possibility.

The levels at 9.7 and 10.1 MeV, already reported [11]), are also observed. The group of neutrons of 3.8 MeV energy at 0° is attributed to the 17.22 MeV state of C^{12} and does not seem to contribute much to the spectra at other angles. The intense group of neutrons of 3.36 MeV energy in the data for 0° must be assigned to the C^{12}(d, n)N^{13} reaction in which the 3.53 MeV state of N^{13} is formed. From other measurements [14]) it is known that the ratio of the intensity of this group to the one leaving N^{13} in the 2.3 MeV level, at 0° and 8 MeV bombarding energy, is about 3.7. This again excludes the possibility of the 4.8 MeV neutrons at 0° being due to the C^{12}(d, n) reaction only, since only about 35 % of the observed intensity can be attributed to this reaction. At 20° the 3.53 MeV N^{13} neutron group contributes to the 10.09 MeV C^{11} level, shifting its peak to lower energies, but at more advanced angles it should not contribute more than 10 % to the observed intensity of 10.09 MeV group.

The 3.1 MeV neutron group at 0° and 20°, the 2.8 at 45°, and the 2.3 at 75° were attributed again to the B^{11}(d, n) reaction in which C^{12} is left in the 17.8 MeV level. The group of neutrons corresponding to a state in C^{11} at 10.7 MeV could not be assigned either to contamination or to the B^{11} content of the target, since it remains in the proper position at all angles, as does also the group corresponding to the reported level of C^{11} at 10.9 MeV excitation. On the other hand the 2.4 MeV neutrons at 0°, the 2.3 at 20°, the 2.0 at 45° and the 1.8 MeV at 75° are assigned to the 18.39 MeV level of C^{12}.

A group of neutrons corresponding to a state in C^{11} at 11.26 MeV was observed only at 75°. Although it seems that there is some contribution from this group to the low energy tail of 18.39 MeV level of C^{12} at other angles, this level in C^{11} will be listed as

uncertain. A level in C^{11} at 11.52 MeV seems well established.

Table II gives the relative intensities in c.m.s. of individual groups of neutrons corresponding to states in 8 to 12 MeV region

TABLE II

Relative intensities of neutron groups.

$E_{exc.}$	0°	20°	45°	75°
8.09	6.5	6	3.5	2.1
8.40	36	23.5	2.5	1.3
8.62	37	28	6	2.1
8.98	10	3.7	4.5	1.7
9.28	12	2.3	2	1
9.69	8	4	2.5	2.3
10.09	10	8.5	4.2	1.5
10.69	15.5	12.5	3.5	1.5
10.89	11	6	3.3	2.5
(11.26)				
11.52				

at 0°, 20°, 45°, and 75° (laboratory system). The data are not sufficient to deduce the angular distributions, especially for groups with low intensities. It is clear, however, that these states are formed mainly by stripping interaction.

4. Angular Distributions

The angular distributions in c.m.s. of the neutrons from the ground state, first, second, and third excited states of C^{11} are shown in fig. 3 to 6. The indicated errors are due to counting statistics only. The curves shown in the figures are theoretical angular distributions calculated from Butler's formula using a value of 5.8×10^{-13} cm for the nuclear radius.

The angular distributions of all these four groups of neutrons can be well fitted with Butler's curves † having $l_p = 1$. As the ground state of B^{10} is known to be a 3+ state, this fixes the parity of the respective states in C^{11} as negative and restricts the spin values to $3/2 \leqq J \leqq 9/2$ for these levels.

Because of the low statistics, it is more difficult to find the best fitting radius. Although for the n_0 and n_1 larger r_0 values would give somewhat better agreement with the experimental points, this could also be achieved by subtracting an isotropic background.

† Since the writing of this article it came to my attention that E. E. Maslin, J. M. Calvert and A. A. Jaffe in Liverpool have obtained the same result for the ground state and first excited state of C^{11} (private communication).

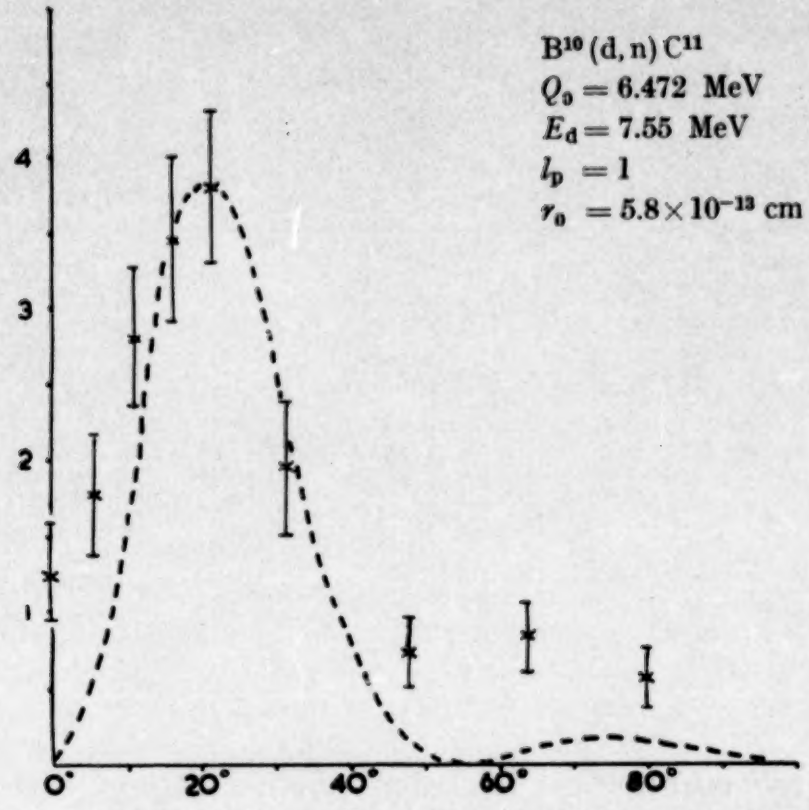

Fig. 3. Angular distribution of the neutrons from the ground state of C^{11}

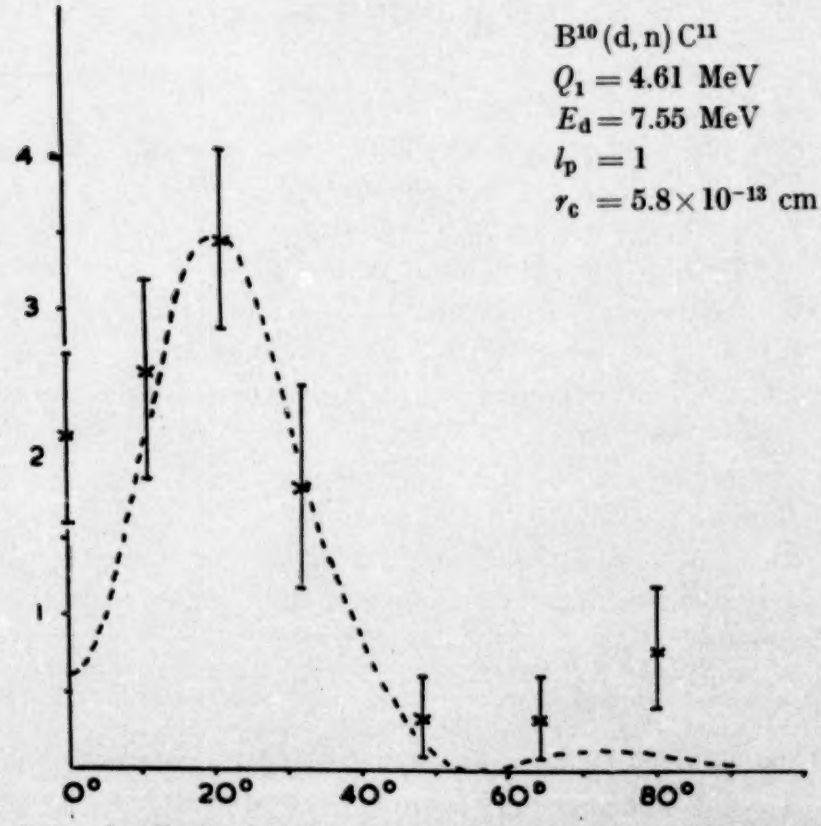

Fig. 4. Angular distribution of the neutrons from the 1st excited state of C^{11}.

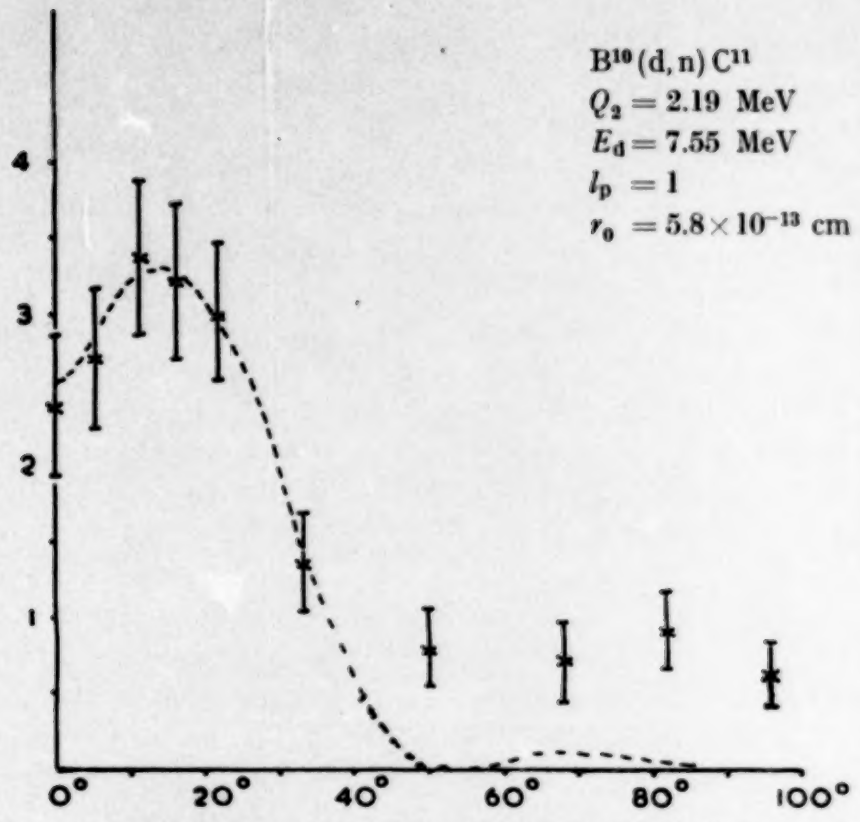

Fig. 5. Angular distribution of the neutrons from the 2nd excited state of C^{11}.

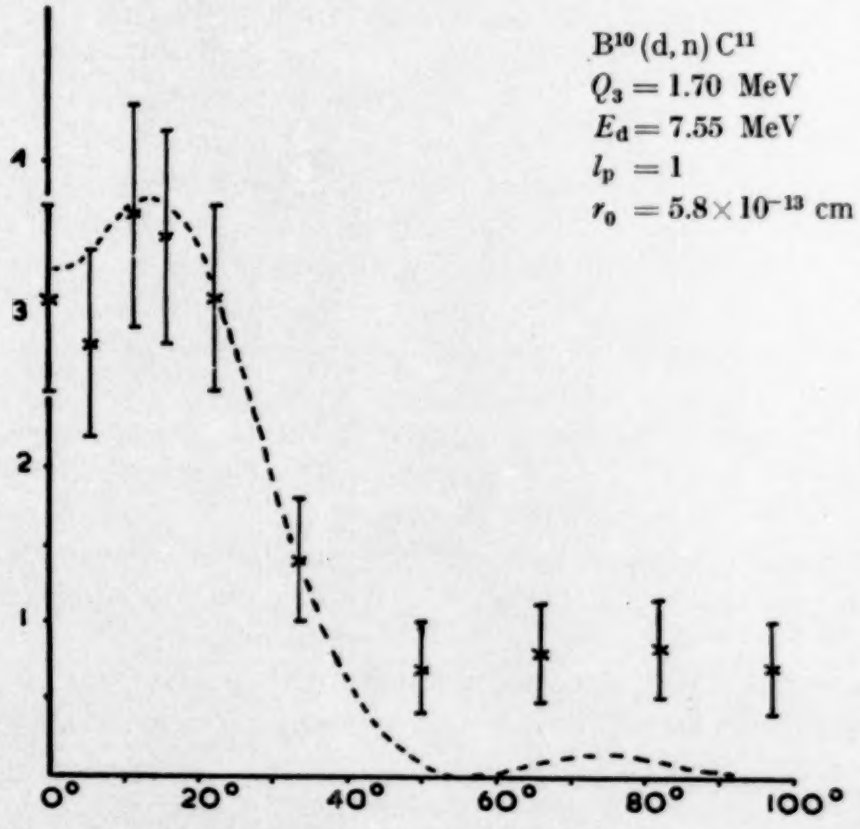

Fig. 6. Angular distribution of the neutrons from the 3rd excited state of C^{11}.

It is surprising, however, that in the case of the first excited state the intensities at large angles amount only to about 15 % of the stripping maximum, whereas for other three states this figure is about 25 %. This could be due to very low statistics for n_1.

Burke *et al.* [2]), using a long counter at 2 MeV bombarding energy obtain an angular distribution for the ground state and first excited state (unresolved) which agrees very well with the assumption of $l_p = 1$. Endt and Paris [1]), using 0.6 MeV deuterons ascribe 1, 3, 0, and 2 for the angular momentum transfer of the captured proton to the ground state, first, second, and third excited states respectively. The disagreement of this result with present measurements seem to confirm that at lower deuteron energies the competition between stripping and compound nucleus formation makes the assignment of l-values on basis of angular distributions rather unreliable.

The assignment of $l_p = 1$ to the first four states in C^{11} is in agreement with the assignment of $l_n = 1$ to the corresponding levels in the mirror reaction $B^{10}(d, p)B^{11}$ at the same bombarding energy [5]). It is most interesting, however, to compare the angular distribution of neutrons leaving the C^{11} nucleus in the first excited state with the corresponding angular distribution of protons in the $B^{10}(d, p)$ reaction. For this state Evans [5]) finds a rather anomalous distribution, that markedly deviates from the theoretical Butler's curve for $l_n = 1$, which he tried to explain by the exchange theory developed by French and Case [15]). Unfortunately, in the C^{11} case, the poor statistics of the neutron group makes it impossible to draw any conclusions about a possible anomaly in the angular distribution. Actually, the experimental points seem to fit quite well the theoretical curve, although the intensity at 0° seems to be somewhat higher than one would expect.

The author is indebted to Dr. A. P. French for suggesting the problem and to Dr. W. G. Parkinson for helpful discussion and kind interest in this publication. Thanks are due to Dr. N. T. S. Evans for his willing help and collaboration during the experiment; to Mr. E. G. T. Morley and Mr. W. R. Phillips for their able operation of the cyclotron during the long exposure of nuclear plates.

The author wishes to express his gratitude to the British Council and the Institute "R. Bošković" whose maintenance grants made this work possible.

References

1) Endt and Paris, Physica **20** (1954) 585
2) Burke, Risser and Phillips, Phys. Rev. **93** (1954) 188
3) Evans and Parkinson, Proc. Phil. Soc. A **67** (1954) 684
4) Rhoderick, University of Cambridge Thesis (1948)
5) Evans, University of Cambrige Thesis (1956)
6) Blau and De Felice, Phys. Rev. **74** (1948) 1198
7) Beiser, Rev. Mod. Phys. **24** (1952) 273
8) Baroni *et al.*, Instituto Nazionale di Fisica Nucleare, Sezione di Roma, B S **9** (1955)
9) Hughes and Harvey, Neutron Cross-Sections, Brookhaven National Laboratory, Upton, N.Y. (1955)
10) Richards, Phys. Rev. **59** (1941) 796
11) Ajzenberg and Lauritsen, Rev. Mod. Phys. **27** (1955) 77
12) Johnson, Phys. Rev. **86** (1952) 302
13) Marion, Cook and Bonner, Phys. Rev. **100** (1955) 847
14) Middleton *et al.*, Proc. Phys. Soc. A **66** (1953) 95
15) French and Case, unpublished (1954)

Nuclear Physics **2** (1956/57) 124—131; *North-Holland Publishing Co., Amsterdam*

DIFFERENTIAL ELASTIC SCATTERING OF 14 MeV NEUTRONS IN LEAD, MERCURY AND ZINC

H. NAUTA

Natuurkundig Laboratorium, Rijksuniversiteit Groningen

Received 16 July 1956

Abstract: The differential cross sections for the elastic scattering of 14 MeV neutrons from lead, mercury and zinc have been measured in a ring geometry using a biased detector with a spherical liquid scintillator. The measurements were taken over the angular range between 15° and 125°.

The results are in qualitative agreement with theoretical predictions.

1. Introduction

Experimental data on the differential cross sections for elastic scattering have been published for some neutron energies between 1 MeV and 14 MeV [1, 7]). Maxima in the forward direction were observed in all cases and in several cases additional maxima at larger angles were found. The results have been compared with the optical model theory developed by Feshbach, Porter and Weisskopf [8]). In this theory the term σ_{se} in the expression for the elastic scattering cross section $\sigma_{el} = \sigma_{se} + \sigma_{ce}$ is calculated; σ_{se} represents elastic scattering without involving compound nucleus formation, while σ_{ce} denotes elastic scattering produced by the decay of the compound nucleus through the entrance channel.

At low energies (smaller than 2 MeV) the comparison of experiment with theory is difficult since the compound nucleus has an excellent chance to decay by the entrance channel, which produces compound elastic scattering. The measurement of the elastic scattering at low energy thus gives an unknown mixture of compound-elastic and shape-elastic scattering which are experimentally undistinguishable. The use of higher energy neutrons presents the advantage that there are more nuclear levels available for inelastic scattering so that the compound-elastic scattering is essentially small and the comparison between theoretical predictions and experimental results becomes a more sensitive test of the theory. Recently the results of an analysis of scattering of 14 MeV

neutrons based on this theory and using exact phase-shift calculations were presented [9]).

2. Experimental Method

Fig. 1 shows the experimental arrangement. The neutrons were generated by the T(d, n)He^4 reaction. A target of T—Zr was bombarded with a magnetically analyzed beam of 200 keV deuterons,

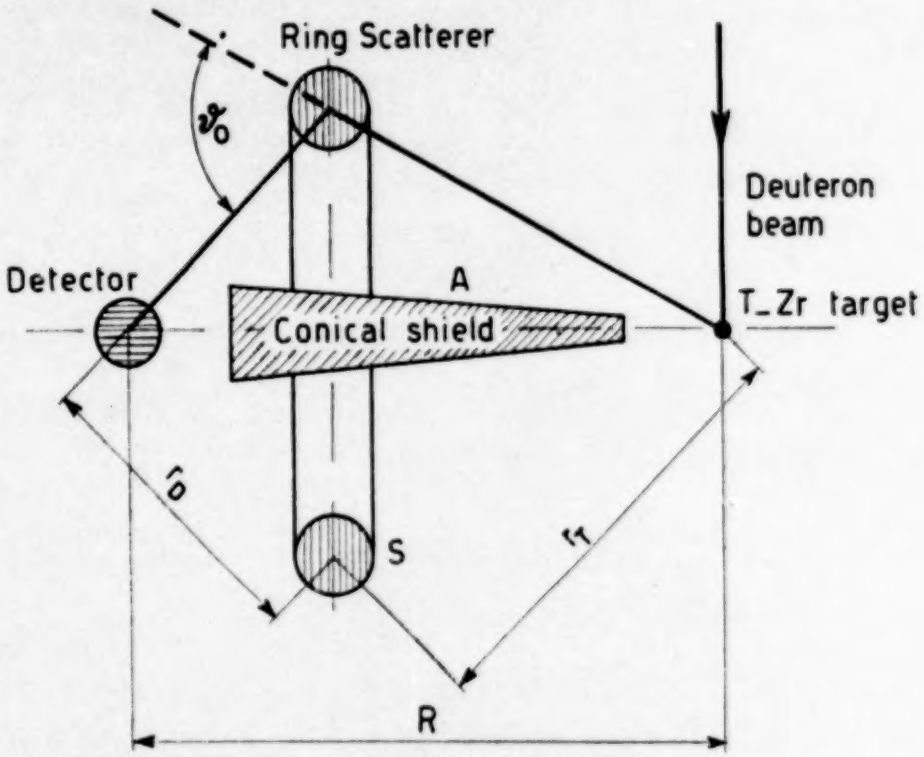

Fig. 1. Schematic diagram of experimental arrangement.

produced by a cascade generator. The production of neutrons during the experiments was monitored by a BF_3-filled proportional counter in a fixed position. The scatterers were rings of different size, two of each element, in order to cover the range of angles from 15° to 125°. Two lead rings of 2 cm thickness, diameters 9.6 cm and 20 cm, two mercury rings of 1.6 cm thickness in thin plastic containers, diameters 11.2 cm and 17.6 cm and two zinc rings of 1.8 cm thickness, diameters 8.0 cm and 20 cm were used. The scattering at various angles was obtained by moving the scatterer laterally while the source and the detector were in a fixed position. The distance R from source to detector in all cases was 75 cm.

The detector was a scintillation counter with a spherical liquid

scintillator consisting of a solution of p-terphenyl (5 g/l) and 1,6-diphenylhexatriene, 1,3 (10 mg/l) in purified xylene, enclosed in a spherical glass bulb, 18 mm in diameter, connected to an R.C.A.-6342 multiplier with a lucite light guide. A discriminator after the linear amplifier was set to detect only pulses corresponding to a recoil proton energy of at least 12 MeV, so that the detection of inelastically scattered neutrons and gamma rays is eliminated, as there do not seem to occur levels in the compound nucleus below 2 MeV.

A conical shield A, 50 cm long, of material of large total cross sectional area (lead) kept the detector from measuring the primary neutrons from the source and reduced the counting rate of the primary neutrons by a factor of 200.

3. Cross Section Calculations and Corrections

If, for a given number of neutrons emitted by the neutron source, N_s is the counting rate with the scatterer S and the conical shield A in position, N_0 the counting rate without S (background) and N_1 the counting rate without S and A, the differential elastic cross section can be calculated from the scattering ratio $f(\vartheta)$, defined as

$$f(\vartheta) = \frac{N_s - N_0}{N_1 - N_0}.$$

The difference $N_s - N_0$ has to be attributed to the neutrons scattered from the ring into the detector.

Then, if multiple scattering of the neutrons in the scatterer is neglected, the relation between the ratio $f(\vartheta)$ and the differential elastic cross section $\sigma_{el}(\vartheta)$ is

$$f(\vartheta) = \int_V \frac{R^2}{r_D^2 \times r_T^2} \times s(E) \times \sigma_{el}(\vartheta) \times \exp(-n\sigma_t x) \times n \, dV \qquad (1)$$

where ϑ is the scattering angle in the laboratory system of coordinates, n the number of nuclei in the scatterer per cm^3, σ_t the total cross section of the element of the scatterer, x the total length of the neutron path in the scatterer, $s(E)$ the sensitivity of the biased detector for scattered neutrons of energy $E(\vartheta)$ normalised for the neutrons with energy $E(\vartheta = 0)$. The meaning of the remaining symbols is clear from fig. 1. The integration has to be extended over the volume V of the scatterer. On account of the spherical

shape of the scintillator the angular sensitivity of the detector is constant and hence does not occur in formula (1), which is derived with the assumption that the neutron source is an isotrope radiator and emits monoenergetic neutrons. This assumption can be justified by the low bombarding energy of the deuterons (200 keV) compared with the high Q-value (17.6 MeV) of the neutron producing reaction. In addition deviations from isotropy cancel out to the first approximation by the symmetric position of detector and scatterers relative to the axis of symmetry of the arrangement, which is at 90° to the direction of the deuteron beam.

The factor $s(E)$ accounts for the relative energy loss of the neutrons in scattering which can approximately be written as

$$\frac{\Delta E}{E} = \frac{2(1-\cos\vartheta)}{A+1-\cos\vartheta}$$

if A is the mass number of the scattering element and ϑ the scattering angle in the laboratory system of coordinates. This correction is appreciable only for high discriminator levels and large scattering angles and the calculated cross sections have been corrected for this effect.

Neglecting the attenuation of the neutrons in the scatterer, so that the exponential factor in formula (1) becomes unity, the cross section can be calculated from the very simple formula

$$\sigma_{el}(\vartheta) = \frac{f(\vartheta)}{s(E)\times nV} \cdot \frac{r_D^2 \times r_T^2}{R^2} . \qquad (2)$$

The attenuation of the neutron beam in the scatterer was calculated as a correction by expanding the exponential factor in formula (1) in a series and integrating term by term. A correction of sufficient accuracy could be obtained; it was of the order of magnitude of 30 %.

Due tc the finite dimensions of the scatterer and the detector a correction for the angular spread was carried out by expanding the integrand of formula (1) in a Taylor series about ϑ_0 and integrating term by term. This correction turned out to be of importance only in the pronounced maxima and minima where the second derivative of $\sigma(\vartheta_0)$ is large. This correction caused the maxima to increase and the minima to decrease. As the mean thickness of all the scattering samples was about $\frac{1}{4}$ of a mean free path for scattering, only a small percentage of the scattered

neutrons was scattered again before leaving the sample. Although the angular distributions are strongly peaked in the forward direction, the multiple scattering effect will cause rather small errors.

The counter efficiency is independent of the counting rates occurring in the experiments. The background counting rate was

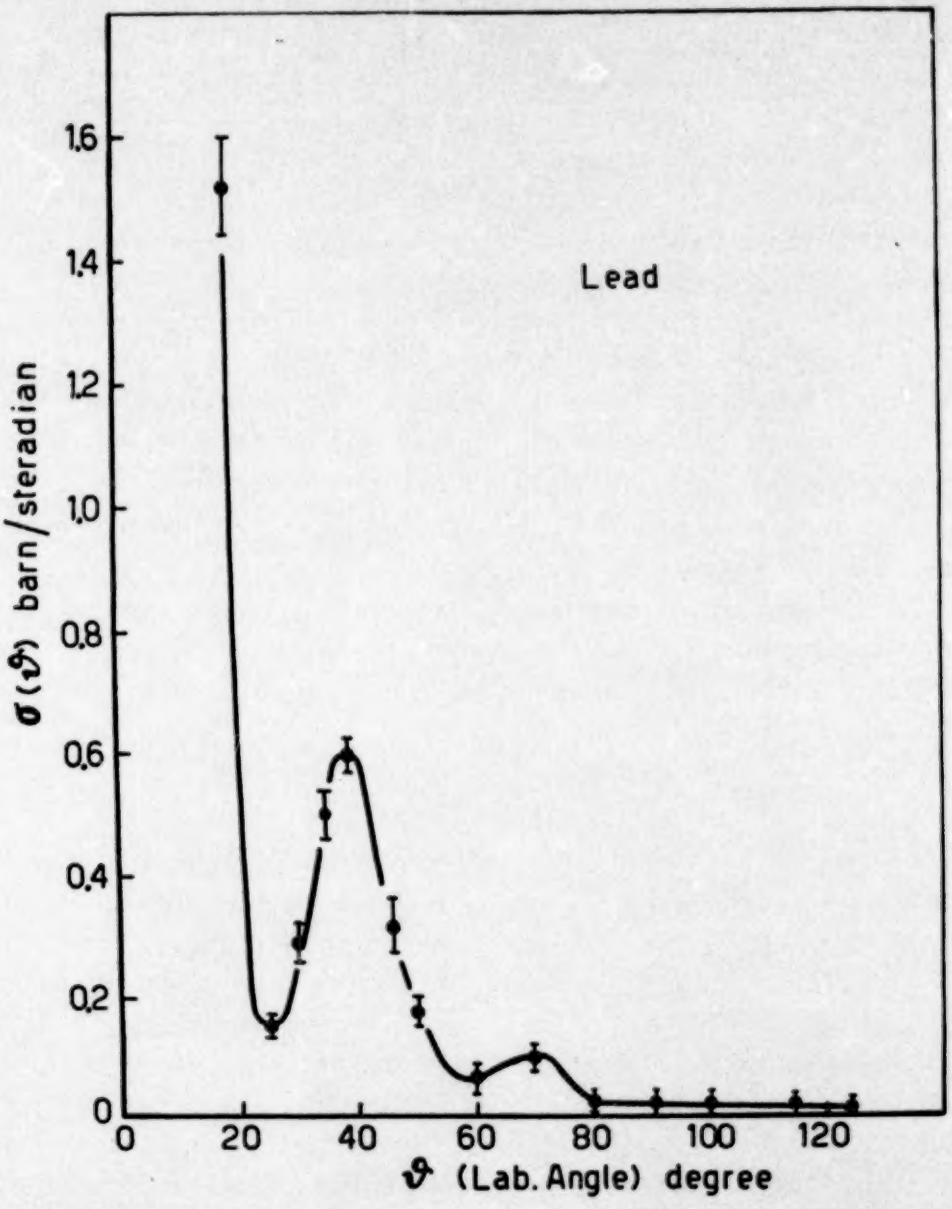

Fig. 2. Differential elastic scattering cross section of 14 MeV neutrons for lead.

about 50 counts per minute. The direct beam count N_1 was about 200 times the background N_0. For mercury the counting rate N_s at 40° was three times N_0; at 70° N_s was 60 % of N_0. The vertical

bars in figs. 2—4 indicate the standard deviation in the measurements of the ratio $f(\vartheta)$. For angles larger than 90° the curves indicate merely the upper limit of the cross section due to the small difference between N_s and N_0.

4. Discussion of the Results

The experimental results, as obtained by the above method, are presented in figs. 2—4. The results for lead are in perfect agreement with the tentative experimental data obtained by J. Coon and

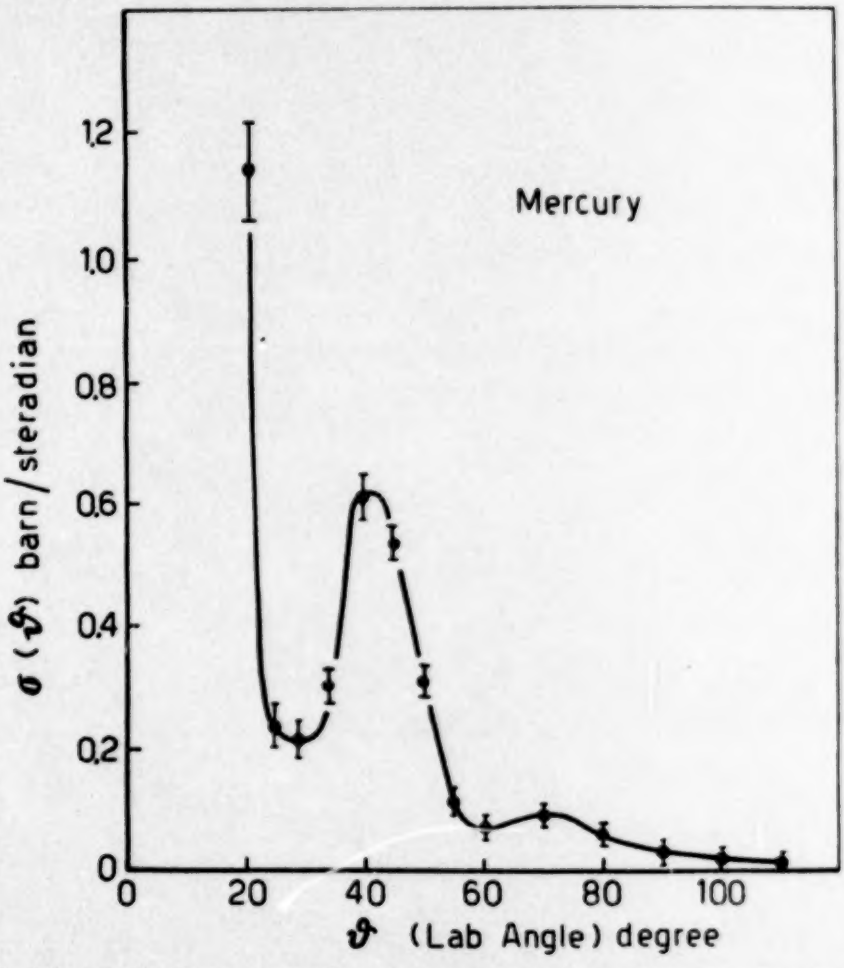

Fig. 3. Differential elastic scattering cross section of 14 MeV neutrons for mercury.

W. Cross, mentioned in ref. [9]). It has been shown that calculations based on the optical model of the nucleus gave better correspondence with the experimental data when the simple complex square well potential was replaced by a potential with step wells [9]). In the case of lead these authors found only qualitative agreement between the

theoretical curve and the tentative experimental data. For example at 40° the experimentally determined cross section differs by a factor of three from the theoretical value. As this discrepancy cannot be explained by multiple scattering, the theoretical prediction of the angular distribution for lead does not sufficiently fit to the experimental data. The angular distributions for mercury and lead

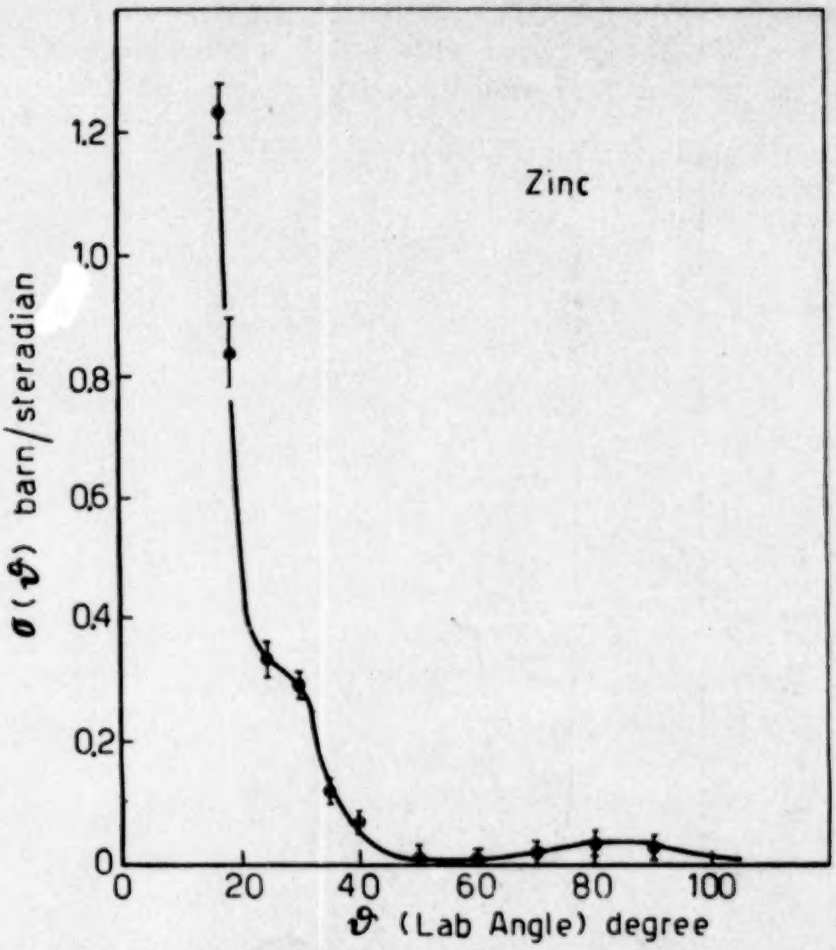

Fig. 4. Differential elastic scattering cross section of 14 MeV neutrons for zinc.

seem to be nearly identical as can be expected from the theory.

The author wishes to acknowledge Professor Dr. H. Brinkman, the Director of the Natuurkundig Laboratorium der Rijksuniversiteit, Groningen, Nederland, for his unfailing interest in this research. Special thanks are further due to Mr. P. J. Pasma and Mr. C. P. Sikkema for their indispensable assistance in solving neutron-generator problems.

References

1) W. D. Whitehead and S. C. Snowdon, Phys. Rev. **92** (1953) 114
2) M. Walt and H. H. Barschall, Phys. Rev. **93** (1954) 1062
3) S. C. Snowdon and W. D. Whitehead, Phys. Rev. **94** (1954) 1267
4) M. Walt and J. R. Beyster, Phys. Rev. **98** (1955) 677
5) R. N. Little Jr *et al.*, Phys. Rev. **98** (1955) 634
6) W. J. Rhein, Phys. Rev. **98** (1955) 1300
7) J. O. Elliot, Phys. Rev. **101** (1956) 684
8) H. Feshbach, C. E. Porter and V. Weisskopf, Phys. Rev. **96** (1954) 448
9) G. Culler, S. Fernbach and N. Sherman, Phys. Rev. **101** (1956) 1047

Nuclear Physics **2** (1956/57) 132—146; *North-Holland Publishing Co., Amsterdam*

PROPERTIES OF LOW LYING LEVELS IN Mg^{25}

H. E. GOVE, G. A. BARTHOLOMEW, E. B. PAUL † and A. E. LITHERLAND

Chalk River Laboratory, Atomic Energy of Canada Limited, Chalk River, Ontario, Canada

Received 25 June 1956

Abstract: The reaction Mg^{25} (pp′γ)Mg^{25} and the negaton decay of Na^{25} have been used to study the first four excited states of Mg^{25} at 0.58, 0.98, 1.61, and 1.96 MeV. The 0.98 MeV level decays to the level at 0.58 MeV or to ground by gamma emission in the intensity ratio 51:49. The 1.61 MeV level decays to ground $> 96\,\%$ of the time. The 1.96 MeV level decays to the level at 0.98 MeV or 0.58 MeV or to ground in the intensity proportions 25:50:25. A study of the gamma rays following negaton decay of Na^{25} shows that the levels in Mg^{25} at 0.98 and 1.61 MeV are fed by negaton transitions. Gamma rays due to negaton transitions to the 0.58 state are less than 3 % of the total. Comparisons between the gamma-ray branching ratios of levels in Mg^{25} and those in Al^{25} indicate that the 0.58, 0.98 and 1.96 MeV levels in Mg^{25} have spins and parities 1/2+, 3/2+ and 5/2+ respectively, while that at 1.61 MeV is probably 7/2+. The most likely spin and parity assignments for the ground state of Na^{25} are 5/2+.

1. Introduction

Inelastic proton scattering from Mg^{25} has been studied by Hausman *et al.* [1]), who observed the scattered protons in a magnetic spectrometer with an accuracy of ± 20 keV. The most accurate knowledge of the level positions in Mg^{25} derives from magnetic analysis of the Mg^{24}(d, p)Mg^{25} and Al^{27}(d, α)Mg^{25} reactions [2]). From this work the positions of the first five excited states are known to ± 6 keV. Angular distribution measurements of the Mg^{24}(d, p)Mg^{25} reaction [3]) indicate spins of 3/2+ or 5/2+ for the ground, 0.98, and 1.96 MeV levels, of 1/2+ for the level at 0.58 MeV, and of 1/2− or 3/2− for the level at 3.40 MeV. The angular distribution of the proton group leading to the 1.61 MeV state is isotropic. The spin of the ground state is almost certainly [4]) 5/2+. In the negaton decay of Na^{25}, Maeder and Stähelin [5]) have deduced allowed β-transitions to the ground, 0.98, and 1.61 MeV levels with a somewhat weaker branch to the 0.58 MeV level. In the positon decay of Al^{25}, the same workers have observed, in

† Now at Physics Division, A.E.R.E., Harwell.

addition to the mirror transition to the ground state, a weak branch to the 1.61 MeV state which is also an allowed transition. Iwersen and Koski [6]) have observed gamma rays of energy 0.98, 0.59, and 0.41 MeV following the negaton decay of Na^{25}. Gamma-ray cascades in Mg^{25} have been observed in the $Mg^{24}(n, \gamma)Mg^{25}$ reaction [7]) in particular, the state at 3.40 MeV is established as 3/2−, and the gamma rays resulting from the decay of this state to the ground and first excited states have been observed.

In the present work, the yield of gamma rays resulting from inelastic proton scattering to the first four excited states of Mg^{25} has been studied over a limited range of proton energy $E_p = 1.7$—3.0 MeV. More detailed studies were made at selected points on the yield curve when the relative feeding of the various states made a study of the cascading feasible. Direct and coincidence gamma-ray spectra measurements were used to establish the cascading from the 0.98, 1.61, and 1.96 MeV states. Some further work on the gamma rays resulting from negaton decay of Na^{25} is also reported. The results are compared to those obtained [8]) for the mirror nucleus Al^{25}.

2. Experimental Details

The proton beam from the Chalk River electrostatic accelerator bombarded a target of metallic magnesium enriched to 96 % in

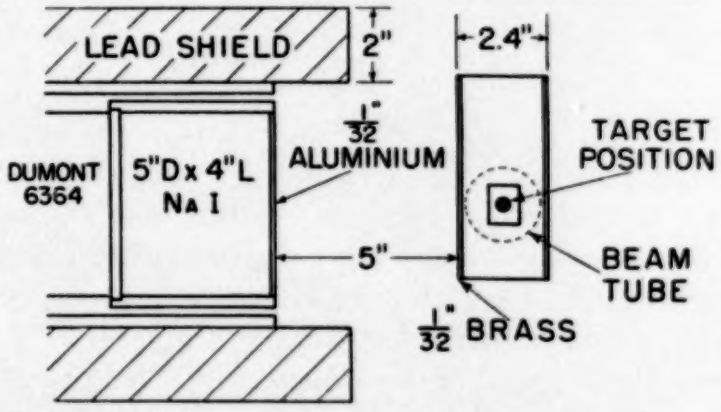

Fig. 1. A schematic diagram of the standard geometry employed to measure gamma-ray spectra.

Mg^{25}. This consisted of a 30 $\mu g/cm^2$ layer of magnesium evaporated onto a 0.020-inch-thick tantalum backing, and was prepared by the Isotope Branch at A.E.R.E., Harwell. The target arrangement

and the scintillation spectrometers used are identical to those already described [8]). In all the measurements to be discussed a standard geometry was employed for which the absolute efficiency vs. gamma-ray energy curve for the total absorption peak and the shapes of standard gamma-ray spectra are known [8]). This geometry is shown schematically in fig. 1. For the measurements of the gamma-ray spectrum following the negaton decay of Na^{25}, the Na^{25} source was placed in the target position. For coincidence measurements, a second NaI crystal and Dumont 6364 photomultiplier similar to the one shown in fig. 1 were placed on the opposite side of the target holder.

The Na^{25} source (with a half-life of about 60 seconds) was prepared by placing a right cylinder of natural magnesium 1—1/2 in. in diameter and 25/32 in. thick, 1/8 in. from a tritium target which was bombarded with deuterons from the 100 keV Cockroft-Walton generator. The intensity of 14 MeV neutrons from the target was about 10^9 per second. Exposure times were about one minute. The following reactions occur: $Mg^{24}(n, p)Na^{24}$, $Mg^{25}(n, p)Na^{25}$, and $Mg^{26}(n, \alpha)Ne^{23}$. Na^{24}, which has a half-life of about 15 hours, gives rise to gamma rays of energy 2.75 and 1.37 MeV. and Ne^{23}, with a half-life of about 40 seconds, gives rise primarily to a gamma ray of 0.44 MeV energy, and undoubtedly accounts for the gamma ray of 0.46 MeV observed by Iwerson and Koski [6]), who used a similar method of producing Na^{25}.

3. Experimental Results

The yield of the reaction $Mg^{25}(pp'\gamma)$ was measured at 90° to the incident proton beam as a function of proton energy between 1.7 and 3.0 MeV. Both scintillation crystals were employed and gates were set on the voltage outputs; the first gate included pulses corresponding to the total absorption peak of 0.40 and 0.58 MeV gamma rays, the second 0.98 MeV gamma rays, the third 1.61 MeV, and the fourth 1.96 MeV gamma rays. These four yield curves, which were measured simultaneously, are shown in fig. 2. For lower energy gamma rays the gates always included tails of the spectra of higher energy transitions and hence the yield curves are principally, but not exclusively, for the gamma ray energies listed. In the case of the yield for the 1.96 MeV gamma ray the background is relatively high due to the low intensity of these gamma rays

and hence the ordinate is not particularly accurate. The absolute energy scale was calibrated just below the resonance marked 1 using the Li^7(p, n) threshold at a proton energy of 1.882 MeV. As can be seen, the situation in the compound nucleus Al^{26} is quite complicated, the level density is very high, and considerable overlapping of levels occurs. The main purpose of this measurement

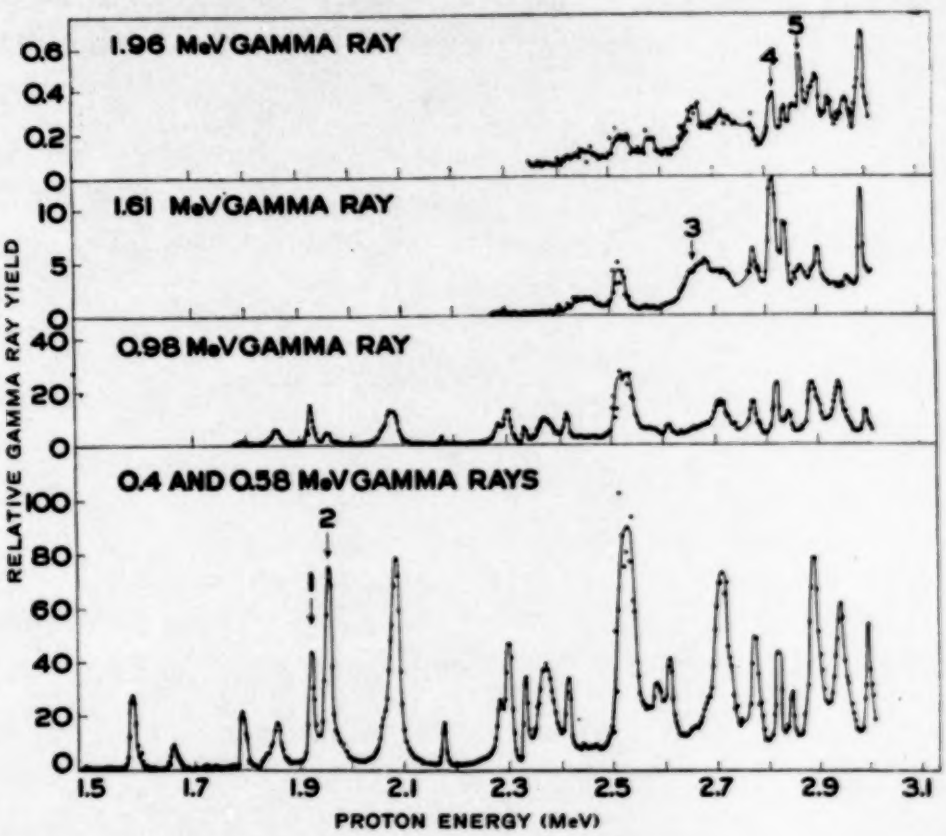

Fig. 2. The yield of gamma rays from the reaction $Mg^{25}(pp'\gamma)$ measured at 90° to the incident proton beam. Two scintillation crystals were employed and gates were set on the voltage outputs. The labels on each curve indicate that the corresponding gates included only the total absorption peaks of the listed gamma rays. The numbers indicate the positions on the yield curve at which gamma-ray branching ratios of various levels in Mg^{25} were measured.

was to choose appropriate resonances for the study of the branching ratio of low-lying levels in Mg^{25} and to compare these with the results obtained [8]) in the mirror nucleus Al^{25}. These measurements are discussed below for the levels in Mg^{25} at 0.98, 1.61, and 1.96 MeV, followed by a description of the results of some measurements of the gamma-ray spectrum following the negaton decay of Na^{25}.

3.1 BRANCHING RATIO OF THE 0.98 MeV LEVEL IN Mg^{25}

Two adjacent resonances (1 and 2, fig. 2) were observed, one of which showed only a gamma ray of 0.58 MeV with a very weak 0.98 MeV, and the other which showed gamma rays of 0.40, 0.58, and 0.98 MeV. The gamma-ray spectra at the two resonances are shown in fig. 3(a) and fig. 3(b), measured at 90°. Measurements of standard gamma-ray spectra [8]) showed that for a gamma ray of about 1 MeV the spectrum has a flat, low-energy tail 18 % of the

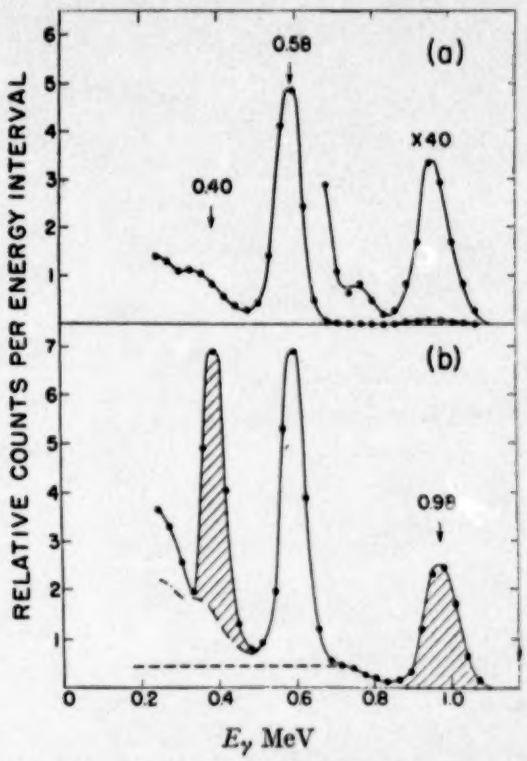

Fig. 3. The gamma ray spectra measured at 90° to the incident proton beam a) at position 2 on the yield curve and b) at position 1 on the yield curve. The areas corresponding to the total absorption peaks for the 0.40 and 0.98 MeV gamma rays are shown shaded. The dotted line indicates the contribution from the low energy portion of the 0.98 MeV gamma ray spectrum and the dot-dash line that for the 0.58 MeV gamma ray.

peak height, and this shape is shown as a dashed line in fig. 3(b). The shape for a 0.58 MeV gamma ray is obtained from fig. 3(a).

In this way, accurate measurements of the area under the total absorption peaks for the 0.98 and 0.40 MeV gamma rays are obtained. These areas are shown shaded in fig. 3(b). When corrected for crystal efficiency [8]), the intensity ratio of 0.98 to 0.40 MeV gamma rays at this resonance is 1.05 ± 0.03, where the error does not include possible errors in the relative efficiency of the crystal for

the two gamma rays concerned. It is difficult to estimate the latter, but it is unlikely to be more than a few percent. The spectrum shown in fig. 3(b) was measured at six angles between 90° and 0° to the incident beam, and the angular distributions of the three gamma rays are shown in fig. 4. The spherical symmetry of the 0.58 MeV radiation is consistent with $J = 1/2$ for the level. Both the 0.4 and 0.98 MeV gamma rays have distributions $P_0+0.1\ P_2$, and hence no correction to the above ratio is required. The ratio of

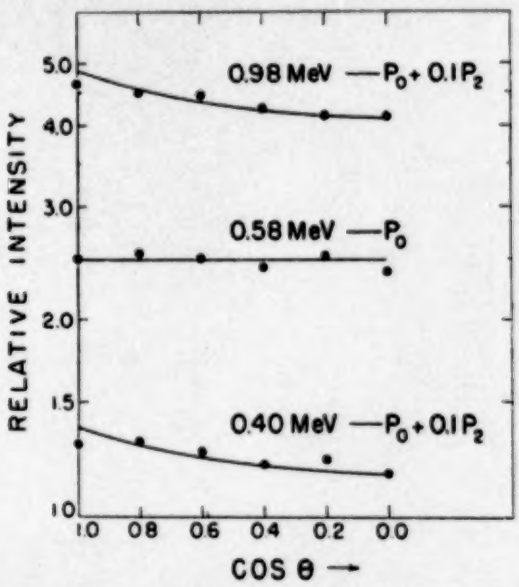

Fig. 4. The angular distributions of the gamma rays measured at position 1 on the yield curve. The solid lines represent Legendre Polynomial fits to the experimental points and their equations are given in each case.

0.98 MeV to 0.40 MeV gamma rays measured by Maeder and Stähelin [5]) from the negaton decay of Na^{25} was 2.27 ± 0.40. The disagreement between these measurements will be discussed later.

3.2 BRANCHING RATIO OF THE 1.61 MeV LEVEL IN Mg^{25}

At a proton energy corresponding to position 3 on the yield curve (fig. 2), the gamma-ray spectrum was measured. This spectrum is shown in fig. 5(a). Gamma rays of energy 0.98, 0.58, and 0.40 MeV were observed, as well as a 1.61 MeV gamma ray. No gamma ray of energy 1.96 MeV was seen, and an upper limit on its intensity can be set at 3 % of that of the 1.61 MeV gamma ray. In addition, the well-known 300 keV gamma ray from coulomb excitation in the tantalum backing was found. If the gamma decay of the level at 1.61 MeV in Mg^{25}, which shows a direct ground state

transition at this energy, cascaded via the levels at 0.98 and 0.58 MeV, primary gamma rays of 0.63 and 1.03 MeV would be emitted. The former would be in coincidence with a gamma ray of 0.58 MeV and the latter with one of 0.98, 0.58, and 0.40 MeV. In order to determine the branching ratio, a voltage window was set on one crystal to include pulses corresponding to the total absorption peak of the 0.58 MeV gamma ray as indicated in fig. 5(a). The spectrum of pulses in coincidence with these was displayed on the 30-channel

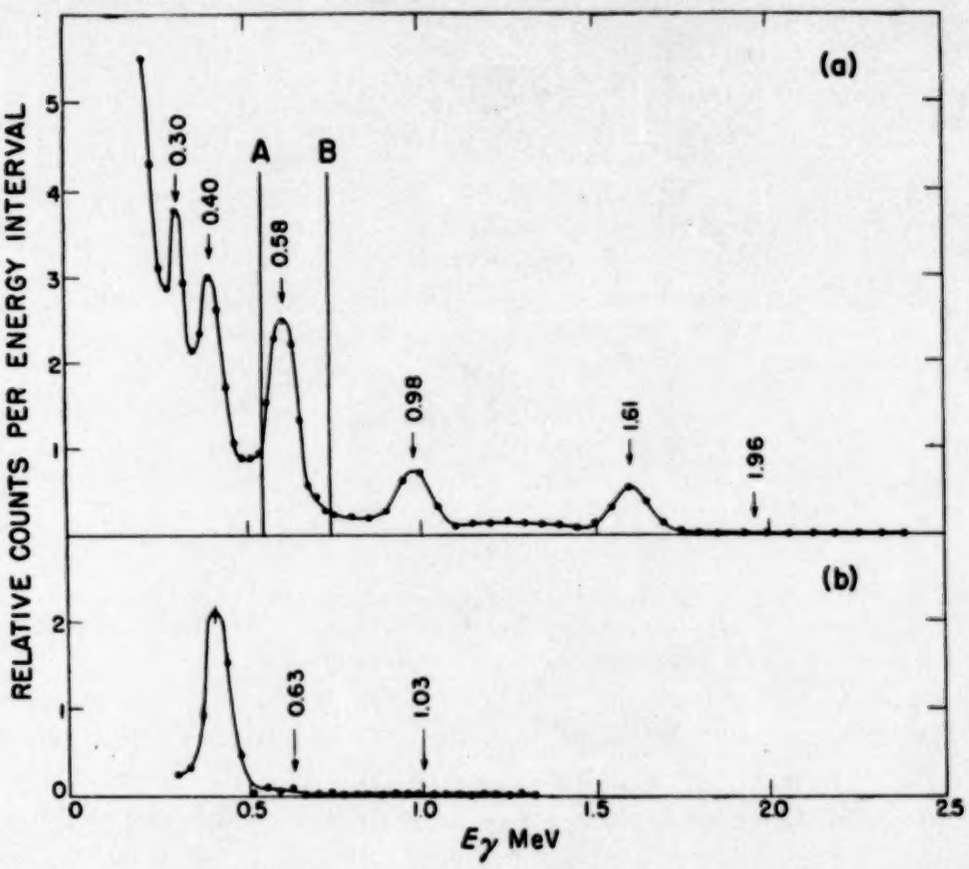

Fig. 5. The gamma ray spectrum measured at 90° to the beam at position 3 on the yield curve is shown in (a). The gamma ray spectrum in coincidence with voltage pulses lying between A and B is shown in (b).

analyser in the manner described previously [8]). and is shown in fig. 5(b). The only gamma ray observed in the coincidence spectrum is that of 0.40 MeV, which arises from direct feeding of the 0.98 MeV level in Mg^{25}. Upper limits on the amount of 0.63 and 1.03 MeV radiation present can be set by comparing the counts observed at positions in the coincidence spectrum corresponding to these energies to that observed for the 0.40 MeV gamma ray, and assuming

that the intensity of 0.40 MeV gamma rays observed in the coincidence spectrum is proportional to that observed in the direct spectrum. This yields the result that the ratio of intensities of 0.63 and 1.03 MeV gamma rays to those of 1.61 MeV is respectively less than 3 % and less than 1 %. Hence the 1.61 MeV level decays directly to the ground state more than 96 % of the time.

3.3 BRANCHING RATIO OF THE 1.96 MeV LEVEL IN Mg^{25}

In order to measure the branching ratio of the 1.96 MeV level it is an advantage to find a proton energy at which the ratio of the yield of 1.96 MeV gamma rays to the yield of 1.61 MeV gamma rays is a maximum. This occurs at the position marked 5 on the yield curve. The direct spectrum measured here at 0° to the beam is shown in fig. 6(b). This is to be compared to a spectrum measured at 4 on the yield curve shown in fig. 6(a). In this case there is practically no 1.96 MeV gamma ray present relative to the 1.61 MeV gamma ray and, in addition, the shape of the spectrum in the region of 1.38 MeV is notably different. Since the shape of a gamma-ray spectrum of around 2.0 MeV is known [8]), the contribution of the 1.96 MeV gamma ray can be subtracted from that of the 1.61 and 1.38 MeV gamma rays. Then the 1.61 MeV gamma ray spectrum can be subtracted by using the spectrum shape obtained from fig. 6(a), and the intensity of 1.38 MeV gamma rays in the spectrum can be determined. Spectra similar to that shown in fig. 6(b) were measured at 14 angles between 0° and 90° to the incident beam. A least square Legendre Polynomial fit gave distributions of the form $P_0+(0.12\pm0.03)P_2$ for the 1.38 MeV gamma ray and $P_0-(0.25\pm0.01)P_2$ for that of 1.61 MeV. The results for the 1.96 MeV gamma ray were only accurate enough to obtain the average intensity. No P_4 term was observed for the distribution of the 1.38 MeV gamma ray. From these measurements the average ratio of the intensity of the 1.38 MeV to the 1.96 MeV gamma ray was found to be 2.04 ± 0.10. In order to ensure that none of the 1.38 MeV gamma ray observed in the spectrum arose from the reaction $Mg^{24}(pp'\gamma)$ [$Q = -1.368$ MeV] a target of the same thickness of Mg^{24} was measured at the same proton energy. Correcting the intensity of the 1.37 MeV gamma ray so observed for the few percent of Mg^{24} in the Mg^{25} target showed that such a contribution was negligible.

In fig. 6(c) is shown a coincidence spectrum with the gate of one

counter set to include the total absorption peak of the 0.58 MeV gamma ray. It shows gamma rays of energy 0.40, 0.58, 0.98, and 1.38 MeV.

This was measured with one counter set at 0° and the other at

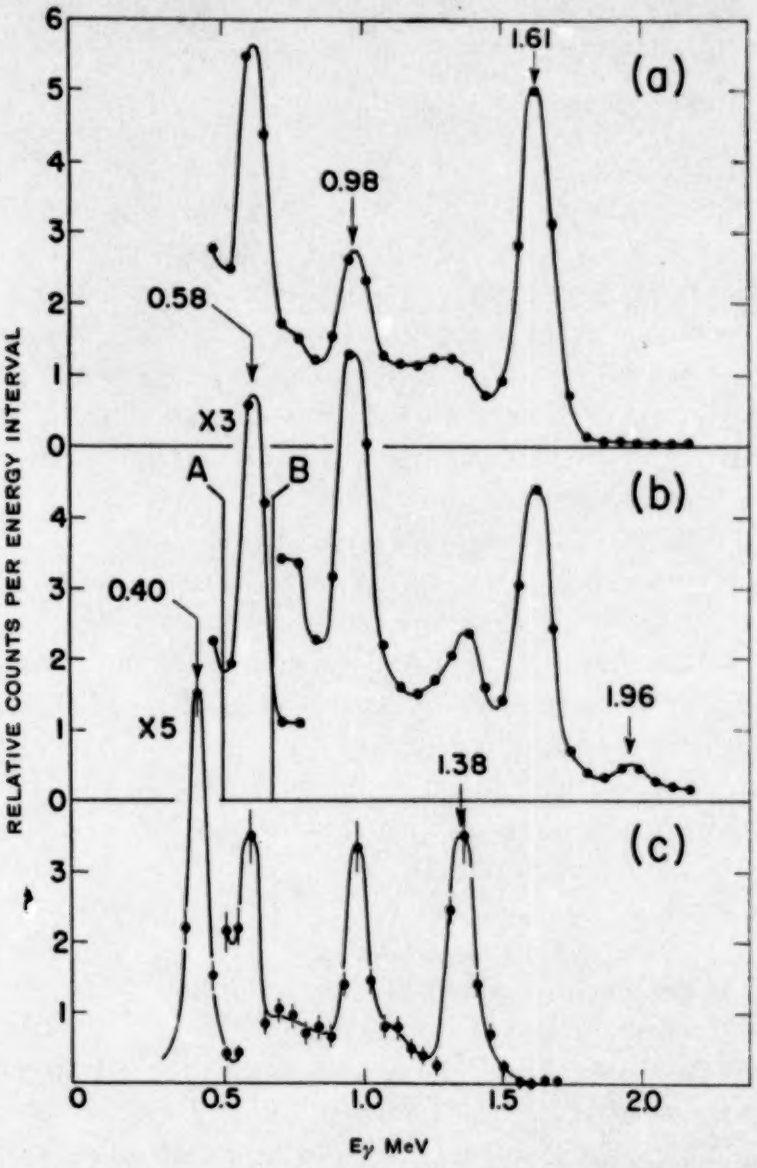

Fig. 6. The gamma ray spectrum measured at 0° to the beam (a) at position 4 on the yield curve, (b) at position 5 on the yield curve. The spectrum of gamma rays at position 5 in coincidence with voltage pulses lying between A and B in (b) is shown in (c).

90° to the beam, so that the two counters were shielded from each other, in order that coincidences, due to annihilation radiation from pair production in one crystal passing into the other, could

be eliminated. The intensity ratio of 1.38 MeV radiation to 0.98 MeV radiation from the 1.96 MeV level has been calculated from this coincidence spectrum assuming spherical symmetry for the angular distribution of the coincidence spectrum. In this calculation it is necessary to take into account that some of the 0.98 MeV gamma rays appearing in the direct spectrum arise from decay of the 0.98 level and some from decay of the 1.96 MeV level and, further, that the gate shown also includes low energy tails from the 0.98 and 1.38 MeV gamma rays. When this is done the ratio of the 1.38 to 0.98 MeV gamma rays from the 1.96 MeV level is 2.0 ± 0.4. From this and the previous ratio, the branching of the 1.96 MeV level is 25 ± 5 % to the 0.98 level, 50 ± 3 % to the 0.58 level, and 25 % to ground. The quoted errors are chiefly statistical and do not take into account any possible angular correlations.

3.4 GAMMA RAYS FROM THE NEGATON DECAY OF Na^{25}

The spectrum of gamma rays following the negaton decay of Na^{25} has been measured using the geometry illustrated in fig. 1,

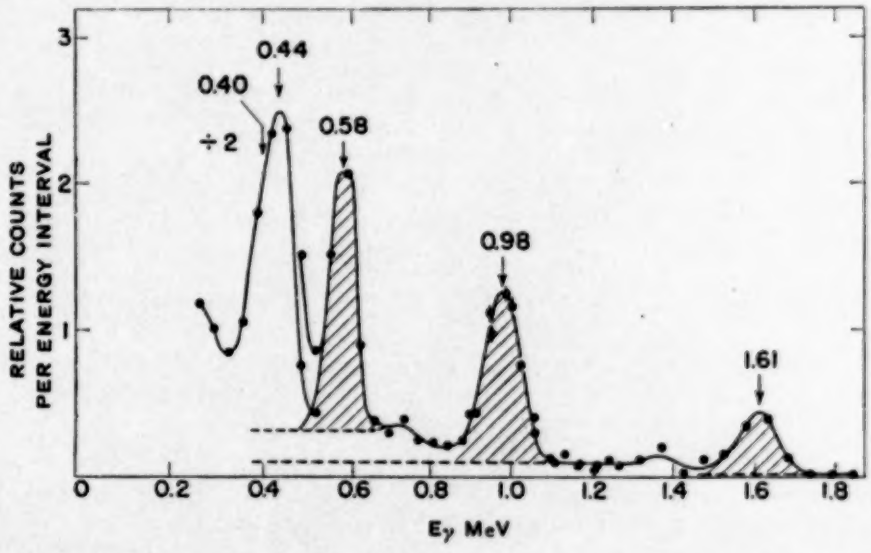

Fig. 7. The gamma ray spectrum following the negaton decay of Na^{25}. The areas corresponding to the total absorption peaks for the 0.58, 0.98, and 1.61 MeV gamma rays are shown shaded. The dotted lines show the contributions of higher energy gamma rays under lower energy ones. The 0.44 gamma ray arises from the negaton decay of Ne^{23} which is produced at the same time as the Na^{25}.

and is shown in fig. 7. This represents the results of measurements of the spectrum taken about a minute after bombardment and then about four minutes later after the activity due to Na^{25} and

Ne^{23} was negligible compared to that from Na^{24}. By subtracting these, the contribution from Na^{24} is essentially eliminated. The 0.44 MeV gamma ray from the negaton decay of Ne^{23} made it impossible to measure the 0.40 MeV intensity in this spectrum with any degree of accuracy. This negaton decay of Ne^{23} also gives rise to a gamma ray of energy 1.63 MeV whose intensity is 4 % of that for the 0.44 MeV gamma ray [9]). This must be subtracted from the peak at 1.61 MeV from the negaton decay of Na^{25}. In addition, a spectrum measurement was made with lower amplifier gain to examine the region around 1.96 MeV. In this measurement the source was placed considerably closer to the target. The relative intensities of the various gamma rays are listed in table I. The value listed for the 0.40 MeV gamma ray is obtained from that

TABLE I

Relative intensity of gamma rays from the negaton decay of Na^{25}.

Gamma-Ray Energy MeV	Relative Intensity
0.40	1181 ± 50
0.58	1108 ± 53
0.98	1241 ± 38
1.61	407 ± 34
1.96	< 30

The value for the 0.40 MeV gamma ray was obtained from that for the 0.98 MeV by using the ratio of intensities of 0.98 to 0.40 of 1.05 ± 0.03 obtained from the $Mg^{25}(pp'\gamma)Mg^{25}$ results.

TABLE II

Relative intensities of negaton transitions to the excited states of Mg^{25}.

Negaton transitions to level in Mg^{25} at	Relative intensity of negaton transitions	Present work		% branching ratio (ref. [5]))
		% branching ratio	log ft	
1.96	< 110	< 1	> 5.9	
1.61	407 ± 34	5	5.6	6.5
0.98	2422 ± 63	30	5.2	25
0.58	-73 ± 76	< 1	> 6.9	≈ 3.5
0		65	5.3	65

To compare the present results with those of ref. [5]), the value of 65 % for the transitions to the ground state given in ref. [5]) has been assumed in the third and fourth columns. The fifth column shows the results of ref. [5]) for comparison.

for the 0.98 MeV gamma rays using the ratio of intensity of the gamma rays of 0.98 to 0.40 MeV measured from the $Mg^{25}(pp'\gamma)Mg^{25}$ reaction. From these values the relative intensities of the negaton transitions to the 0.58, 0.98, 1.61, and 1.96 MeV levels in Mg^{25} can be readily obtained. In the case of the transition to the 1.96 MeV level, the branching ratio for gamma decay of this level measured in the $Mg^{25}(pp'\gamma)$ reaction was used. Table II lists the relative intensities of the various negaton transitions and the percent branching, assuming 65 % of the transitions [5]) go to the ground state of Mg^{25}. Log *ft* values are also listed. The negaton and

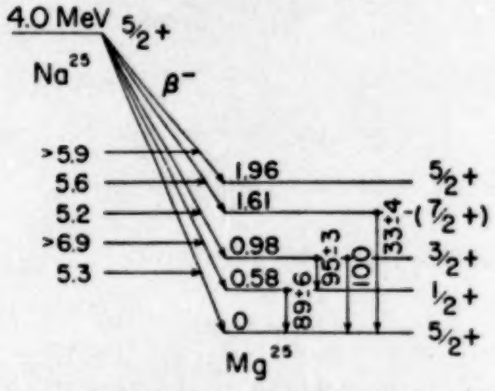

Fig. 8. An energy level diagram illustrating the negaton decay of Na^{25} and the subsequent gamma decay of levels in Mg^{25}. Log_{10} *ft* values are given for each negaton branch and the relative intensities of the gamma rays are also shown.

gamma ray data is summarized in fig. 8. The results obtained by Maeder and Stähelin are shown in the last column in table II for comparison. The main discrepancy between the two results occurs for the negaton transition to the 0.58 MeV level. The results described here are quite compatible with this negaton intensity being zero, while those of Maeder and Stähelin indicate that it is at least greater than one percent.

It was mentioned previously that the gamma-ray branching ratio of the 0.98 MeV state obtained by Maeder and Stähelin was considerably different from that obtained in the $Mg^{25}(pp'\gamma)$ reaction. Table III compares the intensity of the 0.40, 0.58, and 1.61 MeV gamma rays relative to that for the 0.98 MeV gamma ray in the negaton decay of Na^{25} and the $Mg^{25}(pp'\gamma)$ reaction as measured in this work with the values obtained by Maeder and Stähelin. The agreement improves as the gamma-ray energy increases. A possible explanation lies in the difference in the size of NaI crystals used. Maeder and Stähelin used a crystal 3.5 cm in

diameter by 2.5 cm long and employed a rather complicated spectrum analysis to obtain the total number of pulses corresponding to each gamma ray. In the case of a 5 in. diameter by 4 in. long crystal, more of the pulses appear in the total absorption peak, and

TABLE III

Intensity of gamma rays relative to that for the 0.98 MeV gamma ray in the negaton decay of Na^{25} compared to those obtained in ref. [5]).

Gamma ray energy MeV	Intensity relative to that for the 0.98 MeV gamma ray	
	Present work	Maeder and Stähelin [5])
0.40	0.952±.027	0.44±.07
0.58	0.893±.056	0.59±.11
1.61	0.328±.040	0.40±.10

The present value for the 0.40 MeV gamma ray was measured in the $Mg^{25}(pp'\gamma)$ reaction.

spectrum analysis is simpler. This is particularly true for the 0.40 MeV to 0.98 MeV ratio where, in the present work, the spectrum involved only three gamma rays, 0.40, 0.58, and 0.98, and the shape of the 0.58 was known with considerable accuracy. In view of this it is not surprising that the percent negaton branching to the 0.58 level should differ. Considerably greater accuracy than obtained in the present work is required to establish what this branching ratio is.

4. Conclusions

The energy level diagrams for the first four excited states in the mirror nuclei Mg^{25} and Al^{25} with the measured gamma-ray branching ratios are shown in fig. 9. The ground state and the excited states in Al^{25} at 0.45, 0.95, and 1.81 MeV are known [8]) to be 5/2+, 1/2+, 3/2+, and 5/2+ respectively. Comparing the branching ratios and level positions with those in Mg^{25} confirms that the ground state and 0.58 level of Mg^{25} have $J = 5/2+$ and 1/2+ respectively, and indicates $J = 3/2+$ and 5/2+ for the levels at 0.98 and 1.96 MeV respectively. It also indicates a correspondence between the states at 1.61 MeV in the two nuclei. The negaton decay of Na^{25} then goes to levels of spin 5/2+ and 3/2+ in Mg^{25} with log ft values of about 5.3. Hence the spin of Na^{25} is either 3/2+ or 5/2+ and, since the

log *ft* value for the transition to the level in Mg^{25} at 1.61 MeV is 5.4, this level has $J \leqq 7/2$ with positive parity. The angular distribution[3]) of the proton group corresponding to the 1.61 MeV state in Mg^{25} from the Mg^{24}(d, p)Mg^{25} reaction shows no stripping pattern, and hence the 1.61 MeV state may have $J \geqq 7/2$ (and if $J = 7/2$, the parity is probably even). The absence of a stripping pattern, however, need not always imply a high orbital angular momentum of the added particle; for example, the Si^{28}(d, p)Si^{29*}

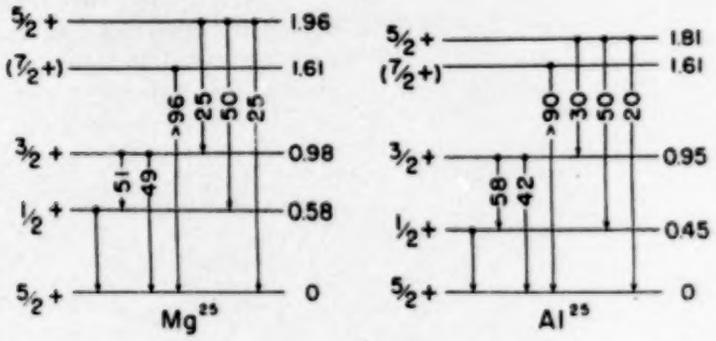

Fig. 9. A comparison between the energies and gamma ray branching ratios of low lying levels in Mg^{25} and Al^{25}.

reaction shows no stripping pattern for the proton group corresponding to the 2.43 MeV level in Si^{29}, which has [2]) $J = 3/2+$. However, to the extent that it may imply a high spin, one concludes that the 1.61 MeV level in Mg^{25} has $J = 7/2+$. There is indirect evidence [8]) that the mirror state at 1.61 MeV in Al^{25} is also $7/2+$. These conclusions about the 1.61 MeV state, coupled with the evidence that the negaton branching to the $1/2+$ state in Mg^{25} at 0.58 MeV is less than 1 %, makes it more attractive to assume that the ground state of Na^{25} is $5/2+$rather than $3/2+$ as suggested by Maeder and Stähelin [5]).

Applying the collective model interpretation used [8]) for Al^{25} to Mg^{25}, the rotational series 0.58 (1/2+), 0.98 (3/2+), and 1.96 (5/2+) would have $K = 1/2$, $3\hbar^2/I = 1.01$ MeV, and $a = -0.2$, where the various parameters are defined by Bohr and Mottelson [10]). This assumes the same rotational-vibrational interaction as used for Al^{25}.

We wish to thank Dr. G. T. Ewan for his helpful comments on this work.

References

1) Hausman, Allen, Arthur, Bender, and McDole, Phys. Rev. **88** (1952) 1296
2) P. M. Endt and J. C. Kluyver, Revs. Modern Phys. **26** (1954) 95; also L. M. Khromchenko, Doklady Akad. Nauk. S.S.S.R. **93** (1953) 451
3) J. R. Holt and T. N. Marsham, Proc. Phys. Soc. A **66** (1953) 258
4) J. E. Mack, Rev. Modern Phys. **22** (1950) 64
5) D. Maeder and P. Stähelin, Helv. Phys. Acta, **28** (1955) 193; also M. E. Nahmias and T. Yuasa, Compt. rend. **239** (1954) 47 and ref. [2]).
6) J. E. Iwersen and W. S. Koski, Phys. Rev. **98** (1955) 1307
7) B. B. Kinsey and G. A. Bartholomew, Phys. Rev. **93** (1954) 1260; P. J. Campion and G. A. Bartholomew, Bull. Am. Phys. Soc. **1** (1956) 28
8) Litherland, Paul, Bartholomew, and Gove, Phys. Rev. **102** (1956) 208
9) J. R. Penning and F. H. Schmidt, Bull. Am. Phys. Soc. **30** (1955) 8
10) A. Bohr and B. R. Mottelson in Beta- and Gamma-Ray Spectroscopy, edited by K. Siegbahn (North-Holland Publishing Co. Amsterdam, 1955) Chapter XVII

Nuclear Physics **2** (1956/57) 147—159; *North-Holland Publishing Co., Amsterdam*

EFFECT OF DISTRIBUTION OF NUCLEAR CHARGE ON ANGULAR CORRELATION IN BETA-DECAY

A. Z. DOLGINOV and I. N. TOPTIGIN

Physico-Technical Institute of the Academy of Sciences, Leningrad

Received 24 May 1956

Abstract: The β—ν and β—γ angular correlation has been computed with consideration of finite electron wavelength for the cases of uniform volume and surface nuclear charge distributions. The calculations were carried out for linear combinations of various forms of beta decay interactions. It is shown that for transitions of first degree of forbiddenness the calculations yield results which perceptibly differ from those of existing approximate calculations. In some cases the difference was as high as 50 %. The problem of choosing a nucleus which is most suitable for β—γ angular correlation studies is discussed. A comparison of the theory with experiment is made for the Tm^{170} nucleus.

1. Introduction

Although an enormous amount of data on β-spectra has been accumulated it has not been possible to uniquely determine the form of the β-interaction. The reason for this is that the form of allowed β-spectra does not depend on the type of theory, whereas the interpretation of forbidden spectra is a difficult problem. The type of β-interaction can be determined by studying the angular distribution of recoil nuclei (β—ν correlation). In this case the angular distribution is anisotropic for allowed transitions and depends on the form of the β-interaction. An investigation of β—ν correlation [1, 2]) showed that β-interaction is a linear combination of tensor and apparently scalar theories. Such experiments, however, cannot yield information on the relative sign of the scalar S and tensor T interaction as only the squares of the matrix elements enter the formulae. Pseudoscalar interaction P does not contribute to the allowed transitions.

For allowed transitions there is no angular correlation between the β-particle and subsequent γ-quantum. For first forbidden transitions the correlation is sensitive to the form of the theory and thus one can completely determine the nature of the β-interaction. However, inasmuch as several unknown matrix elements must be determined from the experiments the accuracy of the experiments must be especially high.

$\beta-\gamma$ angular correlation theory has been developed in a number of papers [3, 4, 5, 6, 7]). In ref. [7]) $\beta-\gamma$ angular correlation formulae were obtained for a linear combination of different variants of theory but it was assumed that the wave function of the β-particle inside the nucleus equalled its value on the nuclear surface. This assumption leads to appreciable errors. Thus, for example, our formulae, which do not involve an assumption of this type yield for the Tm^{170} nucleus an angular correlation which differs from the result presented in ref. [8, 9]) by as much as 50 %.

For $r \to 0$ the relativistic wave function of a β-particle in the field of a point charge tends to ∞. On the nuclear boundary its value appreciably differs from the true value which can be determined more precisely, by fitting the internal solution for an electron in the field of a distributed positive charge on to the external solution. In this case the wave function inside the nucleus approaches 0 and not ∞ for $r \to 0$.

Explicit expressions for $\beta-\nu$ [10]) and $\beta-\gamma$ [5]) angular correlations, taking into account the finite wavelength of the electron have been obtained by one of the authors for various types of theory.

Since the experimental data can be interpreted only by assuming a linear combination of different types of interaction we have correspondingly generalized in the present paper the results obtained in ref. [5, 10]).

Two extreme cases are considered: that of a charge uniformly distributed over the nuclear volume and that of a uniform surface charge. It is found that the $\beta-\gamma$ angular correlation in these two cases may differ by 20 % of the total effect. The angular correlation depends on the accepted nuclear radius and an uncertainty in the radius may mask the true charge distribution.

The assumption that the electron wave function is constant inside the nucleus also leads to errors on calculation of the form of the β-spectrum. This was first noted by L. A. Sliv [11]) who carried out the calculations for various forms of the theory assuming a volume or surface distribution of the nuclear charge. This problem was subsequently considered by other authors [12, 13, 14]).

2. Angular Correlation Formulae for Beta-Decay

The $\beta-\nu$ and $\beta-\gamma$ angular correlation is computed by the method used in ref. [5, 10]). Outside the nucleus we take the expression given

in ref. [15]) for the relativistic wave function of an electron in a point charge Coulomb field possessing a definite momentum at infinity:

$$\psi_{\mathbf{p}\nu} = \sum_{j\mu\lambda} i^{j-\lambda+2\nu} C^{j\mu}_{lm\frac{1}{2}\nu} Y^*_{lm}(\vartheta_p, \varphi_p) \psi_{j\mu\lambda} e^{-i\delta_{j\lambda}} \tag{1}$$

$$\delta_{j\lambda} = \eta_{j\lambda} - \arg \Gamma(\gamma_j + i\alpha ZE/p) - \frac{\pi}{2}(\gamma_j - j + \lambda) \tag{2}$$

$$\exp[2i\eta_{l\lambda}] = [i\alpha Z/p - 2\lambda(j+\tfrac{1}{2})]/(\gamma_j + i\alpha ZE/p) \tag{3}$$

$$\gamma_j = \pm[(j+\tfrac{1}{2})^2 - (\alpha Z)^2]^{\frac{1}{2}}, \ \hbar = c = m = 1.$$

Here E and p are respectively the electron energy and momentum, q the neutrino momentum, $\psi_{j\mu\lambda}$ is a bispinor wave function [16]) with definite total j and orbital $l = j+\lambda$ angular momentum values.

We designate by $F^{\pm}_{j\lambda}$ and $G^{\pm}_{j\lambda}$ the radial parts of $\psi_{j\mu\lambda}$ corresponding to the two possible signs of γ_j. Inside the nucleus solutions with negative γ_j do not satisfy the boundary conditions at the coordinate origin. The radial parts of the internal wave function will be designated as $f_{j\lambda}$ and $g_{j\lambda}$. The expressions for $f_{j\lambda}$ and $g_{j\lambda}$ depend on whether the nuclear charge is distributed over a surface or throughout the volume. The fitting factors for the external and internal solutions enter the angular correlation formulae. We denote them by $A_{j\lambda}$ and we may write [11])

$$A_{j\lambda} = N_{j\lambda}(F^-_{j\lambda}G^+_{j\lambda} - F^+_{j\lambda}G^-_{j\lambda})/(F^-_{j\lambda}g_{j\lambda} - G^-_{j\lambda}f_{j\lambda}) \tag{4}$$

$$N_{j\lambda} = [1 - 2C_{j\lambda}\cos(\delta^+_{j\lambda} - \delta^-_{j\lambda}) + C^2_{j\lambda}]^{-\frac{1}{2}} \tag{5}$$

$$C_{j\lambda} = (f_{j\lambda}G^+_{j\lambda} - g_{j\lambda}F^+_{j\lambda})/(f_{j\lambda}G^-_{j\lambda} - g_{j\lambda}F^-_{j\lambda}). \tag{6}$$

Here $\delta^{\pm}_{j\lambda}$ are the phases in formula (2) corresponding to the two signs of γ_j. The values of $F^{\pm}_{j\lambda}$, $G^{\pm}_{j\lambda}$, $f_{j\lambda}$ and $g_{j\lambda}$ in (4) should be those at the nuclear boundary. The phases $\delta^+_{j\lambda}$ and $\delta^-_{j\lambda}$ do not enter the angular correlation formulae separately but instead a quantity $\Delta_{j\lambda}$ is involved, which is defined by

$$\operatorname{tg} \Delta_{j\lambda} = (\sin\delta^+_{j\lambda} - C_{j\lambda}\sin\delta^-_{j\lambda})/(\cos\delta^+_{j\lambda} - C_{j\lambda}\cos\delta^-_{j\lambda}). \tag{7}$$

The angular correlation between the β-particle and neutrino for transitions of first order of forbiddenness has the form

$$W(\vartheta) = \sum_{n=0}^{2} \sum_{i\le k} [\mathrm{Re}(M_i M^*_k)] C^{(n)}_{ik} P_n(\cos\vartheta) \tag{8}$$

where Re denotes the real part and M_i and M_k are β transition matrix elements the explicit form of which is presented in Appendix I. The condition of invariance with respect to reversal of

time has already been utilized in (8) and the phase shifts have been chosen to satisfy this condition. The quantities $C_{ik}^{(n)}$ are functions of the nuclear charge and of the β-particle energy and depend on the form of the theory. Their explicit expressions are given in Appendix II. The coefficients $C_{ik}^{(n)}$ were computed for linear combinations of (STP) and (VT). Since the experimental data are not consistent with the assumption of an axial vector interaction V the latter is not considered here.

For $Z = 0$ our formulae transform into the Born approximation formulae; for $Z > A^{1/3} E_{\text{MeV}}$ (where E_{MeV} is the total electron energy expressed in MeV) both types of formulae are significantly different.

Thus, for pure scalar theory and $Z = 0$ one obtains

$$W(\vartheta) = (p^2+q^2+2pq\cos\vartheta)[1-(P/E)\cos\vartheta]$$

and for $Z \gg A^{1/3}E_{\text{MeV}}$

$$W(\vartheta) \approx 1+(P/3E)\cos\vartheta. \tag{9}$$

For vector theory and $Z \gg A^{1/3}\ E_{\text{MeV}}$ one obtains
A similar result is obtained in other variants of β-decay theory.

$$W(\vartheta) \approx 1-(P/3E)\cos\vartheta.$$

It was demonstrated in ref. [10]) that even if the finite electron wave length (in the field of a spherical nucleus) is taken into account the form of the $\beta-\nu$ angular correlation for allowed transitions will not be dependent on Z.

For transitions of first order of forbiddenness the expression for the $\beta-\gamma$ angular correlation can be written as follows:

$$W(\vartheta) = \sum_{n=0,2} \sum_{J\leq J'} \sum_{i\leq k} [\mathrm{Re}(M_i M_k^*)]\, U_{JJ'}^n C_{ik}^{nJJ'} B_n P_n(\cos\vartheta) \tag{10}$$

$$U_{JJ'}^n \equiv U(Jj_1nj_2;\ j_2J') = [(2j_2+1)(2J'+1)]^{\frac{1}{2}} W(Jj_1nj_2;\ j_2J') \tag{11}$$

where $W(Jj_1nj_2;\ j_2J')$ is the Racah function. The quantities $C_{ik}^{nJJ'}$ for the (STP) and (VT) forms of the theory are presented in Appendix III. $j_1 \xrightarrow{\beta} j_2 \xrightarrow{\gamma} j_3$ are the angular momenta of the three nuclear levels involved in the transitions. B_n refers to a γ-transition and for a γ-quantum of multipole order 2^L it has the form

$$B_n = \left[1-\frac{n(n+1)}{2L(L+1)}\right] U(Lj_3nj_2;\ j_2L)\, C_{L0n0}^{L0}. \tag{12}$$

In the case of mixed magnetic radiation of multipole order 2^L and electric radiation of multipole order 2^{L+1} one finds

$$B_n = B_n^{(L)} + |a|^2 B_n^{(L+1)} \pm .$$
$$\pm 2a \sqrt{\frac{2L+3}{L+2}} U(L1nL;\ LL+1) U(j_2 j_3 nL+1;\ Lj_2) C^{L0}_{L0n0} \qquad (13)$$

where $B_n^{(L)}$ is identical with (12) and $B_n^{(L+1)}$ differs from $B_n^{(L)}$ by replacement of L by $L+1$; $|a|^2$ is the ratio between the intensities of the electric and magnetic radiations and $a = \pm|a|$ since the phase shift between the matrix elements for the electric and magnetic transitions is either 0 or π.

If correlation between a β-particle and conversion electron is being studied then together with B_n an auxiliary factor which was presented for example in ref. [17]) (see also ref. [18])) must be introduced in (10).

If the observed gamma quantum is not promptly emitted after beta decay but is preceded in the common cascade by one or several quanta whose direction is not determined by the experiment, a factor Q_n should be introduced in expression (10) which is equal to[19])

$$Q_n = \prod_{k=3}^{N-1} U(j_k L_k n j_{k-1};\ j_{k-1} j_k) \qquad (14)$$

where the transition $j_{N-1} \to j_N$ is accompanied by emission of the observed gamma quantum; the L_k are the multipole orders of the γ-quanta emitted on transition of the nucleus from a state with angular momentum j_{k-1} to a state with angular momentum j_k. If mixed radiation is emitted in intermediate transitions the intensities add up since the interference terms drop out.

In order to illustrate the importance of correctly taking into account the behaviour of the electron wave function within the nucleus consider the $\beta-\gamma$ angular correlation for $Z = 71$ and $A = 170$. The interaction between the electron and Coulomb field is independent of the magnitude of the nuclear matrix elements. Therefore, in order to estimate the magnitude of the effect it will suffice to consider the angular correlation for one of the matrix elements. Writing $W(\vartheta) = \text{const.}\,[1+f(E)P_2(\cos\vartheta)]$ and omitting in $W(\vartheta)$ all terms except those which refer to the matrix element M_3, one obtains for $f(E)$ the curves shown in fig. 1. Curves (2) and (4) refer to the case of uniform volume distribution of charge for nuclear radii $R = 1.2\times10^{-13}\,A^{1/3}$cm and $R = 1.5\times10^{-13}\,A^{1/3}$ cm and curve (3) to the case of a surface charge with $R = 1.2\times10^{-13}\,A^{1/3}$ cm. Our curves differ by $\approx 50\,\%$ from curve (1) plotted on the

basis of the formulae obtained in ref. [6]) in which it was assumed that the electron wave function is constant within the nucleus. For non-spherical nuclei the electron orbital angular momentum is not an integral of motion. However, the β-particle wave length greatly exceeds the nuclear dimensions and therefore the contribution from states with values of l larger than those already considered in the formulae are vanishingly small. The influence of non-sphericity may be different for states with $l = 0$ and $l = 1$ and this may affect the angular distribution. However, the main part of this effect may be taken into account by slightly modifying the effective nuclear radius.

If one retains in formula (8) only the term with $n = 0$ and multiplies it by $g^2\varkappa(2j_2+1)/108\pi^3(2j_1+1)$ (the values of $\varkappa$ for volume and surface distribution of charge are given in Appendix II), then one obtains beta spectrum expressions for (STP) or (VT) interaction.

APPENDIX I

Matrix elements $M_i = \int \psi^*_{j_2 m_2} \tau O_i \psi_{j_1 m_1} \mathrm{d}\mathbf{r}$,

$$O_1 = g_S C_1 r \beta Y_{1M} \qquad O_2 = g_T C_0 r \beta \boldsymbol{\sigma} \mathbf{Y}^1_{00}$$
$$O_3 = g_T C_1 r\ \beta \boldsymbol{\sigma} \mathbf{Y}^0_{1M} \qquad O_4 = g_T C_2 r \beta \boldsymbol{\sigma} \mathbf{Y}^{-1}_{2M}$$
$$O_5 = i g_T C_1 \beta \boldsymbol{\alpha} \mathbf{Y}^{-1}_{1M} \qquad O_6 = g_V C_1 r Y_{1M}$$
$$O_7 = i g_V C_1 \boldsymbol{\alpha} \mathbf{Y}^{-1}_{1M} \qquad O_8 = -i g_P C_0 \beta \gamma_5 Y_{00}\,.$$

$\psi_{j_1 m_1}$ and $\psi_{j_2 m_2}$ are the wave-functions for the initial and final nuclear states; τ is an operator acting on the isobaric spin variables, the g's are the beta interaction constants, β, γ_s, $\boldsymbol{\sigma}$ and $\boldsymbol{\alpha}$ are Dirac matrices, $\mathbf{Y}^{\lambda}_{JM}$ is a spherical vector [15]):

$$\boldsymbol{\sigma}\mathbf{Y}^1_{JM} = -\sum_{\nu=-1}^{1} C^{JM}_{J+\lambda\, M+\nu\, 1-\nu} \sigma_{-\nu} Y_{j+\lambda\, M+\nu}(\vartheta, \varphi), \tag{15}$$
$$C_J \equiv [C^{j_2 m_2}_{J M j_1 m_1}]^{-1}, \qquad \sigma_0 = \sigma_z, \qquad \sigma_{\pm 1} = \pm 2^{-\frac{1}{2}}(\sigma_x \pm i\sigma_y);$$

$C^{jm}_{j_1 m_1 j_2 m_2}$ are Clebsch-Gordan coefficients.

APPENDIX II

$$C^{(0)}_{11}(q) = C^{(0)}_{66}(-q) = 3a_1^+ q^2 - 2a_2^+ q + 2a_4^+ + a_5^+$$
$$C^{(0)}_{22} = 3(a_1^+ q^2 - 2a_2^+ q + a_5^+); \qquad C^{(0)}_{33} = 3a_1^+ q^2 + 4a_2^+ q + a_4^+ + 2a_5^+$$
$$C^{(0)}_{44} = 3(a_1^+ q^2 + a_4^+); \qquad C^{(0)}_{55} = C^{(0)}_{77} = C^{(0)}_{88} = 27a_1^+; \qquad C^{(0)}_{13} = 2\sqrt{2}(a_4^+ - a_5^+)$$
$$\sqrt{2}\, C^{(0)}_{28}(q) = \sqrt{6}\, C^{(0)}_{15}(q) = \sqrt{6}\, C^{(0)}_{67}(-q) = -\sqrt{3}\, C^{(0)}_{35}(-q) = -18\sqrt{2}(a_1^+ q - a_2^+)$$
$$C^{(0)}_{57} = -54a_1^-; \qquad C^{(0)}_{37} = -\sqrt{2}\, C^{(0)}_{56} = 6\sqrt{6}(a_1^- q + a_2^-)$$

$$C_{36}^{(0)} = 2\sqrt{2}(2a_2^- q + a_4^- + a_5^-)$$
$$3C_{11}^{(1)}(q) = -3C_{66}^{(1)}(-q) = -18a_7q^2 + 12(a_8^+ + a_9^+)q + 2a_{10} - 8a_{11}^+ - 4a_{12}$$
$$C_{22}^{(1)} = -6(a_7q^2 - 2a_8^+ q + a_{10}); \qquad 5C_{14}^{(1)} = 6a_7q^2 + 30a_9^+ q + 6a_{12}$$
$$3C_{33}^{(1)} = 18a_7q^2 + 6(a_9^+ + 4a_8^+)q + 4a_{10} + 8a_{11}^+ - 2a_{12}$$
$$3C_{55}^{(1)} = -3C_{77}^{(1)} = -C_{88}^{(1)} = 54a_7; \qquad C_{35}^{(1)} = -4\sqrt{6}(3a_7q + a_8^+ + a_9^+)$$
$$3C_{13}^{(1)} = 4\sqrt{2}(3a_9^+ q - 6a_8^+ q + a_{11}^+ - a_{10} - a_{12})$$
$$C_{15}^{(1)}(q) = -C_{67}^{(1)}(-q) = 4\sqrt{3}(3a_7q + a_8^+ - 2a_9^+)$$
$$C_{36}^{(1)} = 4\sqrt{2}(2a_8^- q + a_9^- q + a_{11}^-); \qquad C_{56}^{(1} = -4\sqrt{3}(a_8^- + 2a_9^-)$$
$$C_{37}^{(1)} = 4\sqrt{6}(a_9^- - a_8^-); \qquad C_{28}^{(1)} = 36(a_7q - a_8^+)$$
$$3C_{11}^{(2)} = -6C_{33}^{(2)} = -10C_{44}^{(2)} = -3C_{66}^{(2)} = -12a_3^+ q; \qquad C_{36}^{(2)} = -4\sqrt{2}\,a_3^- q.$$

The remaining $C_{ik}^{(n)}$ are zero. Here and in the following $C_{ik}^{(n)}(-q)$ signifies that in the corresponding expression q is replaced by $-q$.

For a uniform volume distribution of charge the $a_i^{\pm}$ are

$$a_1^{\pm} = \varphi_0[(\varepsilon-1)\beta_1 \pm (\varepsilon+1)\beta_2]; \qquad \varphi_0 = 1 - 11(\varkappa R)^2/75$$
$$a_2^{\pm} = \varphi_4(\beta_1 \pm \beta_2)\varkappa^2 - (3\alpha Z/10R)[(\varepsilon-1)\beta_1 \pm (\varepsilon+1)\beta_2]; \qquad \varphi_4 = 1 - 7(\varkappa R)^2/75$$
$$a_3^{\pm} = \varphi_5(\beta_7 \pm \beta_8)\varkappa^2; \qquad \varphi_5 = 1 - 4(\varkappa R)^2/35$$
$$a_4^{\pm} = \varphi_2[(\varepsilon-1)\beta_3 \pm (\varepsilon+1)\beta_4]\varkappa^2; \qquad \varphi_2 = 1 - 3(\varkappa R)^2/35$$
$$a_5^{\pm} = \varphi_1[(\varepsilon+1)\beta_1 \pm (\varepsilon-1)\beta_2]\varkappa^2 - (3\alpha Z/5R)(\beta_1 \pm \beta_2)\varkappa^2$$
$$+ (3\alpha Z/10R)^2[(\varepsilon-1)\beta_1 \pm (\varepsilon+1)\beta_2]; \qquad \varphi_1 = 1 - 2(\varkappa R)^2/35$$
$$a_6^{\pm} = \varphi_3[(\varepsilon+1)\beta_7 \pm (\varepsilon-1)\beta_8]\varkappa^2 - (3\alpha Z/10R)(\beta_7 \pm \beta_8)\varkappa^2$$
$$a_7 = \varphi_0\beta_5\varkappa; \qquad \varphi_3 = 1 - 12(\varkappa R)^2/175$$
$$a_8 = \varphi_4\beta_5\varepsilon\varkappa - (3\alpha Z/10R)\beta_5\varkappa; \quad a_8^- = \varphi_4\beta_5\varkappa$$
$$a_9^{\pm} = \varphi_5[(\varepsilon-1)\beta_6 \pm (\varepsilon+1)\beta_9]\varkappa$$
$$a_{10} = \varphi_1\beta_5\varkappa^3 - (3\alpha Z/5R)\beta_5\varepsilon\varkappa + (3\alpha Z/10R)^2\beta_5\varkappa$$
$$a_{11}^{\pm} = \varphi_3(\beta_6 \pm \beta_9)\varkappa^3 - (3\alpha Z/10R)[(\varepsilon-1)\beta_6 \pm (\varepsilon+1)\beta_9]\varkappa$$
$$a_{12} = \varphi_2\beta_{10}\varkappa^3$$
$$\varepsilon = E + 3\alpha Z/2R; \qquad \varkappa = (\varepsilon^2-1)^{\frac{1}{2}}.$$

For a surface distribution of charge the $a_i^{\pm}$ are

$$a_1^{\pm} = \varphi_0[(\varepsilon-1)\beta_1 \pm (\varepsilon+1)\beta_2]; \qquad a_2^{\pm} = \varphi_2(\beta_1 \pm \beta_2)\varkappa^2$$
$$a_3^{\pm} = \varphi_2(\beta_7 \pm \beta_8)\varkappa^2; \qquad a_4^{\pm} = \varphi_1[(\varepsilon-1)\beta_3 \pm (\varepsilon+1)\beta_4]\varkappa^2$$
$$a_5^{\pm} = \varphi_1[(\varepsilon+1)\beta_1 \pm (\varepsilon-1)\beta_2]\varkappa^2; \qquad a_6^{\pm} = \varphi_1[(\varepsilon+1)\beta_7 \pm (\varepsilon-1)\beta_8]\varkappa^2$$
$$a_7 = \varphi_0\beta_5\varkappa; \qquad a_{8]}^{+} = \varphi_2\beta_5\varepsilon\varkappa; \qquad a_8^- = \varphi_2\beta_5\varkappa$$
$$a_9^{\pm} = \varphi_2[(\varepsilon-1)\beta_6 \pm (\varepsilon+1)\beta_9]\varkappa; \qquad a_{10} = \varphi_1\beta_5\varkappa^3$$
$$a_{11}^{\pm} = \varphi_1(\beta_6 \pm \beta_9)\varkappa^3; \qquad a_{12} = \varphi_1\beta_{10}\varkappa^3$$

$\varphi_0 = 1-(\varkappa R)^2/5; \quad \varphi_1 = 1-3(\varkappa R)^2/25; \quad \varphi_2 = 1-4(\varkappa R)^2/25$

$\varepsilon = E+\alpha Z/R; \quad \varkappa = (\varepsilon^2-1)^{\frac{1}{2}}.$

The quantities β_i which enter the a_i^+ are determined by the fitting factors (4) and phases (7):

$$\beta_1 = A^2_{\frac{1}{2}\frac{1}{2}}; \quad \beta_2 = A^2_{\frac{1}{2}-\frac{1}{2}}; \quad \beta_3 = A^2_{\frac{3}{2}\frac{1}{2}}; \quad \beta_4 = A^2_{\frac{3}{2}-\frac{1}{2}};$$

$$\beta_5 = A_{\frac{1}{2}\frac{1}{2}}A_{\frac{1}{2}-\frac{1}{2}}\cos(\Delta_{\frac{1}{2}\frac{1}{2}}-\Delta_{\frac{1}{2}-\frac{1}{2}}); \quad \beta_6 = A_{\frac{1}{2}\frac{1}{2}}A_{\frac{3}{2}\frac{1}{2}}\cos(\Delta_{\frac{1}{2}\frac{1}{2}}-\Delta_{\frac{3}{2}\frac{1}{2}});$$

$$\beta_7 = A_{\frac{1}{2}\frac{1}{2}}A_{\frac{3}{2}-\frac{1}{2}}\cos(\Delta_{\frac{1}{2}\frac{1}{2}}-\Delta_{\frac{3}{2}-\frac{1}{2}}); \quad \beta_8 = A_{\frac{1}{2}-\frac{1}{2}}A_{\frac{3}{2}\frac{1}{2}}\cos(\Delta_{\frac{1}{2}-\frac{1}{2}}-\Delta_{\frac{3}{2}\frac{1}{2}});$$

$$\beta_9 = A_{\frac{1}{2}-\frac{1}{2}}A_{\frac{3}{2}-\frac{1}{2}}\cos(\Delta_{\frac{1}{2}-\frac{1}{2}}-\Delta_{\frac{3}{2}-\frac{1}{2}}); \quad \beta_{10} = A_{\frac{3}{2}\frac{1}{2}}A_{\frac{3}{2}-\frac{1}{2}}\cos(\Delta_{\frac{3}{2}\frac{1}{2}}-\Delta_{\frac{3}{2}-\frac{1}{2}}).$$

In the case when $(\alpha Z)^2 \ll 1$ and $(\alpha Z)^2 \ll p^2$ simple expressions for β_i can be obtained

$\beta_1 = p(E-1)/\varkappa(\varepsilon-1); \quad \beta_2 = p(E+1)/\varkappa(\varepsilon+1); \quad \beta_3 = (p/\varkappa)^3\beta_1$

$\beta_4 = (p/\varkappa)^3\beta_2; \quad \beta_5 = (p/\varkappa)^2; \quad \beta_6 = (p/\varkappa)^2\beta_1\cos\omega$

$\beta_7 = \beta_8 = (p/\varkappa)^3\cos\omega; \quad \beta_9 = (p/\varkappa)^2\beta_2\cos\omega; \quad \beta_{10} = (p/\varkappa)^4;$

$\omega = \text{arc tg}\,(\alpha ZE/p); \quad \varphi_k = 1.$

APPENDIX III

The quantities $C_{ik}^{0JJ'}$ are equal to the $C_{ik}^{(0)}$ from table II.

$3C_{11}^{211}(q) = 3C_{66}^{211}(-q) = -\sqrt{5}\,C_{34}^{212}(-q) = 3\sqrt{10}\,(2a_3^+q-a_4^+-2a_6^+)$

$\sqrt{2}\,C_{33}^{211} = \sqrt{5}\,(4a_3^+q-a_4^++4a_6^+); \quad \sqrt{2}\,C_{44}^{222} = -3\sqrt{7}\,a_4^+$

$3C_{15}^{211} = 3C_{67}^{211} = \sqrt{15}\,C_{48}^{202} = \sqrt{10}\,C_{45}^{212} = 3\sqrt{2}\,C_{35}^{211} = -18\sqrt{30}\,a_3^+$

$C_{24}^{202} = 6\sqrt{2}\,(a_3^+q-a_6^+); \quad C_{13}^{211} = 2\sqrt{5}\,(3a_3^+q-a_4^++a_6^+)$

$3C_{36}^{211} = -\sqrt{5}\,C_{46}^{212} = -6\sqrt{5}\,(a_3^-q+a_4^-+a_6^-)$

$3C_{56}^{211} = 3\sqrt{2}\,C_{37}^{211} = \sqrt{10}\,C_{47}^{212} = 18\sqrt{30}\,a_3^-$

$C_{14}^{212} = 6(a_3^+q+a_4^+-a_6^+).$

The remaining $C_{ik}^{nJJ'}$ are equal zero.

3. Comparison with Experiment and Selection of a Suitable Nucleus for β—γ Angular Correlation Studies

The main criterion to be used when choosing a nucleus for $\beta-\gamma$ angular correlation experiments is that one should be able to give an unambiguous interpretation of the experimental facts. Inasmuch as the type of beta decay theory has not been established, there is not much sense in carrying out the experiments with the purpose of determining the nuclear angular momenta. It is desirable

to use nuclei whose angular momenta and parities of levels are known in order to refine the beta decay theory.

If the change of the nuclear angular momentum Δj exceeds the order of forbiddenness by one unit, a single matrix element will contribute. The angular correlation is then independent of the form of the linear combination of the various types of theory and therefore ceases to be of interest. If Δj is one unit less then the order of forbiddenness the pseudoscalar theory will contribute to the linear combination of the various types of theory. If the relative sign of S and T interaction is the point of interest one should select transitions for which Δj equals the order of forbiddenness. In this case the formulae contain the minimum number of unknown matrix elements.

If the initial and final states of the nucleus are satisfactorily described by the nuclear shell model the ratio between the matrix elements can be determined theoretically. In order to find the signs of the S and T variants it is sufficient to know roughly (but with correct sign) the magnitude of these ratios. Let us now consider from this standpoint some nuclei which are apparently more suitable than others for this type of study.

1. Transition of $_{49}In^{117}$ from the isomeric state to the excited 0.161 MeV level of $_{50}Sn^{117}$ is a transition of first order of forbiddenness with $\Delta j = 1$.

It may be assumed that the beta decay of In^{117} involves a single-nucleon transition since the observed properties of the levels agree with predictions of the shell model [20]). The isomeric In^{117} state corresponds to the $p_{1/2}$ and the excited level Sn^{117} to the $d_{3/2}$ state. Transition to the ground $s_{1/2}$ level is accompanied by magnetic dipole radiation.

2. Beta decay from the ground state of $_{56}Ba^{139}$ to the excited 0.163 MeV level of $_{57}La^{139}$ is also a first order forbidden transition [21]) with $\Delta j = 1$. Ba^{139} has one neutron in excess of the closed shell in the $f_{7/2}$ state. On beta decay this neutron transforms into a proton on the $d_{3/2}$ level. The transition from the $d_{3/2}$ to the $g_{7/2}$ ground state is accompanied by magnetic dipole radiation.

3. Similarly to Ba^{139} the $_{58}Ce^{141}$ nucleus has one neutron in excess of the closed shell. This neutron passes from the $f_{7/2}$ state to the 0.145 MeV level of $_{59}Pr^{141}$. The $g_{7/2} \rightarrow d_{3/2}$ transition to the ground state of Pr^{141} involves magnetic dipole radiation [22]). In distinction to La^{139} the proton $g_{7/2}$ state of Pr^{141} lies above the $d_{3/2}$

state. This is not inconsistent with the shell model as the $g_{7/2}$ and $d_{5/2}$ levels are close to each other and may intersect. Ce^{141} decays with $\Delta j = 0$ and this, generally speaking, should permit one to determine the contribution from pseudoscalar interaction; however, this circumstance also complicates the interpretation of the experiments since instead of a single unknown ratio g_S/g_T and of three matrix element ratios two unknown ratios g_S/g_T and g_P/g_T become involved together with five matrix element ratios.

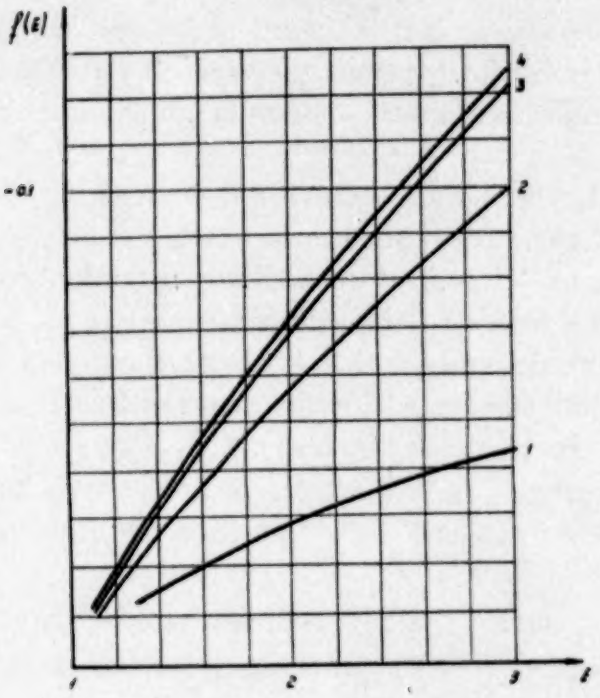

Fig. 1. Factor $f(E)$ for a nucleus with $Z = 71$ and $A = 170$; curves (2) and 4) correspond to a volume charge distribution and nuclear radii $R = 1.2\times10^{-13}\,A^{1/3}$ cm and $R = 1.5\times10^{-13}\,A^{1/3}$ cm and curve (3) to a surface charge distribution of radius $R = 1.2\times10^{-13}\,A^{1/3}$ cm; curve (1) was plotted according to the formulae given in ref. [6]) for a radius $R = 1.2\times10^{-13}\,A^{1/3}$ cm.

There is a number of other nuclei which apparently satisfy the conditions formulated above; examples are $_{80}Hg^{203}$ [23, 24, 25]) $_{81}Tl^{208}$ [26, 27, 28]).

If the $\beta-\gamma$ angular correlation for such nuclei as In^{117}, Ba^{139} or Ce^{141} is investigated with at least the same degree of accuracy as that already attained in correlation measurements it will probably be possible unambiguously to interpret the experiments by determining the ratio of the matrix elements with help of the shell model.

The most interesting nucleus of those studied experimentally is

$_{69}Tm^{170}$ as the angular momenta of its levels are known and first order forbidden beta decay takes place with $\Delta j = 1$.

We denote the ratios of the quantities M_i as follows:

$$M_1/M_3 = x; \qquad M_5/M_3 = (\alpha Z/2R)y; \qquad M_4/M_3 = u$$

(x is the product of g_S/g_T and the matrix element ratio). The requirement of invariance with respect to reflection in time leads to such a choice of the matrix element phases that the quantities x, y, u turn out to be real. The angular momenta of the Tm^{170} $\beta-\gamma$ transition are, according to ref. [29, 30]) equal to $1^- \to 2^+ \to 0^+$. The $\beta-\gamma$ angular correlation experimental points [29]) are presented

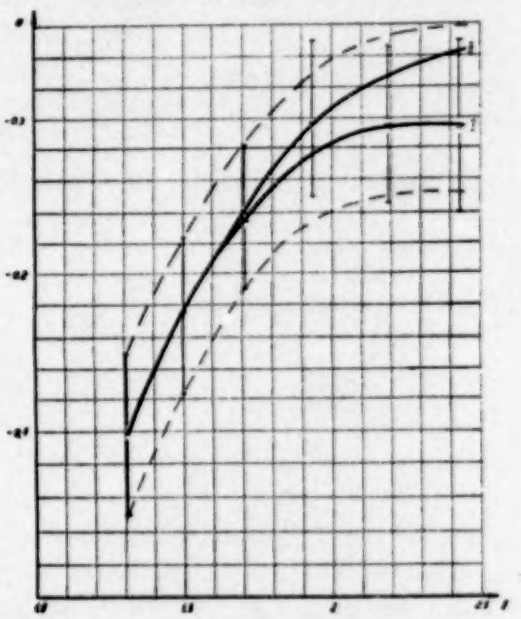

Fig. 2. $\beta-\gamma$ angular correlation experimental points for the Tm^{170} nucleus according to the data presented in ref. [29]).

in fig. 2. The values of $a(E)$, which enters formula (10) if the latter is written as $W(\vartheta) = 1-a(E)\cos^2\vartheta$, are plotted along the ordinate axis. Without making any assumptions regarding the nuclear matrix elements we determined the region for x and y (for a real u) in which the angular correlation curve remains within the region of spread of the experimental points. This region is bounded by curve II in fig. 3. If the spread of the exprimental points is restricted to points which lie above those in curve I of fig. 2 the region of permissible values of x, y will be considerably smaller (curve I in fig. 3). In this case $x > 0$ for any y and in order to determine the sign of g_S/g_T it should be sufficient to establish the sign of the ratio between the matrix elements.

There is no serious ground for assuming a single-nucleon β-transition in Tm^{170}. If, however, in order to make a rough estimation this assumption is made and the results of ref. [31]) are used to calculate the ratio between the matrix elements, then

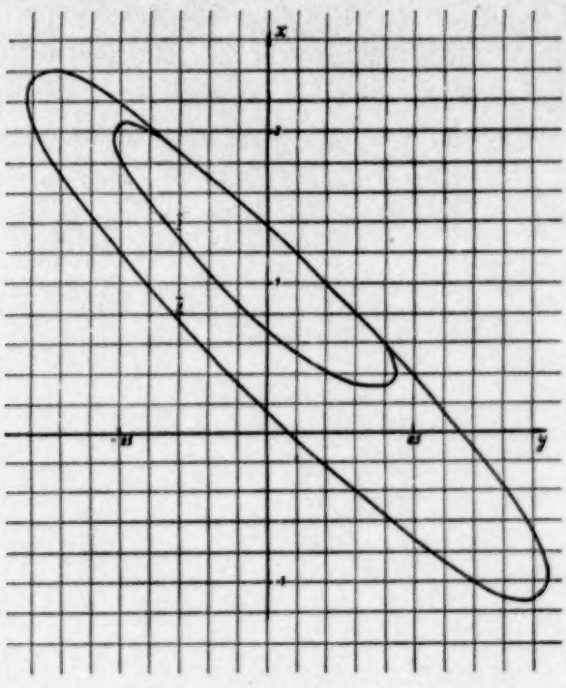

Fig. 3. Region of permissible values of the parameters x and y for the Tm^{170} nucleus. Curve II restricts the region of the values of x and y for which $a(E)$ lies within the boundaries of the spread of the experimental points. Curve I refers to those values of x and y for which $a(E)$ lies above curve I in Fig. 2.

for the $p_{1/2} \rightarrow s_{1/2}$ transition (see ref. [30])) comparison with experiment yields $g_S/g_T < 0$ whereas if one assumes $p_{3/2} \rightarrow s_{1/2}$, it is found that $g_S/g_T > 0$.

References

1) B. N. Rustad and S. L. Ruby, Phys. Rev. **89** (1953) 880
2) D. R. Maxon, J. S. Allen, W. K. Jentschke, Phys. Rev. **97** (1955) 109
3) A. Z. Dolginov, JETP **20** (1950) 636
4) D. L. Falkoff and G. F. Uhlenbeck, Phys. Rev. **79** (1950) 334
5) A. Z. Dolginov, JETP **22** (1952) 668
6) M. Yamada and M. Morita, Progr. Theor. Phys. **8** (1952) 431
7) M. Morita, Progr. Theor. Phys. **10** (1954) 363
8) M. Morita and M. Yamada, Progr. Theor. Phys. **11** (1954) 219
9) Y. Kato and M. Morita, Progr. Theor. Phys. **13** (1955) 276
10) A. Z. Dolginov, JETP **22** (1952) 658

11) L. A. Sliv, JETP **17** (1947) 1049
12) M. F. Rose and D. K. Holmes, Phys. Rev. **83** (1951) 190
13) M. Yamada, Progr. Theor. Phys. **10** (1953) 241
14) I. Malcolm, Phil. Mag. **43** (1952) 1011
15) V. B. Berestetsky, A. Z. Dolginov and K. A. Ter-Martirosyan, JETP **20**, (1950) 527,
16) M. E. Rose, Phys. Rev. **51** (1937) 484
17) L. C. Biedenharn and M. F. Rose, Revs. Mod. Phys. **25** (1953) 729
18) A. Z. Dolginov, Izv. Akad. Nauk SSSR ser. fys. **17** (1952) 322
19) A. Z. Dolginov, JETP **23** (1952) 493
20) C. L. McGinnis, Phys. Rev. **97** (1955) 93
21) A. C. G. Mitchell and E. Hebb, Phys. Rev. **95** (1954) 727
22) J. T. Jones and F. N. Jensen, Phys. Rev. **97** (1955) 1031
23) S. Thulin and K. Nybö, Ark. Fys. **7** (1953) 289
24) A. H. Wapstra, D. Macder, G. J. Nijgh and L. Th. M. Ornstein, Physica **20** (1954) 169
25) N. Marty, C. R. Acad. Sci. **240** (1955) 291
26) L. G. Elliott, R. L. Graham, J. Wlaker and J. L. Wolfson, Phys. Rev. **93** (1954) 356
27) N. Feather, I. Kyles, R. W. Pringle, Proc. Phys. Soc. **61** (1948) 466
28) D. G. E. Martin, H. O. W. Richardson and Yun-Kuei Hsü, Proc. Phys. Soc. A **60** (1948) 466
29) H. Rose, Phil. Mag. **43** (1952) 1146
30) R. Richmond and H. Rose, Phil. Mag. **43** (1952) 367
31) M. E. Rose and R. K. Osborn, Phys. Rev. **93** (1954) 1326

Nuclear Physics **2** (1956/57) 160—168; *North-Holland Publishing Co., Amsterdam*

INTERPRETATION DES RESULTATS EXPERIMENTAUX DE CORRELATION ANGULAIRE

P. C. MACQ† et M. DE HEMPTINNE

Centre de Physique Nucléaire, Université de Louvain

Reçu le 20 juin 1956

Abstract: Fuchs' theory of angular correlation for the β—γ cascade of type $2^- \to 2^+ \to 0^+$ is generalized and applied to the discussion of the experimental results for Rb^{86} and Cl^{38}.

A l'occasion de l'étude [1, 2]) de la corrélation angulaire du Cl^{38}, nous avons repris l'interprétation des résultats du Rb^{86} fournie par Fuchs [3]) et en avons précisé la portée. Ces deux radioéléments présentent, en effet, le même type de cascade

$$2^- \underset{\beta}{\to} 2^+ \underset{\gamma}{\to} 0^+$$

ce qui en permet une étude parallèle.

1. Introduction

Dans le cas du Rb^{86} étudié expérimentalement par Deutsch and Stevenson [4]), comme dans celui du Cl^{38}, l'émission β entre les niveaux 2^- et 2^+ est une fois défendue: le moment angulaire emporté dans l'émission bêta sera donc 0, 1 ou 2. L'émission gamma subséquente est pure avec un moment $L = 2$; elle résulte en effet de transitions entre les niveaux nucléaires de moments et parités 2^+ et 0^+.

Nous limitant pour l'émission β à l'hypothèse d'une interaction tensorielle, les éléments de matrices liés aux moments 0, 1 ou 2 des leptons sont ††

$$\begin{aligned} \text{pour } L = 0 &: \langle \beta\boldsymbol{\sigma} \cdot \mathbf{r} \rangle \\ L = 1 &: \langle \beta\boldsymbol{\alpha} \rangle \text{ et } \langle \beta\boldsymbol{\sigma} \times \mathbf{r} \rangle \\ L = 2 &: B^{\beta}_{ij}. \end{aligned}$$

Les courbes a, b, c de la figure 1 donnent le coefficient d'anisotropie ε du Rb^{86} en fonction de l'énergie des particules dans l'hypothèse d'une attribution de moment angulaire bien défini (moment angu-

† Boursier de l'I.R.S.I.A. Extrait de thèse de Doctorat (mai 1955).

†† Nous utilisons ici les notations de Konopinski [5]).

laire pur) aux leptons libérés à l'occasion de la transition. Le coefficient ε est défini à partir de la fonction de distribution

$$W(\theta) = 1+\varepsilon \cos^2 \theta$$

représentant l'intensité de l'émission β en fonction de l'angle entre les directions d'émission de la particule β et du photon émis subséquemment dans le processus de désexcitation du noyau formé. Le désaccord entre l'expérience (région hachurée) et la théorie (courbes a, b, c,) est complet. Dans le cas du Cl^{38} (fig. 2) on est arrivé aux mêmes conclusions.

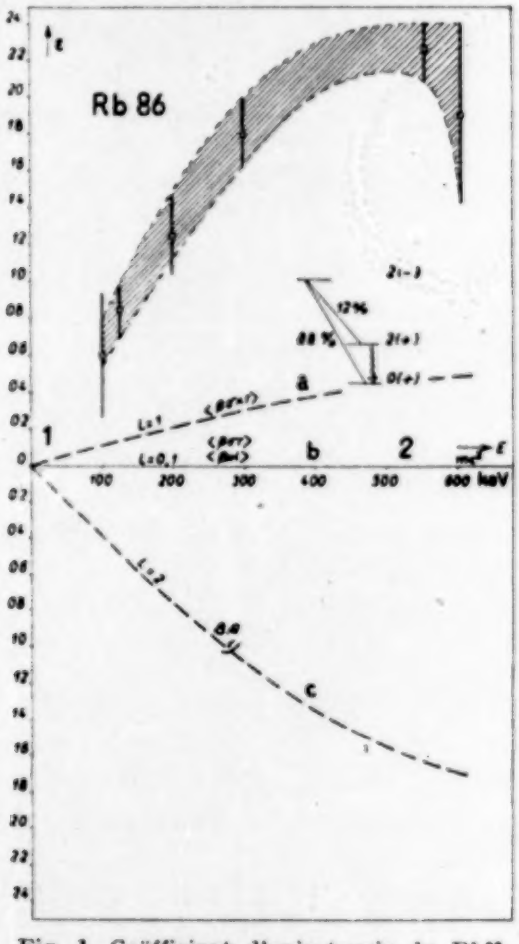

Fig. 1. Coëfficient d'anisotropie du Rb^{86}.

Fuchs [3]) fut le premier à introduire l'hypothèse d'un mélange de moments angulaires pour les leptons dans la théorie de la corrélation angulaire β—γ: les leptons n'emportent pas un moment bien défini mais bien une superposition de ceux-ci. Une telle hypothèse s'avère d'ailleurs indispensable pour interpréter la forme des spectres β obtenue expérimentalement. Il a montré qu'un

mélange des éléments de matrice $\langle\beta\alpha\rangle$ et B^{β}_{ij} dans le rapport $\langle\beta\alpha\rangle/B^{\beta}_{ij} = ix$, $(x = -0.78)$ rétablissait apparemment l'accord entre la théorie et l'expérience.

Son étude a le grand mérite d'avoir prouvé que l'hypothèse du mélange introduisait dans la fonction $W(\theta)$ des termes d'interférence entre les différents éléments de matrice. Ces termes s'annulent lorsqu'on intègre $W(\theta)$ sur toutes les directions. On comprend

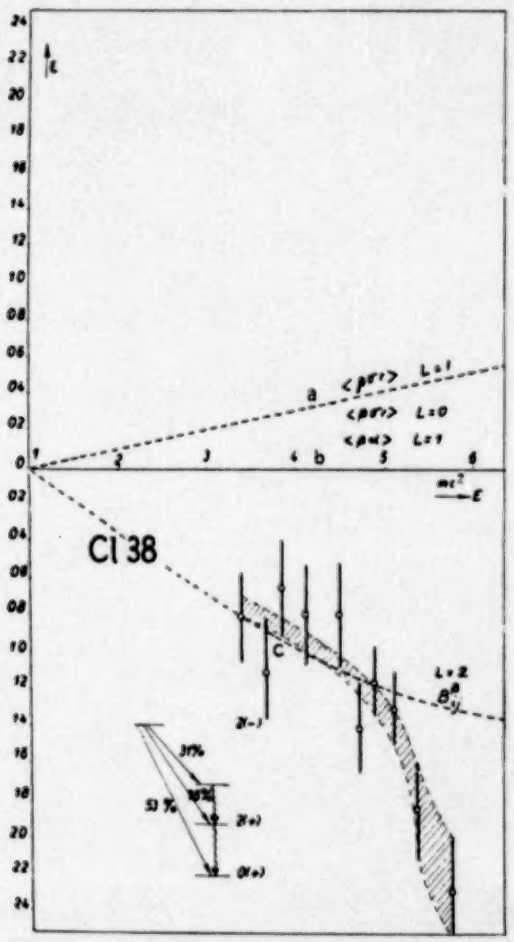

Fig. 2. Coëfficient d'anisotropie du Cl^{38}.

dès lors pourquoi les expériences qui ne tenaient pas compte des propriétés directionnelles n'étaient pas parvenues à mettre en évidence ce phénomène d'interférence. Un examen de la fig. 4 montre clairement que les courbes (a) obtenues en tenant compte de ce phénomène sont totalement différentes de celles obtenues par une addition quelconque de courbes (b) représentatives des cas purs.

2. Théorie de Fuchs généralisée

Nous avons étendu le travail de Fuchs en nous limitant cependant au cas le plus général d'interaction tensorielle †. Nous définissons les variables x, y, z, k, p, E, ξ de la façon suivante:

$$\frac{\langle\beta\alpha\rangle}{B^{\beta}_{ij}} = ix, \quad \frac{\langle\beta\sigma\times\mathbf{r}\rangle}{B^{\beta}_{ij}} = iy, \quad \frac{\langle\beta\sigma\cdot\mathbf{r}\rangle}{B^{\beta}_{ij}} = z;$$

k — moment du neutrino,
p — moment de la particule β,
E — énergie de la particule β;
$\xi = \alpha Z/2R$,
Z — nombre atomique,
R — rayon nucléaire.

La fonction de corrélation prend la forme

$$\begin{aligned}W(\theta) = {} & \tfrac{1}{6}[k^2+p^2]+2x^2 \\ & +2y^2\left[\frac{1}{6}(k^2+p^2)+\frac{2}{3}k\left(\frac{p^2}{3E}+\xi\right)+\xi^2+\frac{2\xi p^2}{3E}\right] \\ & +2z^2\left[\frac{1}{9}(k^2+p^2)-\frac{2}{3}k\left(\frac{p^2}{3E}+\xi\right)+\xi^2+\frac{2\xi p^2}{3E}\right] \\ & -4xy\left[\frac{1}{3}k+\frac{p^2}{3E}+\xi\right] \\ & -p^2\left[\frac{1}{56}+\frac{x}{\sqrt{14}}\frac{1}{E}-\frac{y}{\sqrt{14}}\left(\frac{k}{3E}+\frac{1}{2}+\frac{\xi}{E}\right)+\frac{2z}{\sqrt{21}}\left(-\frac{k}{3E}+\frac{1}{3}+\frac{\xi}{E}\right)\right. \\ & \left.-\frac{1}{6}y^2\left(\frac{2k}{3E}+\frac{1}{2}+\frac{2\xi}{E}\right)+\frac{xy}{3E}\right]P_2(\cos\theta) \\ \approx {} & 1+\varepsilon(x,\ y,\ z,\ E,\ Z)\cos^2\theta.\end{aligned}$$

Remarquons que

1) $\varepsilon = 0$ pour $p = 0$: l'émission est isotrope pour une énergie cinétique nulle des particules β,
2) ε n'est pas nécessairement maximum pour une énergie maximum des particules β,
3) un poids atomique petit favorise l'anisotropie, car ε est de l'ordre de grandeur de $1/Z$ pour Z grand.

Si on fait abstraction du cas du K^{42} pour lequel on ne possède à ce jour de valeur de ε que pour deux énergies, le Rb^{86}, de nombre

† Le même calcul a été repris depuis par Morita [6]) pour tous les types possibles d'interaction.

atomique 37, était le corps le plus léger étudié avant notre travail sur le Cl^{38} ($Z = 17$).

Nous avons examiné successivement chacun des cas

$$y = z = 0,$$
$$x = y = 0,$$
$$x = z = 0.$$

2.1 CAS OÙ $y = z = 0$.

Dans ce cas, nous avons affaire à un mélange de moments angulaires $L = 1$ et $L = 2$. La fonction de corrélation angulaire se présente alors sous la forme

$$W(\theta) = \frac{1}{6}(k^2+p^2)+2x^2-p^2\left(\frac{1}{56}+\frac{x}{\sqrt{14}}\frac{1}{E}\right)P_2(\cos\theta)$$
$$\approx 1+\varepsilon\cos^2\theta.$$

Le facteur d'anisotropie est uniquement fonction de l'énergie E et de x. En se fixant E et en utilisant la valeur expérimentale de ε, on obtient une équation du second ordre en x avec les solutions $x_1(E)$ et $x_2(E)$. Les résultats expérimentaux fournissent deux valeurs extrêmes ε_{max} et ε_{min} pour chaque valeur de l'énergie. Le domaine de x sera donc limité soit par les courbes $x_1(E)_{max}$ et $x_1(E)_{min}$ soit par les courbes $x_2(E)_{max}$ et $x_2(E)_{min}$.

La fig. 3 donne en hachuré la zone permise pour x. Comme x

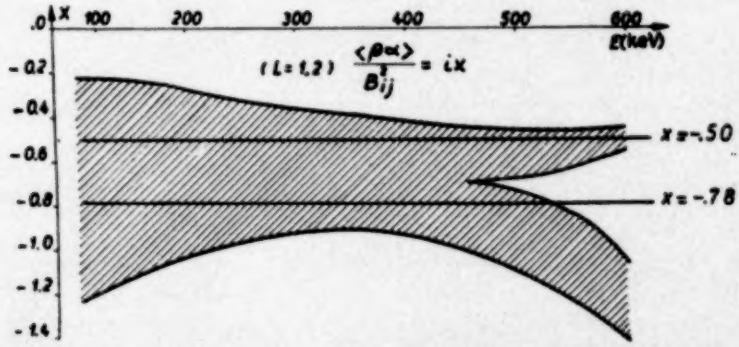

Fig. 3. Zônes permises pour le paramètre x ($y = z = 0$).

représente un rapport d'éléments de matrices nucléaires, il doit rester constant pour toute énergie des particules; x devra donc nécessairement se trouver dans un des deux domaines horizontaux:

a) soit $x = -0.8$ à -0.9, ce qui correspond à la valeur de -0.78 proposée par Fuchs; on remarque immédiatement sur la fig. 3 que l'on s'écarte de la région permise pour des énergies élevées;

b) soit $x = -0.45$ à -0.55; x reste dans la région hachurée pour tout le spectre d'énergie.

Nous avons repris sur la fig. 4 les courbes représentatives de ε en fonction de E pour différentes valeurs du paramètre x. La comparaison des fig. 3 et 4 fait apparaître tout l'intérêt de la discussion des valeurs permises pour x; dès qu'une horizontale tracée

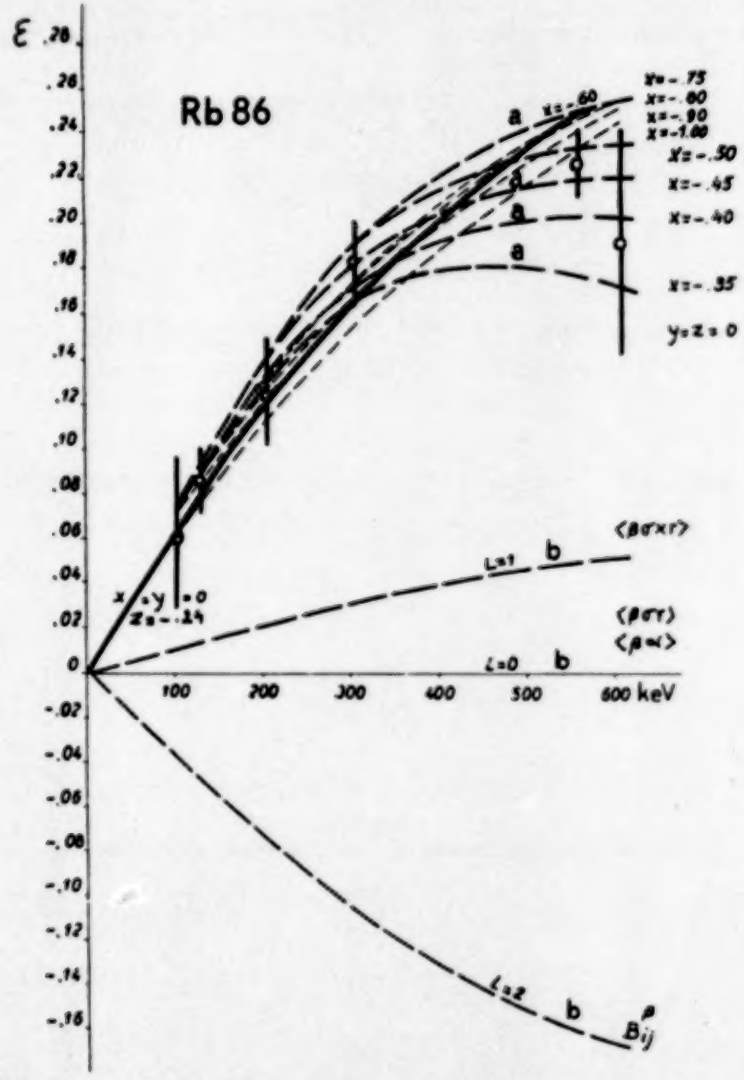

Fig. 4. Coëfficient d'anisotropie du Rb^{86} calculé pour différentes valeurs des paramètres x, y, z.

sur la fig. 3 sort de la zone permise, la courbe correspondante de la fig. 4 s'écarte des limites fixées par l'expérience.

D'autre part, l'étude du spectre β donne une courbe de Kurie

droite, aux erreurs expérimentales près; cela signifie que le facteur de correction A_0 dans

$$W(\theta) = A_0 + A_2 P_2 (\cos\theta)$$

est à peu près constant. La table I donne les valeurs de A_0 pour $x = -0.78$ et -0.50.

TABLE I

Comparaison des valeurs de A_0 pour $x = -0.78$ et $x = -0.50$

x \ E	100 keV	200 keV	300 keV	400 keV	500 keV	600 keV
−0.78	1.21	1.20	1.17	1.13	1.07	1
−0.50	1.40	1.38	1.31	1.22	1.11	1

La valeur $x = -0.78$ semblerait donc plus favorable si l'on s'arrêtait à cette combinaison de moments angulaires.

2.2 CAS OÙ $x = y = 0$.

On a alors affaire à un mélange de moments angulaires $L = 0$ et $L = 2$. La fonction de corrélation angulaire aura la forme

$$W(\theta) = \frac{1}{6}(k^2+p^2) + 2z^2\left[\frac{1}{9}(k^2+p^2) - \frac{2}{3}k\left(\frac{p^2}{3E}+\xi\right) + \xi^2 + \frac{2\xi p^2}{3E}\right]$$
$$-p^2\left[\frac{1}{56} + \frac{2z}{\sqrt{21}}\left(-\frac{k}{3E}+\frac{1}{3}+\frac{\xi}{E}\right)\right] P_2(\cos\theta).$$

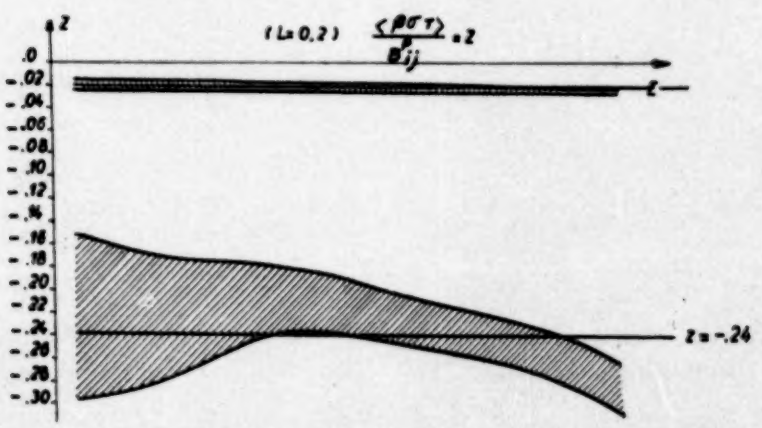

Fig. 5. Zônes permises pour le paramètre z ($x = y = 0$).

Reprenant la même méthode que dans le paragraphe précédent, nous déterminons deux régions possibles pour z (fig. 5):

a) $z \approx -0.02$,
b) $z \approx -0.24$.

La courbe de $\varepsilon(z, E)$ pour $z = -0.24$ est reprise en trait plein sur la fig. 4. On remarque qu'elle concorde tout aussi bien avec les résultats expérimentaux que la courbe $\varepsilon(x, E)$ pour $x = -0.78$.

Le facteur $A_0(z, E)$ de correction est d'ailleurs aussi constant que pour le mélange considéré par Fuchs; il est donné dans la table II en regard de $A_0\ (x, E)$.

TABLE II

Comparaison des valeurs de A_0 pour $x = -0.78$ et $z = -0.24$

A_0 \ E(keV)	100	200	300	400	500	600
$A_0(x, E)$ pour $x = -0.78$	1.21	1.20	1.17	1.13	1.07	1.00
$A_0(z, E)$ pour $z = -0.24$	1.24	1.21	1.14	1.09	1.04	1.00

2.3. CAS OÙ $x = z = 0$.

Le mélange de moments angulaires sera $L = 1$ et $L = 2$ et la fonction $W(\theta)$ devient

$$W(\theta) = \frac{1}{6}(k^2+p^2)+2y^2\left[\frac{1}{6}(k^2+p^2)+\frac{2k}{3}\left(\frac{p^2}{3E}+\xi\right)+\xi^2+\frac{2\xi p^2}{3E}\right]$$

$$-p^2\left[\frac{1}{56}-\frac{y}{\sqrt{14}}\left(\frac{k}{3E}+\frac{1}{2}+\frac{\xi}{E}\right)-\frac{1}{6}y^2\left(\frac{2k}{3E}+\frac{1}{2}+\frac{2\xi}{E}\right)\right]P_2(\cos\theta).$$

La fig. 6 fait apparaître directement les domaines permis pour y:

a) $y \approx +0.04$,
b) $y \approx +0.14$.

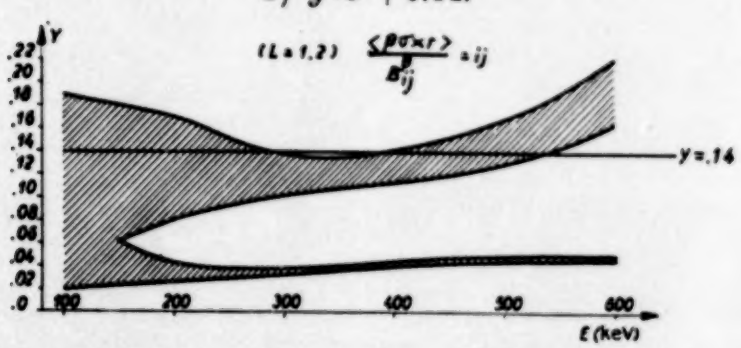

Fig. 6. Zônes permises pour le paramètre $y(x = z = 0)$.

De ce qui précède, on peut déduire par le seul examen de cette figure, qu'il existe des valeurs non nulles de y satisfaisant aux résultats expérimentaux.

3. Conclusion

Si l'on s'en tient à une interaction du type tensoriel il est impossible d'interpréter les résultats expérimentaux en attribuant un moment angulaire pur ($L = 0$, 1 ou 2) aux leptons émis. Nous avons vu, par contre, qu'un mélange de deux quelconques de ces moments était satisfaisant. Il est clair que l'hypothèse d'un mélange plus complexe et même d'autres types d'interaction permettrait aussi de trouver un accord avec l'expérience. Dans l'état actuel de la question, il est donc difficile de tirer des conclusions nettes des quelques cas expérimentaux étudiés. Toutefois, il semble que des expériences de corrélation angulaire triple pourront préciser la nature du mélange dont l'existence a été mise en évidence [7]).

Bibliographie

1) P. C. Macq, Bull. Acad. Roy. Belg. **40** (1954) 802
2) P. C. Macq, Bull. Acad. Roy. Belg. **40** (1955) 467
3) M. Fuchs, Doctoral Thesis (Michigan 1951)
4) D. T. Stevenson and M. Deutsch, Phys. Rev. **83** (1951) 1202
5) E. Konopinski, Rev. Mod. Phys. **15** (1943) 209
6) M. Morita, Prog. Theor. Phys. **14** (1955) 27
7) M. Morita, communication privée (1956)

Nuclear Physics **2** (1956/57) 169—172; *North-Holland Publishing Co., Amsterdam*

COLLECTIVE NUCLEAR MOTION AND THE EFFECTIVE MASS OF A NUCLEON

R. J. BLIN-STOYLE
Clarendon Laboratory, Oxford

Received 10 July 1956

Abstract: It is suggested that the energies of rotational levels in nuclei indicate that the effective mass of a nucleon in a nucleus is approximately one-half the actual mass.

1. Introduction

The following discussion is an attempt to account for certain aspects of the collective motion of a nucleus. For some time now it has been known that the deformation of a nucleus, as calculated from the energies of rotational levels on the assumption of the irrotational flow of nuclear matter, differs considerably from the deformation obtained from static quadrupole moments and transition probabilities, etc. The measured moments of inertia appear to be several times larger than would be expected for irrotational flow (e.g. ref. [1])). This fact has led to the investigation by various authors [2, 3, 4]) of the moment of inertia for particles moving independently in a rotating deformed potential well. The surprising result is obtained that for this case the moment of inertia is approximately that for rigid rotation. However, it is shown by the above authors that the effect of internucleon forces is to reduce this value so that the experimental values can be accounted for qualitatively. For large deformations, nevertheless, the moment of inertia should approach that for rigid rotation and a saturation effect is to be expected.

Recent experimental work seems to give evidence of such an effect but I (the moment of inertia) seems to saturate at about $\frac{1}{2}I_{\text{rigid}}$ rather than I_{rigid}. It is suggested in the following that this is a manifestation of a nucleon "effective mass" in the nucleus.

2. Experimental Results

It is well known that the energy levels, quadrupole moments, etc., of nuclei in the range $150 < A < 180$ can be satisfactorily

interpreted in terms of collective nuclear motion. In fig. 1 a plot is given of I/I_{rigid} against β for these nuclei, where β is a measure

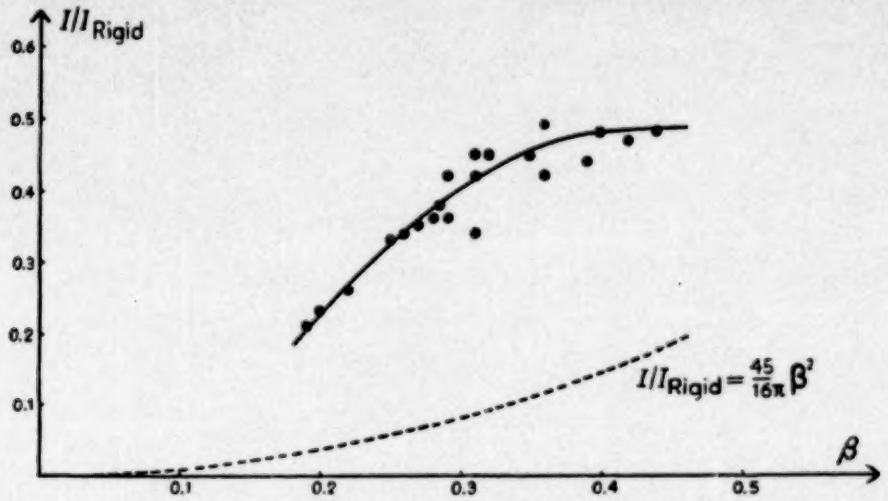

Fig. 1. Plot of I/I_{rigid} against β. The full line is drawn through the experimental points to demonstrate the saturation effect. The broken line is the curve obtained theoretically for irrotational flow.

of the distortion of the nuclei obtained from electrical properties and defined by

$$\beta = \frac{4}{3}\sqrt{\frac{\pi}{5}}\,\frac{\Delta R}{R_0},$$

where R_0 is the mean nuclear radius and ΔR the difference between major and minor semi-axes. I is the moment of inertia calculated from the observed rotational level spacing and

$$I_{\text{rigid}} = \tfrac{2}{5}MAR_0^2(1+0.31\beta+\ldots)$$

is the rigid moment of inertia for an ellipsoid of constant density. The points clearly do not lie on the parabola $I/I_{\text{rigid}} = (45/16\pi)\beta^2$ which is obtained for irrotational flow. The values of I/I_{rigid} however do seem to approach approximately one-half for large β.

Unfortunately in the rotational region $A > 230$ values of β are not known so that a similar analysis cannot be made. However, the energies E_2 of spin 2 first excited states of even nuclei in this region seem [5, 6]) to saturate at about 44 keV for $A \approx 236$ so that we can estimate the saturation value of the moment of inertia from the relation $E_2 = 3\hbar^2/I_{\text{sat}}$. Then taking $0.31\beta \approx 0.1$ in the expression for I_{rigid} gives $I_{\text{sat}}/I_{\text{rigid}} \approx 15\hbar^2/(2.2E_2\, r_0^2 A^{5/3})$. Assuming $r_0 = 1.2\times 10^{-13}$ cm (as used by Bohr for $150 < A < 188$) gives $I_{\text{sat}}/I_{\text{rigid}} \approx \frac{1}{2}$.

An alternative way of demonstrating the saturation effect is

to plot the energies E_2 of the spin 2 first excited states of even nuclei against A. This is done in fig. 2 using the collection of values given by Scharff-Goldhaber [5]). Also plotted on this diagram are

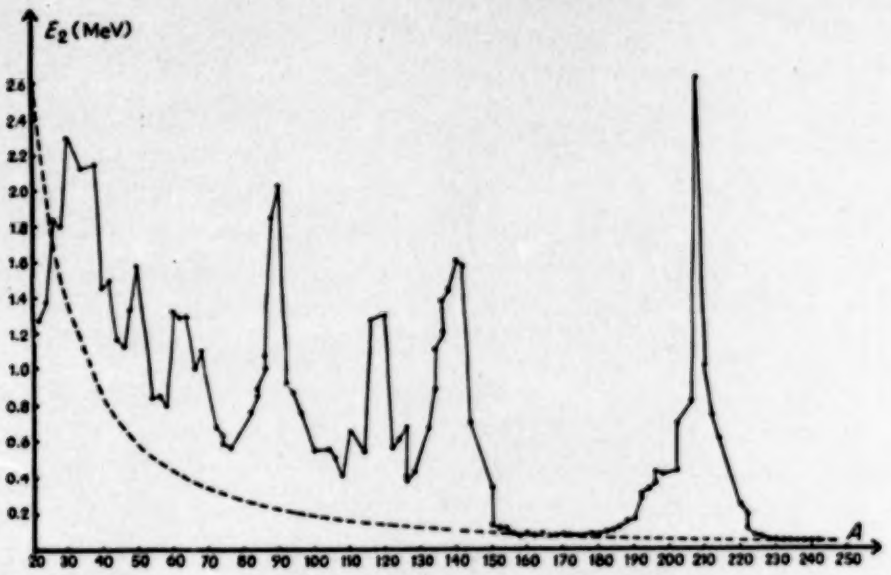

Fig. 2. Plot of E_2 against A. The full line is drawn through the experimental points whilst the broken line indicates the theoretical values for E_2 assuming rigid rotation for an effective nucleon mass $m^* = \frac{1}{2}m$.

the energies of the first excited states calculated assuming saturation, i.e., assuming that the nucleus is undergoing rigid rotation with moment of inertia $\frac{1}{2}I_{\text{rigid}}$; I_{rigid}, of course, depends on β and, as before, we have taken $0.31\,\beta \approx 0.1$, which, for $r_0 = 1.2\times 10^{-13}$ cm, gives $E_2 = 396A^{-5/3}$ MeV. The saturation is strikingly demonstrated for the two regions $160 < A < 170$ and $A > 230$. It is interesting to note that the experimental and theoretical curves also coincide around $A = 24-28$ since nuclei with these mass numbers have been postulated to have strong rotational properties.

3. Interpretation in terms of a nucleon „effective mass"

Recent work of Brueckner *et al.* [7, 8]) implies that in nuclear matter a nucleon can be considered to move in a constant, uniform potential but with a very different "effective mass". Thus if the collective rotational motion of a nucleus is to be represented by particles moving in a rotating deformed potential well it might be expected that the nucleon mass m has to be replaced by an "effective mass" m^*. It then follows that for large distortions the moment of inertia should saturate at $I = (m^*/m)I_{\text{rigid}}$. Thus to agree with

experiment one must have $m^* \approx \frac{1}{2}m$. This is in accord with Brueckner's estimate of m^*.

4. Discussion

Formally, Brueckner's results can be expressed in the following way. If Φ is the wave function of a nucleus then in the limit of many particles $\Phi = F\Psi$ where F is a unitary operator and Ψ describes particles moving in a uniform potential well with an effective mass m^*. Ψ will be referred to as the model wave function. If the nucleus is rotating, for example, about the x-axis with angular velocity ω, the perturbation producing the rotation of the deformed potential well is $-\omega L_x$ where $\mathbf{L}$ is the total angular momentum operator for the system. Now it seems fairly certain that $\mathbf{L}$ commutes with F (see ref. [8])) so that it is sufficient to consider rotation of the model described by Ψ and this will give the results already presented. Thus in the limit of large distortions the model rotates rigidly but not the actual nucleus. Clearly these ideas will break down in the limit of extremely large distortions (a needle-shaped nucleus) when the nucleus also rotates rigidly. This is because the idea of an effective mass arises mainly from consideration of volume effects whereas for such a hypothetical nucleus surface effects completely predominate.

With these ideas, then, it is possible to account for nuclear moments of inertia in the regions of large distortions. The variation of I with β for small distortions, however, still requires more quantitative investigation.

The author is indebted to Professor V. F. Weisskopf for comments on the above ideas.

References

1) A. W. Sunyar, Phys. Rev. **98** (1955) 653
2) D. Inglis, Phys. Rev. **96** (1955) 1059
3) A. Bohr and B. R. Mottelson, Dan. Mat. Fys. Medd. **30** (1955) No. 1
A. Bohr, P. O. Froman and B. R. Mottelson, Dan. Mat. Fys. Medd. **29** (1955) No. 10
4) S. A. Moszkowski, Phys. Rev. to be published
5) G. Scharff-Goldhaber, Phys. Rev. **90** (1953) 587
6) A. Bohr, Rotational States of Atomic Nuclei (Ejnar Munksgaard, Copenhagen, 1954)
7) K. A. Brueckner, C. A. Levinson and H. M. Mahmoud, Phys. Rev. **95** (1954) 217
K. A. Brueckner, Phys. Rev. **96** (1955) 508
K. A. Brueckner, Phys. Rev. **97** (1955) 1344
K. A. Brueckner and C. A. Levinson, Phys. Rev. **97** (1955) 1353
8) R. J. Eden and N. C. Francis, Phys. Rev. **97** (1955) 1366

Nuclear Physics **2** (1956/57) 173—176; *North-Holland Publishing Co., Amsterdam*

THE INTERACTION LAGRANGIAN FOR FUNDAMENTAL PARTICLES

ABDUS SALAM

St. John's College, Cambridge

Received 24 May 1956

Abstract: On the basis of d'Espagnat and Prentki's classification, the interaction Lagrangian is written down for all strong reactions of fundamental particles. Use is made of the invariance requirement for particle-antiparticle conjugation.

1. Introduction

In this paper we consider the problem of writing down the interaction Lagrangian involving all strong reactions of fundamental particles †. Besides invariance for proper Lorentz and parity transformations, the Lagrangian is assumed invariant

(1) for particle-antiparticle conjugation;

(2) for charge-conserving gauge transformations of operators $\phi' = \phi \exp(iQ\alpha)$, where Q is the charge and α a constant parameter;

(3) for rotations in a [3] isobaric space.

It is assumed that the Λ field is scalar, the

$$\boldsymbol{\pi} = \begin{pmatrix} \pi_1 \\ \pi_2 \\ \pi_3 \end{pmatrix} \text{ and } \boldsymbol{\Sigma} = \begin{pmatrix} \Sigma_1 \\ \Sigma_2 \\ \Sigma_3 \end{pmatrix}$$

fields are vectors, the

$$\mathrm{N} = \begin{pmatrix} \mathrm{p} \\ \mathrm{n} \end{pmatrix}, \ \mathrm{K} = \begin{pmatrix} \mathrm{K}^+ \\ \mathrm{K}^0 \end{pmatrix} \text{ and } \Xi = \begin{pmatrix} \Xi^0 \\ \Xi^- \end{pmatrix}$$

fields are spinors in this space. We have $\pi^{\pm} = 2^{-\frac{1}{2}}(\pi^1 \mp i\pi^2)$, $\Sigma^{\pm} = 2^{-\frac{1}{2}}(\Sigma^1 \mp i\Sigma^2)$. In writing these vectors and spinors [(Ξ^0, Ξ^-) rather than (Ξ^-, Ξ^0) for example], it is assumed that T_3 is positive for all positively charged particles. This is not a new assumption however. Once the vector or spinor character of the particles is

† This problem has been considered previously by Utiyama [1]) and d'Espagnat and Prentki [2]). The present paper is based on d'Espagnat and Prentki's work.

fixed and the sign of T_3 (arbitrarily) assigned for one particle (e.g. $T_3 = +\frac{1}{2}$ for a proton), the observed (charge-conserving, charge independent) reactions $p \to n+\pi^+$, $\pi^-+p \to \Lambda^0+K^0$ etc. determine the sign of T_3 for all other particles.

2. Reflections in Isobaric Space

Let us briefly consider the role of reflections in the isobaric space. Racah [3]) and d'Espagnat and Prentki [2, 4]) have made the important remark that the gauge transformation $\exp(iQ\alpha)$ for the particular angle $\alpha = \pi$ acquires the significance of a parity operation ($z \to -z$) in the isobaric space, provided π and Σ particles are considered as pseudovectors, Λ as scalar, and N and Ξ as spinors with opposite reflection properties †. The operation $\exp(iQ\pi)$ transforms $\Sigma \to (-\Sigma_1, -\Sigma_2, \Sigma_3)$, $N \to -\tau_3 N$, $\Xi \to \tau_3 \Xi$. Thus any Lagrangian invariant for transformations (2) and (3) of section 1 is automatically isobaric reflection invariant.

The operations $P_1 = \exp[i(Q-T_3)\pi]$, $P_2 = \exp[i(Q+T_3)\pi]$ clearly correspond to the full reflection $x, y, z \to -x, -y, -z$. It is important to remark that one of the two operators $Q-T_3$ or $Q+T_3$ must in any case be a multiple of the unit operator. This follows from the role of T_3 as component of a spin, so that the eigenvalues of T_3 (like the charge) differ by one unit for two neighbouring components of any multiplet (e.g. $T_3(p)-T_3(n) = 1 = Q_p-Q_n$). This is the content of Gell-Mann's strangeness hypothesis. The fact that it is $Q-T_3$ which uniformly occurs as a multiple of the unit matrix for all multiplets, follows from the remark in section 1, that all positively charged particles come to acquire positive isobaric spin if we assign $T_3 = +\frac{1}{2}$ to the proton. Of the two operators P_1 and P_2, only P_1 commutes with T_1, T_2: P_1, then, gives the correct characterization of the parity operation. Since $\exp(iQ\pi)$ does not commute with T_1 or T_2, it would appear that only full reflections ($x, y, z \to -x, -y, -z$ and not merely $z \to -z$) have a significance in the isobaric space.

3. Particle-antiparticle Conjugation

Before writing down the Lagrangian we wish to consider in this section the role of particle-antiparticle conjugation in providing

† Unlike the presentation in ref. [2]) the approach here towards reflections in the isobaric space makes it unnecessary to exclude from the Lagrangian 4-Fermi or more complicated interactions, although in practice we shall do so.

reality conditions for the coupling constants. Pauli [5]) † has recently derived similar conditions for the meson-nucleon case from Wigner's Time Reversal Operation (WR). In this same paper Pauli has shown that WR and particle-antiparticle conjugation impose identical restrictions and this latter (and perhaps more familiar) approach is used here.

Particle-antiparticle conjugation (AC) is the unitary transformation $\phi' = U\phi U^{-1}$, where the relation of the ϕ' field to "antiparticles" is isomorphic with the relation of the ϕ field to "particles". The Lagrangian as well as other operators representing physical quantities (e.g. Q, T_3 etc.) should be invariant for this unitary transformation ††. Thus $\mathscr{L} = \frac{1}{2}[\mathscr{L}(\phi)+U\mathscr{L}(\phi)U^{-1}]$.

For a complex Bose field ϕ, we might expect $\phi' = U\phi U^{-1} = \exp(i\alpha)\cdot\phi^*$, but the unitarity of U implies $\alpha = 0$ or π. There are thus just two independent types of fields, either those for which $\phi_1' = \phi_1^*$ or $\phi_2' = -\phi_2^*$ and any given field can belong to one of these two types. For ϕ_2 fields it is always possible (irrespective of the presence of any interactions) to redefine the field variable $\Phi = i\phi_2$ such that $\Phi' = \Phi^*$. This same result holds for a complex Dirac field. To see this it is simplest to use a Majorana ††† representation where in general in close analogy with the Bose case $\psi_1' = \psi^*$ or $\psi_2' = -\psi_2^*$ and the second possibility is again removed by a redefinition. For a real (neutral) field it is well known that a redefinition will not remove the negative sign in the second case without destroying the reality of the field.

Consider a hermitian coupling of 3 distinct fields, e.g. $\mathscr{L}(\phi) = C\bar{\Lambda}\mathrm{n}\theta^0 + C^*\bar{\mathrm{n}}\Lambda\theta^{0*}$. The invariance for anti-particle conjugation requires

$$\mathscr{L} = \tfrac{1}{2}[\mathscr{L}(\phi)+\mathscr{L}(\phi')] = \tfrac{1}{2}(C+C^*)\,[\bar{\Lambda}\mathrm{n}\theta^0+\bar{\mathrm{n}}\Lambda\theta^{0*}].$$

The coupling constant, therefore, must be real and this is Pauli's result [5]).

4. Interaction Lagrangian

We are now in a position to write down the fundamental La-

† I would like to acknowledge my indebtedness to Prof. Pauli's stimulating paper.

†† The role of U as a unitary transformation is destroyed if the viewpoint of earlier presentations is adopted, where invariance of $e\bar{\psi}_p\gamma_\mu\psi_p A_\mu$ for $\psi\to\psi'$ is secured by $e\to -e$ rather than by simultaneously transforming $A_\mu \to A'_\mu = UA_\mu U^{-1}$ (see ref. [6,7])).

††† In the Majorana representation of hermitian γ matrices, γ_1, γ_3, γ_5 are real, γ_4 pure imaginary.

grangian, with all possible interactions allowed by (1), (2) and (3) of section 1. Assume for simplicity that all fermions are $(\frac{1}{2}+)$ and θ's are $(0+)$ particles. Then

$$\begin{aligned}\mathscr{L} = & g_1 \overline{\mathrm{N}}(i\gamma_5)\,\boldsymbol{\tau}\cdot\boldsymbol{\pi}\,\mathrm{N} \\ & + g_2\,[\overline{\Lambda}(i\gamma_5)\,\boldsymbol{\pi}\cdot\boldsymbol{\Sigma} + \overline{\boldsymbol{\Sigma}}\cdot\boldsymbol{\pi}(i\gamma_5)\,\Lambda] \\ & + g_3\, i\overline{\boldsymbol{\Sigma}}(i\gamma_5)\wedge\boldsymbol{\pi}\cdot\boldsymbol{\Sigma} \\ & + g_4\,\overline{\Xi}(i\gamma_5)\,\boldsymbol{\tau}\cdot\boldsymbol{\pi}\,\Xi \\ & + g_5\,[\overline{\mathrm{N}}\,\theta\,\Lambda^0 + \overline{\Lambda}^0\,\theta^*\,\mathrm{N}] \\ & + g_6[\overline{\mathrm{N}}\,\boldsymbol{\tau}\cdot\boldsymbol{\Sigma}\,\theta + \theta^*\,\overline{\boldsymbol{\Sigma}}\cdot\boldsymbol{\tau}\,\mathrm{N}] \\ & + g_7\,[\overline{\Xi}\,\tau_2\,\theta^*\,\Lambda^0 + \overline{\Lambda}^0\,\theta\,\tau_2\,\Xi] \\ & + g_8\,[\overline{\Xi}\,\tau_2\,\boldsymbol{\tau}\cdot\boldsymbol{\Sigma}\,\theta^* + \theta\,\boldsymbol{\tau}\cdot\overline{\boldsymbol{\Sigma}}\,\tau_2\,\Xi].\end{aligned}$$

The present sign of g_3 makes the $\boldsymbol{\pi}$ couplings similar ($g_1\ \bar{\mathrm{p}}\mathrm{p}\pi^0$ and $g_3\,\overline{\Sigma}^+\,\Sigma^+\,\pi^0$, and $-g_1\,\bar{\mathrm{n}}\mathrm{n}\pi^0$ and $-g_3\,\overline{\Sigma}^-\,\Sigma^-\,\pi^0$ etc.). It is tempting to speculate on the possibility $g_1 = g_2 = g_3 = g_4$ and $g_5 = g_6 = g_7 = g_8$, and even perhaps $g_1 = g_5$ which present experimental evidence does not exclude (cf. ref. [8])).

To the group of π interactions, we could add pseudovector interactions $f_1\,\overline{\mathrm{N}}(i\gamma_5\,\gamma_\mu)\boldsymbol{\tau}\cdot(\partial\boldsymbol{\phi}/\partial x_\mu)\mathrm{N}$ etc. (f_1 real). However if Λ and Σ have opposite parities $(\frac{1}{2}+)$ and $(\frac{1}{2}-)$, this could not be done without destroying charge-independence.

To the group involving θ interactions, τ particle $(0-)$ interactions could likewise be added, replacing the Dirac unit-matrix by $i\gamma_5$. There is no restriction here (on account of the complex nature of the τ^0 field) on introducing charge-independent pseudovector interactions, whatever the parity assignments for the Fermi particles.

References

1) R. Utiyama, Phys. Rev. **100** (1955) 248
2) B. d'Espagnat and J. Prentki, Nuc. Phys. **1** (1956) 33
3) G. Racah, Nuc. Phys. **1** (1956) 301
4) B. d'Espagnat and J. Prentki, Phys. Rev. (in print)
5) W. Pauli in Niels Bohr and the development of physics (Pergamon Press, 1955) p. 30
6) Jost and Pais, Phys. Rev. **87** (1952) 871
7) Ravenhall and Wolfenstein, Phys. Rev. **88** (1952) 279
8) S. Oneda and A. Wakasa, Nuc. Phys. **1** (1956) 445

Nuclear Physics **2**)1956/57) 177—187; *North-Holland Publishing Co., Amsterdam*

RADIALLY SYMMETRIC SOLUTIONS OF BETHE-SALPETER EQUATION

S. N. BISWAS and H. S. GREEN
University of Adelaide, S-Australia
Received 18 June 1956

Abstract: New exact solutions are obtained of the Bethe-Salpeter equation for a pair of fermions, in the ladder approximation and for zero boson mass. The solutions are applicable for small but non-vanishing total energy, and for scalar or pseudoscalar boson fields with ordinary or derivate coupling. A boundary condition, similar to that applied to the Schrödinger equation in three dimensions, is proposed, which reduces the continuum of eigenvalues for the coupling constant to a set of discrete values, except in the case of s(s) coupling. It is pointed out that this boundary condition also implies the existence of a new quantum number, with properties similar to those of the "strangeness" number already used to classify the new particles.

1. Introduction

The Bethe-Salpeter equation [1]) is a fully covariant integral equation describing the interaction of two elementary particles. It was originally solved with the help of non-covariant approximations, and the results so obtained were not radically different from those obtained by means of the non-covariant Schrödinger equation. They fostered the hope that one could predict the energies of bound states within the framework of relativistic field theories.

Attempts to solve the covariant equation in a covariant way have, however, led to difficulties. The homogeneous equation for the interaction of a pair of nucleons can be simplified by adopting the covariant 'ladder approximation', neglecting the meson mass, and finally equating the total energy of the system to zero, in the barycentric frame of reference. Goldstein [2]) found, under these conditions, that the proper values of the coupling constant were not discrete, as expected of a system with discrete energy levels, but continuous. He did suggest a procedure for extracting a discrete value from the continuous spectrum, but it has been shown by one of the authors [3]) that this procedure is unsuccessful. The question remained open whether this unnatural behaviour of the predicted spectrum was associated with the unnatural value assumed for the total energy, or not. Another possibility was that some special

condition ought to be applied to the relativistic wave-function, but no such condition was clearly indicated.

Some light has been shed on these questions by the researches of Wick [4]), Scarf [5]) and Cutkosky [6]). They have considered the application of the Bethe-Salpeter formalism to the interaction of two spinless particles. For this problem an exact solution of the integral equation is possible, with arbitrary binding energy. A discrete spectrum results from the adoption of a physically reasonable condition on the wave-function, which is also necessary for the existence of its Fourier transform. But, as Wick has pointed out, the existence of a discrete spectrum is assured provided that the integral equation can be solved by the Fredholm method, and in this respect there is a fundamental difference between the equations for spinless and spin $\frac{1}{2}$ particles. The Fredholm method is directly applicable to the B.-S. equation for spinless particles, but not to the equation for two fermions treated by Goldstein. It would seem, therefore, that there is an essential difference between the properties of the equation considered by Wick, Scarf and Cutkosky and that appropriate to the interaction of a pair of fermions.

In this paper we propose to examine the effect of a condition on the wave function which appears not to have been properly considered. We shall require that the solution of the B.-S. equation together with its spatio-temporal derivatives should be finite and continuous everywhere, and particularly on the light cone. This is a natural generalization of the condition on the solution of a Schrödinger equation, and, as we shall show, has the merit of crystallizing discrete eigenvalues from the continua in the physically interesting cases. It also has merits which we cannot discuss at length in this paper, but shall mention in § 4.

Our boundary condition has the effect of eliminating completely the solution of the B.-S. equation obtained by Goldstein, along with its continuum of eigenvalues, for both s(s) and ps(ps) coupling. The disappearance of this solution may, of course, be merely a feature of the extreme binding energy. But there is another solution of the equation considered by Goldstein which for ps(ps) coupling is not similarly eliminated, for certain discrete values of the coupling constant. This second solution will be derived not merely for zero total energy, but for total energies somewhat exceeding zero. It is interesting to notice that there is no corresponding solution with s(s) coupling.

Recently [1]) attention has been given to the possibility that field theories with derivative coupling may be renormalizable, by extensions of the conventional methods. Even if this possibility were fully realized, it might of course be difficult to justify the B.-S. equation in the ladder approximation. But, in spite of the highly singular nature of the kernel, the equation can be solved without difficulty for both s(v) and ps(pv) coupling. The solutions will be obtained, and it will be shown that the eigenvalue problem is determinate, except possibly for solutions of Goldstein's type. The solutions obtained are valid only for zero boson mass and total energies sufficiently near to zero. There is nothing, however, to indicate that these solutions cannot be continued to non-vanishing values of the meson mass and more realistic values of the total energy. The results obtained therefore provide the first definite indication that the B.-S. equation possesses covariant solutions representing the bound states of two fermions.

2. Solutions of the Bethe-Salpeter Equation

We write the Bethe-Salpeter two-nucleon equation in the momentum representation in the form

$$\phi(k) = -\frac{\lambda}{i\pi^2}\int \Gamma_l \frac{1}{p+l-m}\phi(l)\frac{1}{p-l-m}\Gamma_l^+ \frac{\mathrm{d}^4 l}{(k-l)^2}, \ldots . \quad (1)$$

where natural units are used, the interaction is restricted to 'ladder' approximation with zero boson mass, λ is the coupling constant and Γ_l has the values 1, $-il$, $i\gamma_5$ and $\gamma_5 l$ for s(s), s(v), ps(ps) and ps(pv) neutral fields respectively. Γ_l^+ is the adjoint of Γ_l.

Defining $\theta(k) = (p+k-m)^{-1}\phi\,(k)(p-k-m)^{-1}$ and $\theta(x)$ as the fourier transform of $\theta(k)$, i.e.,

$$\theta(x) = \frac{1}{i(2\pi)^4}\int \theta(k)\ \mathrm{e}^{-ik\cdot x}\mathrm{d}^4 k$$

one obtains easily from equation (1) the following differential equations in the coordinate representation for $\theta(x)$:

$$(p+i\nabla-m)\theta(x)(p-i\overleftarrow{\nabla}-m) = \frac{4\lambda}{x^2}\Gamma_x\theta(x)\Gamma_x^+ \ . \ . \ . \ . \quad (2)$$

where $\Gamma_x = 1$, $\gamma\cdot\partial/\partial x$, $i\gamma_5$ or $i\gamma_5\gamma\cdot\partial/\partial x$ for the s(s), s(v), ps(ps) or ps(pv) theories respectively. (Note that $\Gamma_x^+ = -\gamma\partial/\partial x$ in s(v) theory and $-i\gamma_5\gamma\cdot\overleftarrow{\partial}/\partial x$ in ps(pv) theory).

Our object is now to solve the differential equation (2) by assuming a special form of $\theta(x)$. We require that $\theta(x)$ be capable of expansion in the form

$$\theta(x) = \theta_0(x)+\theta_1(x) + \ldots\ldots \tag{3}$$

where $\theta_0(x)$ is of the form $x \cdot \sigma(x^2)$ and $\theta_1(x)$ of the form $(p \cdot x)\omega(x^2)$. The equation (1) can however be solved in the momentum representation by transforming it to a differential equation, operating on both sides of (1) with the operator $\Box = \partial^2/\partial k^\mu \partial k_\mu$. Since the boundary conditions of the wave function are directly applicable to the solutions of the wave equation only in coordinate space we shall continue our investigation in the coordinate representation. We shall merely state the corresponding solutions in the momentum representation so as to make clear that the solutions in coordinate space admit fourier transformation.

Introducing (3) in both sides of (2) one gets the following system of differential equations:

$$(i\nabla-m)\theta_0(x)(\overleftarrow{i\nabla}+m)-\frac{4\lambda}{x^2}\Gamma_x\theta_0(x)\Gamma_x^+=0, \tag{4}$$

$$(i\nabla-m)\theta_1(x)(\overrightarrow{i\nabla}+m)-\frac{4\pi}{x^2}\Gamma_x\theta_1(x)\Gamma_x^+ = -p\theta_0(\overleftarrow{i\nabla}+m)+(i\nabla-m)\theta_0 p. \tag{5}$$

Our procedure will now be to solve the equation (4) to obtain θ_0. It will then be possible to write down the solutions of the homogeneous equations (5) immediately, since the Green's function for this equation can be constructed from the independent solutions of (4). We now proceed to the solution of (4).

Assuming $\theta_0 = x\sigma(x^2)$ and $\theta_1 = (p \cdot x)\bar{\omega}(x^2)$, then one can at once write down the following for (4) and (5):

$$(\Box+m^2)\theta_0+\frac{4\lambda}{x^2}\Gamma_x\theta_0\Gamma_x^+ = 0,$$

$$(\Box+m^2)\theta_1+\frac{4\lambda}{x^2}\theta_1\Gamma_x^+ = m(p\theta_0+\theta_0 p). \tag{6}$$

For s(s) and ps(ps) couplings one obtains with $s = m^2x^2$ from the first equation of (6):

$$\sigma''(s)+\frac{3}{s}\sigma'(s)+\frac{s\pm 4\lambda}{4s^2}\sigma(s) = 0; \tag{7}$$

the upper or lower sign is taken according as the coupling is s(s) or ps(ps). A very similar equation to (7) holds for $\bar{\omega}(s)$ buth with an inhomogeneous term given by the right-hand side of (5.). The solution of (7) is given by

$$\sigma_\nu(s) = s^{-1}B_\nu(s^{\frac{1}{2}}) \text{ with } \nu = (4\mp 4\lambda)^{\frac{1}{2}}$$

where B_ν is a cylindrical function. The two solutions J_ν and $J_{-\nu}$ (or Y_ν) are both finite at infinity but only J_ν is finite at the origin so that the solutions of (4) and (5) may be written down in the form

$$\theta_0 = s^{-1}B_\nu(s^{\frac{1}{2}})x,$$

$$\theta_1 = c_\pm(p\cdot x)\left\{\chi_1(s)\int_0^s \chi_2(\xi)\sigma_\nu(\xi)\xi^{-1}\,d\xi + \chi_2(s)\int_s^\infty \chi_1(\xi)\sigma_\nu(\xi)\xi^{-1}\,d\xi\right\}, \quad (8)$$

where $\chi_1(s) = s^{-1}J_{-\mu}(s^{\frac{1}{2}})$, $\chi_2(s) = s^{-1}J_\mu(s^{\frac{1}{2}})$, and $\mu = (4-4\lambda)^{\frac{1}{2}}$; $\sigma_\nu(s)$ is the chosen solution of (7) and $c_\pm$ are constants differing in signs according as one considers s(s) or ps(ps) coupling. The precise determination of these constants is unimportant for our purposes. To the solution for θ_1 one may add any linear combination of χ_1 and χ_2 multiplied by $(p\cdot x)$.

We now discuss the solutions of (4) with the assumption that $\theta_0(x) = \theta_0(x^2)$, a purely scalar function of x^2. This is essentially Goldstein's solution. We get the following differential equation for $\theta_0(s)$:

$$4s^2\theta_0''(s) + 8s\theta_0'(s) + (s+4\lambda)\theta_0(s) = 0$$

admitting at once the solution

$$\theta_0(s) = s^{-\frac{1}{2}}B_\nu(s^{\frac{1}{2}}) \text{ with } \nu = (1-4\lambda)^{\frac{1}{2}}. \quad (9)$$

Next consider the derivative coupling theories. The equations (4) and (5) can now be brought to the forms given below. Assuming as before that $\theta_0(x)$ has the form $x\cdot\chi(x^2)$ and θ_1 the form $(p\cdot x)\tau(x^2)$ one writes the differential equations for χ together in the form

$$(s\pm\lambda)\left(\chi''(s) + \frac{3}{s}\chi'(s)\right) + \frac{1}{4}\chi(s) = 0 \quad (10)$$

where $s = m^2x^2$ and for convenience we set $m = 1$. For τ the following equation is then obtained:

$$\tau''(s) + \frac{3}{s}\tau'(s) + \frac{\tau(s)}{4(s+\lambda)} = \frac{2\chi(s)}{(s+\lambda)} \quad (11)$$

where $\chi(s)$ is the solution of (10).

The upper or lower sign in (10) is taken according as one considers s(v) or ps(pv) coupling. Introducing a new variable t by $s = \mp\lambda t$ one obtains for (10)

$$\chi''(t)+\frac{3}{t}\chi'(t)\mp\frac{\lambda\chi(t)}{4(t-1)}=0. \tag{12}$$

The equation (12) is a confluent form of Heun's equation [8]) and its general solution is a confluent Heun's function. One may in fact write down the explicit solution of (12) in terms of the established notation for Heun's function [9]):

$$\chi(t)=\lim_{a\to\infty} F(a, h;\ \alpha, \beta, \gamma, \delta;\ t),$$

where $h = 0$, $\alpha\beta = \mp(\lambda a)/4$, $\alpha+\beta = 3$, $\gamma = 3$, $\delta=0$ and $t=s/(\pm\lambda)$; the upper or lower sign indicates the corresponding solution of (12). For the solution of (11) one follows the same method as used in the direct coupling theory. We construct the Green's function of the differential equation (11) from the two independent solutions of the homogeneous equation obtainable from (11). This has just the form of (12) when one restricts to the upper sign only. The two solutions, for convenience, are denoted by $\tau_1(s)$ and $\tau_2(s)$; $\tau_1(s)$ is finite at the origin and behaves as s^4, and τ_2 is singular and behaves like s^{-3}. Both solutions tend to zero for large values of s. For general values of λ, τ_1 is finite but not zero, and τ_2 can be made to vanish at $s = -\lambda$. For *special* values of λ [solutions of $\tau_1(-\lambda) = 0$], τ_1 vanishes and τ_2 is finite but not zero at $s = -\lambda$.

The solution of (11) can be written down in a form similar to the second equation of (8):

$$\theta_1^{(\pm)}(x) = c^{\pm}(p\cdot x)\left\{\tau_2(s)\int_0^s \tau_1(\xi)\chi^{\pm}(\xi)(\xi+\lambda)^{-1}\mathrm{d}\xi + \tau_1(s)\int_s^{\infty}\tau_2(\xi)\chi^{\pm}(\xi)(\xi+\lambda)^{-1}\mathrm{d}\xi\right\}, \tag{13}$$

where the $\pm$ sign refers to the s(v) or ps(pv) coupling respectively, $\chi^{\pm}$ are the solutions of (10) with the upper or lower sign and $c^{\pm}$ is a constant whose value need not be determined for our purposes. To this solution (13) one can of course add a complementary function which is a linear combination of $\tau_1(s)$ and $\tau_2(s)$ multiplied by $(p\cdot x)$.

If one instead assumes with Goldstein that $\theta_0(x)$ is of the form

$\theta_0(x^2)$, then one obtains easily the following differential equation for both s(v) and ps(pv) theory:

$$4(s+\lambda)\left\{\theta_0''(s)+\frac{2\theta_0'(s)}{s}\right\}+\theta_0(s)=0. \tag{14}$$

The solution of (14) is given in terms of a cylindrical function with argument $(s+\lambda)$:

$$\theta_0(s)=s^{-1}(s+\lambda)^{\frac{1}{2}}B_1(\sqrt{s+\lambda}), \tag{15}$$

where B_1 denotes any linear combination of J_1 and Y_1.

It remains to show that Fourier transforms exist of the solutions we have already obtained in the coordinate representation, and that they have no unexpected singularity. In the case of Bessel functions the fourier transform could be taken directly, but little is yet known concerning Heun's function, and it seems necessary to return to the integral equation (1) to obtain the transforms. To determine $\theta(k)$ which is the fourier transform of $\theta(x)$ we assume $\theta(k)=\theta_0(k)+\theta_1(k)+\cdots$ where θ_0 is independent of p and θ_1 depends linearly on p. Assuming a similar form of $\phi(k)$ i.e. $\phi(k)=\phi_0+\phi_1$ where ϕ_0 and ϕ_1 are of the same type as θ_0 and θ_1 one notes that from the relation

$$\theta(k)=(p+k-m)^{-1}\phi(k)(p-k-m)^{-1}$$

it follows that

$$\theta_0(k)=(m^2-k^2)^{-1}\phi_0 \tag{16}$$

and

$$\theta_1(k)=(m^2-k^2)^{-1}\theta_1+m(k^2-m^2)^{-2}(p\phi_0+\phi_0 p). \tag{17}$$

Hence it appears that the determination of $\theta_0(k)$ and $\theta_1(k)$ amounts to finding the unknown functions ϕ_0 and ϕ_1.

For s(s) and ps(ps) coupling one has

$$\phi_0=F(a, b;\ 3, s)k$$

where $s=k^2/m^2$, $a=1+(1\mp\lambda)^{\frac{1}{2}}$ and $b=1-(1\mp\lambda)^{\frac{1}{2}}$. The $-$ or $+$ sign is taken for the s(s) or ps(ps) case.

Similarly, for s(v) or ps(pv) coupling one obtains a confluent form of Heun's equation, whose solution may be written down in the form

$$\theta_0=\lim_{a\to\infty}F(a, h;\ \alpha, \beta, \gamma, \delta;\ s)k \tag{19}$$

with $h=0$, $\alpha\beta=\mp\lambda a$, $\alpha+\beta=3$, $\gamma=3$, $\delta=0$. The upper or lower sign of λ is taken according as the coupling is s(v) or ps(pv).

For the determination of ϕ_1 we can adopt the same procedure we have followed in the coordinate representation.

It is worth mentioning that the solutions reduce to simpler well known functions when one assumes with Goldstein that ϕ_0 is of the form $\phi_0(k^2)$. For s(s) and ps(ps) coupling one has

$$\phi_0(s) = F(a, b;\ 2,\ s)$$

where $a = \frac{1}{2}\{1+(1-4\lambda)^{\frac{1}{2}}\}$, $b = \frac{1}{2}\{1-(1-4\lambda)^{\frac{1}{2}}\}$. Also $\theta_0(s)$ reduces to a Bessel function in case of derivative coupling theory, i.e.

$$\phi_0(s) = s^{-1}(s-1)^{\frac{1}{2}} B_1(2\sqrt{\lambda(s-1)})$$

where B_1 is any cylindrical function.

3. Boundary Conditions and Eigenvalue Problem

The attempt will now be made to formulate a boundary condition, similar to the boundary condition applied to the non-relativistic Schrödinger equation in the following respect: that it isolates certain discrete states from the continuum, which can be identified with the bound states of the pair of fermions considered. Boundary conditions have already been proposed by Wick [4]) and Scarf [5]) for the equations of spinless particles which they have considered. In the present context these conditions are satisfied, provided the fourier transform of the wave function exists; and it has already been seen that the fourier transform does exist independently of the choice of special values of λ. Something more is evidently required.

An examination of the solutions of the B.-S. equation obtained in the previous section suggests a boundary condition for the derivative coupling theories more readily than for s(s) or ps(ps) coupling. The solution $\theta_0(x)$ for zero total energy must obviously not have a singularity as strong as $(x^2)^{-3}$ on the light-cone, since this would mean, among other things, that the wave function would not be normalizable on a space-like surface†; one is therefore restricted to the solution of (10) which vanishes like s^4 near $s = 0$. So long as one confines one's attention to zero energy, there is no apparent restriction on λ. But an examination of (13) shows that, for non-vanishing total energy and general values of λ, there is a singularity at $s = -\lambda$. The precise nature of this singularity is resolved by giving the nucleon mass, and hence s, a small imaginary term which is ultimately made to vanish. It then appears that, though $\theta_1^{(\pm)}(x)$

† This is of course necessary for a bound state solution only.

is finite and continuous everywhere, its first derivatives are usually discontinuous for $s = -\lambda$. To avoid this discontinuity, it is necessary to choose λ in such a way that $\chi^{\pm}(-\lambda) = 0$, i.e., so that $-\lambda$ is one of the zeros of the confluent Heun's function concerned.

The following boundary condition is therefore suggested: *$\theta(x)$and its first spatio-temporal derivatives should be finite and continuous everywhere.* This is a natural extension to four dimensions of the condition customarily applied to the Schrödinger wave function in three dimensions. It has the effect of making the eigenvalue problem determinate, at least for the derivate coupling theories. There seems to be no reason to make an exception for the light-cone.

Now consider the application of this condition to the s(s) and ps(ps) theories. At zero total energy the solution (8) reduces to $\theta_0 = s^{-1}J_\nu(s^{\frac{1}{2}})x$, if the cylindrical function is identified with the Bessel function. To satisfy the condition one must obviously take $\mathrm{Re}\,\nu \geqq 1$, which is impossible for positive values of λ, in the s(s) theory where $\nu = 2(1-\lambda)^{\frac{1}{2}}$. In the ps(ps) theory $\nu = 2(1+\lambda)^{\frac{1}{2}}$, and this difficulty does not arise. Actually the condition that θ_0 should be continuous, and therefore single-valued, on the light-cone may be quite a rigorous one. It would on the present interpretation exclude the possibility that θ_0 should involve some fractional power of s, since this would inply a many-valued wave function with a branch-point on the light-cone. To avoid such a singularity, ν would have to be an even integer greater than 2, and λ would have to be of the form $n^2 - 1$, where n is an integer greater than 1, in the ps(ps) theory. Provided λ is given one of its eigenvalues, both θ_0 and θ_1 as defined by (11) are well behaved functions satisfying the boundary condition, in the ps(ps) theory. There is, however, no satisfactory solution in the s(s) theory.

The condition which has been proposed eliminates solutions for which θ_0 is a function of s only, like that obtained by Goldstein, except perhaps in the derivative coupling theories. It is difficult to reach any final conclusion without continuing the solution to non-vanishing energies, since there is no guarantee that θ_1 will satisfy the 'boundary condition', and we have not succeeded in finding θ_1 when θ_0 is a function of s only. Nor have we succeeded in finding θ_2 explicitly, even where we have determined θ_1; to do so we should have to solve a set of three simultaneous equations of the second order. † But the existence of a solution can be proved,

† This has since been done.

and though we do not know in advance that θ_2 could be found to satisfy the 'boundary condition', it is worth noticing that λ can probably be represented as a power series of the type $\lambda = \lambda_0 + \lambda_2 p^2 + \lambda_4 (p^2)^2 + \cdots$, and the coefficient λ_2 is disposable for the determination of θ_2 and θ_3, just as λ_0 was disposable for the determination of θ_0 and θ_1.

4. Additional Remarks

In this paper we have studied only the radially symmetric solutions of the B.-S. equation. We have, however, made an investigation of the solutions which are not radially symmetric, but depend on the generalized angular variables α, β and γ defined by $x_4 = R\cosh\alpha$, $x_1 = r\sin\beta\cos\gamma$, $x_2 = r\sin\beta\sin\gamma$, $x_3 = r\cos\beta$ with $r = R\sinh\alpha$, so that in the notation of § 2, $s = R^2$. The radial dependence of these solutions does not appear to be essentially different from that of the solutions already derived. It remains to discuss the effect of the boundary condition on the angular dependence of the solutions.

The eigenfunctions of the B.-S. equation for zero total energy can be classified according to the effect of the covariant angular momentum operator $M_{\lambda\mu}$, defined by

$$M_{\lambda\mu} = i\left(x_\lambda \frac{\partial}{\partial x^\mu} - x_\mu \frac{\partial}{\partial x^\lambda}\right) + S_{\lambda\mu},$$

$$S_{\lambda\mu}\theta = \frac{1}{4} i\{(\gamma_\lambda\gamma_\mu - \gamma_\mu\gamma_\lambda)\theta + \theta(\gamma_\lambda\gamma_\mu - \gamma_\mu\gamma_\lambda)\}. \tag{20}$$

Simultaneous eigenfunctions [10]) can be determined of S_{12}, M_{12}, $S_{12}^2+S_{23}^2+S_{31}^2$ and $M_{12}^2+M_{23}^2+M_{31}^2$, in the usual way, and also of $M^{\lambda\mu}M_{\lambda\mu}$. The restrictions imposed by the boundary condition on the eigenfunctions of S_{12}, M_{12}, $S_{12}^2+S_{23}^2+S_{31}^2$ and $M_{12}^2+M_{23}^2+M_{31}^2$ are well known, but few attempts have been made to quantize the invariant $M^{\lambda\mu}M_{\lambda\mu}$. Assuming, however, that the wave function θ is finite and continuous on the light-cone, it can be shown that a new quantum number is required to enumerate the permitted eigenvalues of $M^{\lambda\mu}M_{\lambda\mu}$. The physical meaning of this new quantum number, and the conservation equation (for M_{14}, M_{24} and M_{34}) associated with it, is not transparent in the present state of relativistic quantum mechanics. It has, however, been found necessary[11]) to introduce at least one new quantum number for the classification

of the heavy mesons and hyperons, and Pais [12]) has already suggested that this new quantum number should arise from the quantization of the M_{14}, M_{24}, M_{34} components of the angular momentum tensor. It is important to notice that such a quantization procedure has a meaning only in relation to a boundary condition on the wave function, such as we have formulated above.

When the total energy is not zero, the selection rules are rigorous only if the angular momentum of the centre of mass of the system about the origin of co-ordinates is included with $M_{\lambda\mu}$. This circumstance may help to account for the fact that, in decay processes, the apparent violation of the selection rules is observed.

References

1) E. E. Salpeter and H. A. Bethe, Phys. Rev. **84** (1951) 1232
2) J. S. Goldstein, Phys. Rev. **91** (1953) 1516
3) H. S. Green, Phys. Rev. **97** (1955) 540
4) G. C. Wick, Phys. Rev. **96** (1954) 1124
5) F. L. Scarf, Phys. Rev. **100** (1955) 912
6) R. E. Cutkosky, Phys. Rev. **96** (1954) 1135
7) R. Arnowitt and S. Deser, Phys. Rev. **100** (1955) 349
   See also H. S. Green, Nuc. Phys. **1** (1956) 360
8) G. C. Lambe and D. R. Ward, Quart. J. of Math. **5** (1934) 81
9) C. Snow, Hypergeometric and Legendre Functions, Natl. Bur. of Stds. Applied Mathematics Series **19** (1952) Chapt. VII
10) Max Born and K. Fuchs, Proc. Roy. Soc. Edin. **60** (1939—40) 141
    See also, K. Fuchs, Proc. Roy. Soc. Edin. **60** (1939—40) 147
11) M. Gell-Mann and A. Pais, Proceedings of the 1954 Glasgow Conference on Nuclear and Meson Physics p. 342
    A. Pais, Proc. Nat. Acad. Sci. **40** (1954) 484
    M. Gell-Mann, Phys. Rev. **92** (1953) 833
12) A. Pais, Proc. Nat. Acad. Sci. **40** (1954) 835

Nuclear Physics **2** (1956/57) 188—191; *North-Holland Publishing Co., Amsterdam*

ON THE CHARGE INDEPENDENCE OF NUCLEAR FORCES

RIAZUDDIN
Fitzwilliam House, Cambridge

Received 27 June 1956

Abstract: The possibility that the discrepancy between the zero energy scattering lengths A_{NP}, A_{PP} for ^1S states of the NP and PP systems may be due to the mass difference between charged and neutral pions is investigated.

One test for the hypothesis of charge independence of nuclear forces consists in comparing the zero energy scattering lengths A_{NP}, A_{PP} for the ^1S states of the NP and PP systems. This comparison shows that there is a definite discrepancy between the nuclear forces in ^1S states of NP and PP systems. Schwinger [1]) has pointed out that this discrepancy may be due to non-nuclear interaction. To be precise, the magnetic interaction between nucleons gives different contributions to the effective potentials for NP and PP systems in ^1S states. Schwinger found that A^1_{NP} and A^1_{PP}, the effective scattering lengths resulting from purely nuclear potentials alone, are in definite disagreement for a square well potential but in very satisfactory agreement for a Yukawa potential.

Modern theory, however, postulates a repulsive core of radius about 0.6×10^{-13} cm. Therefore Salpeter [2]) re-investigated this question assuming repulsive cores of radii $\geqq 0.3\times10^{-13}$ cm in addition to an attractive potential of any shape. He found that the magnetic interaction energy is considerably reduced in comparison with Schwinger's result and that a sizeable discrepancy between A^1_{NP} and A^1_{PP} and hence between the effective strengths of the two potentials is again obtained even if the attractive part of the potential is of the Yukawa or Hulthén type.

Now the masses of the charged and neutral pions are determined very accurately by experiment: the neutral pion is about 9 electron masses lighter than its charged counterpart. All deviations from isobaric spin symmetry being due solely to electromagnetic effects, the mass difference between charged and neutral pions would have

to be just of electrodynamic origin. Feynman [3]) and Petermann [3]) have shown that this is a reasonable possibility. Also Schwinger [1]) has pointed out that a difference between NP and PP nuclear interaction is to be anticipated theoretically as a consequence of electrical pertubation of the mesons responsible for the nuclear force. Therefore it is reasonable to examine whether the difference between A_{NP} and A_{PP} is due to the mass difference between charged and neutral pions. The purpose of this note is to consider this possibility.

Using symmetric pseudo-scalar theory with pseudoscalar coupling and taking into consideration the mass difference between neutral and charged pions we find, using the procedure of Klein [4]), for the second order potential

$$V_2' = V_2 + \delta V_2,$$

where V_2 is the usual charge independent potential and δV_2, the correction due to the mass difference, is given by

$$\delta V_2 = -\frac{1}{3}(\tau_3^{(1)}\,\tau_3^{(2)})\frac{g^2}{4\pi}\delta\mu^2 \times \frac{\partial}{\partial\mu^2}\left[\left(\frac{\mu}{2M}\right)^2 \cdot \left\{(\sigma_1\cdot\sigma_2)+S_{12}\left[1+\frac{3}{\mu r}+\frac{3}{(\mu r)^2}\right]\right\}\frac{e^{-\mu r}}{r}\right].$$

Hence for a ^1S state the effective NP and PP interactions are given by

$$V_2^{NP} = V_2 + \delta\mu^2\frac{\partial}{\partial\mu^2}(V_2)$$

$$V_2^{PP} = V_2 - \delta\mu^2\frac{\partial}{\partial\mu^2}(V_2)$$

where V_2, the charge independent potential, is

$$-\frac{g^2}{4\pi}\left(\frac{\mu}{2M}\right)^2\frac{e^{-\mu r}}{r}$$

and

$$\frac{\delta\mu^2}{\mu^2} = 0.064.$$

This means that the depth of the effective NP interaction is greater than that of the PP interaction, showing that we would get the right sign for removing the discrepancy between A_{NP} and A_{PP}.

The effect of mass difference on fourth order interaction can be similarly calculated. In Lévy's [5]) notation, the change in fourth order potential due to mass difference is given by

$$\delta V_{4,2}^{\mathrm{NP}} = 0, \qquad \delta V_{4,2}^{\mathrm{PP}} = -\frac{1}{3}\delta\mu^2 \frac{\partial}{\partial\mu^2} V_{4,2},$$

$$\delta V_{4,1}^{\mathrm{NP}} = 0, \qquad \delta V_{4,1}^{\mathrm{PP}} = -\frac{1}{3}\delta\mu^2 \frac{\partial}{\partial\mu^2} V_{4,1},$$

to order $\delta\mu^2$. Here $V_{4,2}$ is that part of the fourth order charge independent potential which arises from two-pair terms, while $V_{4,1}$ is that arising from one-pair terms. We shall not, however, consider the effects of $\delta(V_{4,2}^{\mathrm{NP}}+V_{4,1}^{\mathrm{NP}})$ and $\delta(V_{4,2}^{\mathrm{PP}}+V_{4,1}^{\mathrm{PP}})$ on the scattering lengths.

Having found how the charge independent potential is affected by the mass difference between neutral and charged pions, we take the effective NP and PP potentials in ^{1}S states as

$$V_2^{\mathrm{NP}} = -V_0 \frac{\mathrm{e}^{-\beta r}}{\beta r} - 0.064\, V_0 \frac{\mathrm{e}^{-\beta r}}{\beta r} + 0.032\, V_0\, \mathrm{e}^{-\beta r},$$

$$V_2^{\mathrm{PP}} = -V_0 \frac{\mathrm{e}^{-\beta r}}{\beta r} + 0.064\, V_0 \frac{\mathrm{e}^{-\beta r}}{\beta r} - 0.032\, V_0\, \mathrm{e}^{-\beta r},$$

where the values of V_0 and β are to be fixed from low energy data and can be calculated from the tables of Blatt and Jackson [6]).

We shall now find the effect of

$$\delta V = -0.064\, V_0 \frac{\mathrm{e}^{-\beta r}}{\beta r} + 0.032\, V_0\, \mathrm{e}^{-\beta r}$$

on the scattering lengths first without repulsive core and then with repulsive core. The experimental value of $1/A_{\mathrm{NP}}$ is -0.422×10^{12} and for a Yakawa potential without repulsive core the corresponding value of $1/A_{\mathrm{PP}}$ is -0.5521×10^{12}.

Denoting by A_{NP}^1 and A_{PP}^1 the charge independent scattering lengths and using the formula

$$\delta\left(\frac{1}{A}\right) \equiv \frac{1}{A} - \frac{1}{A^1} = \int_0^\infty \delta W u_0^2\, \mathrm{d}r$$

where $W = -(M/\hbar^2)V$ and u_0 is the zero energy radial function, we find

$$\delta\left(\frac{1}{A_{\mathrm{NP}}}\right) = +0.21\times 10^{12},$$

$$\delta\left(\frac{1}{A_{\mathrm{PP}}}\right) = -0.21\times 10^{12}.$$

This shows that for a Yukawa potential without repulsive core the effect of mass difference on the scattering lengths is of the right sign but is much larger in magnitude than required.

Let us now consider a Yukawa potential with repulsive core. According to Hafner *et al.* [7]), Fig. 15, the well shape parameter $P = -0.04$ for a hard core potential of radius 0.6×10^{-13} cm. Since $P = -0.037$ for a square well, a Yukawa well with repulsive core behaves like a square well and for a square well without repulsive core the effective NP interaction [6]) should be greater by 3.3 % than the effective PP interaction to obtain the experimental values of A_{NP} and A_{PP}. But the effective NP interaction as given above is greater by about 6 % than the effective PP interaction. So even for a Yukawa potential with a repulsive core of radius 0.6×10^{-13} cm, the magnitude of the effect of mass difference will be larger than required, although the agreement between A^1_{NP} and A^1_{PP} would be better in this case than for a Yukawa potential without repulsive core.

The author is deeply indebted to Dr. A. Salam for guidance and encouragement. A scholarship awarded by the Ministry of Education, Government of Pakistan, is gratefully acknowledged.

References

1) J. Schwinger, Phys. Rev. **78** (1950) 135
2) E. Salpeter, Phys. Rev. **91** (1953) 994
3) R. P. Feynman, Phys. Rev. **94** (1954) 500L; A. Petermann, Helv. Phys. Acta **27** (1954) 441
4) A. Klein, Phys. Rev. **90** (1953) 1101
5) M. M. Lévy, Phys. Rev. **88** (1952) 725
6) Blatt and Jackson, Phys. Rev. **76** (1949) 18; Rev. Mod. Phys. **22** (1950) 77
7) Hafner *et al.*, Phys. Rev. **89** (1953) 204

BOOK REVIEW

H. UMEZAWA, *Quantum Field Theory*. (North-Holland Publishing Co, Amsterdam 1956. xvi—350 pages. 35 fl.).

As is inevitable in a "fashionable" subject developing at a rapid rate, a time arrives when the need for up to date books becomes urgent. Until recently this was the situation in the quantum theory of fields. Apart from the two "classics", Heitler's on quantum electrodynamics and Wentzel's on quantum field theory, as a whole a would-be student had to rely on original papers supplemented, with luck, by mimeographed lecture notes of which several sets have become classics in their own way.

Fortunately matters have now improved very greatly. The new quantum electrodynamics has received a thorough, scholarly treatment by Jauch and Rohrlich, (a comparison of this work with even the recent revised edition of Heitler's book shows clearly how things have moved in this subject!) and the same subject is also dealt with in a shorter monograph by Thirring, admirable for the advanced student. (The reviewer regrets not knowing the reputedly admirable Russian book by Akhiezer and Berestetski.).

Nowadays the theory of the π-meson has replaced electrodynamics as the centre of interest, but, as is well known, the theoretical situation here is far from satisfactory. Nevertheless, for better or for worse, the student can learn of it from the book by Bethe, de Hoffmann and Schweber.

The author of the book under review sets himself a much less limited task than any of the authors previously mentioned. His subject is quantum field theory as a whole and, in spite of the book's moderate size, the adjective encyplopaedic is appropriate to it. Everyone acquainted with the literature must have seen, if not read, the many papers in which familiar results are consolidated by more rigorous derivation, examined for their applicability to all conceivable variants of the theory and stated in absolutely general form. Japanese authors have probably contributed more than any others to this type of work. The present author sets out to build up a presentation encompassing all this. Side by side with the "useful" field theories of particles of spin 0 and $\frac{1}{2}$, those for spin 1 and higher receive his careful attention and where there are alternative treatments possible there is usually mention of all of them.

This is not a book for the reader impatient to acquire the equipment for a topical research problem and even less a book for the person with predominantly experimental interests. However, accepting the author's intentions, the effectiveness of his treatment is remarkable. The presentation is surprisingly free from the pedantry into which work of this nature could so easily lapse. It is by no means dull reading; the general plan and the notation are very well thought out and a real unity of outlook is apparent throughout. It is by no means impossible to follow through the thread of development of, say, electrodynamics and one finds a coherent and clear presentation of the whole subject including renormalisation and the difficulties beyond. When a deep point in the theory is discussed, one may regret that it is passed over too briefly for full appreciation by a beginner, but at the same time one notes the incisiveness of the argument and the author's full mastery of the subject.

In its own way this is an authoritative book; it will be useful to many for reference (the end-of-chapter bibliographies are admirable) and he who has time and disposition to ponder the breadth as well as the depth of the subject will derive enjoyment also.

The printing of text and formulae alike is pleasing, but even with the allowance due to a book written by a Japanese and produced in the Netherlands one could have wished for a little more care in avoidance of trivial misprints in the text.

Finally may one ask why the author chooses to depart from one of the few absolutely universal notational conventions in the subject by denoting the velocity of light by a capital C?

N.Kemmer.

NOTICE

We have just printed Instructions to Contributors of articles to be published in NUCLEAR PHYSICS. We beg all contributors to consult these instructions before typing their final manuscript.
Copies of these instructions are obtainable free of charge from the publishers or from the members of the editorial board.

Editorial Board

K B Adams
E Amaldi
H L Anderson
K T Bainbridge
C J Bakker
P R Bell
R E Bell
S. de Benedetti
A Berthelot
H Brinkman
G von Dardel
M Deutsch
W Gentner
P C. Gugelot
H Halban
O Haxel
M de Hemptinne
P Huber
D. J Hughes
S Kikuchi
J. Koch
S Livingston
E. M McMillan
P B. Moon
M. L. Oliphant
W. Paul
A. S. Rao
G. Salvini
P. Savic
P. Scherrer
C. Schmelzer
A. de Shalit
H. W. B. Skinner
R. Tangen
D. Taylor
S. du Toit
O. Wernholm
R. R. Wilson
S. D. Winter

A NEW JOURNAL

NUCLEAR INSTRUMENTS

A journal on accelerators, instrumentation and techniques in nuclear physics

EDITOR: K. SIEGBAHN
UPPSALA

It will contain

Original papers
Short notes
Survey articles
Progress reports
News items
Book reviews

Nuclear Instruments will be published in bi-monthly issues. It is planned to publish annually one volume of approx. 350 pages, but this may be increased to more volumes if required. Subscription price 130 sh; $ 17.00, postage free.

NORTH-HOLLAND PUBLISHING COMPANY AMSTERDAM

Subscriptions for USA are to be sent exclusively to
INTERSCIENCE PUBLISHERS, INC. - NEW YORK, N.Y.